MECHANISMS OF IMMUNE CELL MEDIATED REGULATION OF FIBROSIS AROUND SILICONE IMPLANTS: IN VIVO AND IN VITRO INVESTIGATIVE STUDY

A THESIS SUBMITTED

BY

JOSNA JOSEPH

IN PARTIAL FULFILLMENT OF THE REQUIREMENTS

FOR THE DEGREE OF

DOCTOR OF PHIOLOSOPHY

SEPTEMBER 2009

SREE CHITRA TIRUNAL INSTITUTE FOR
MEDICAL SCIENCES AND TECHNOLOGY
THIRUVANANTHAPURAM - 695011

The thesis

titled

MECHANISMS OF IMMUNE CELL MEDIATED REGULATION OF FIBROSIS AROUND SILICONE IMPLANTS: IN VIVO AND IN VITRO INVESTIGATIVE STUDY

Submitted

by

Josna Joseph

for

Doctor of Philosophy

of

Sree Chitra Tirunal Institute
For Medical Sciences and Technology
Thiruvananthapuram - 695011

Evaluated and approved

By

Mira Mohanty 10/5/10

Dr. Mira Mohanty
Head
Implant Biology Division
SCTIMST

10th May '10

Prof. Sarah Kuruvilla
Dept. of Pathology
Sri Ramachandra Medical college
& Research Institute
Chennai

Dr. Mira Mohanty
Scientist G

Histopathology Laboratory
Division of Implant Biology
Biomedical Technology Wing
Sree Chitra Tirunal Institute for Medical Sciences & Technology
Poojappura, Thiruvananthapuram, Kerala

CERTIFICATE

This is to certify that Ms. Josna Joseph, in the Division of Implant Biology of this Institute, has fulfilled the requirements of the regulations relating to the nature and prescribed period of research for the PhD degree of the Sree Chitra Tirunal Institute for Medical Sciences and Technology, Thiruvananthapuram. The work relating to her thesis entitled "**MECHANISMS OF IMMUNE CELL MEDIATED REGULATION OF FIBROSIS AROUND SILICONE IMPLANTS : *IN VIVO* AND *IN VITRO* INVESTIGATIVE STUDY**" was carried out under my direct supervision.

Mira Mohanty

Dr. Mira Mohanty

DECLARATION

I, Josna Joseph, hereby declare that I had personally carried out the wok depicted in the thesis entitled "**Mechanisms of immune cell mediated regulation of fibrosis around silicone implants : *in vivo* and *in vitro* investigative study**" under the direct supervision of Dr. Mira Mohanty, Scientist G, Division of Implant Biology, Biomedical Technology Wing, Sree Chitra Tirunal Institute for Medical Sciences and Technology, Thiruvananthapuram, Kerala, India, except where external help sought and acknowledged.

Josna Joseph

.....At Thy Cross's Feet.....

CONTENTS

ACKNOWLEDGEMENTS

First and foremost I offer my sincere and profound gratitude to my supervisor, Dr. Mira Mohanty who have supported me thorough out this work with her patience and knowledge. Her meticulous guidance and ardent encouragement helped in the successful completion of this thesis.

I wish to express sincere thanks to my Doctoral Advisory Committee members, Dr. Prabha Balram and Dr. Roy Joseph for their valuable comments and timely advice during the entire period of this study. Deepest gratitude are due to Dr. T. V. Kumari for her helpful discussions and constructive suggestions regarding the in vitro studies.

I am grateful to the Director, SCTIMST and the Head, BMT Wing for providing the excellent facilities for this study. Sincere thanks are due to the Registrar, SCTIMST for the academic support rendered.

I wish to acknowledge CSIR, India for the funding this doctoral study. I am thankful to Jawaharlal Nehru Memorial Fund for awarding me the JNMF scholarship that helped me to carry out the in vitro molecular studies at National University of Singapore.

I am cordially obliged to Prof. Alirio Melendez, Head, Department of Cellular and Molecular immunology, National University of Singapore for accepting me as an intern student in his laboratory and guiding me in the in vitro molecular studies. Thanks and gratitude to all staff and students of the lab, especially to Ms. Shiau Chen, who gave the essential technical support throughout the study.

Hindustan Latex Limited, Thiruvananthapuram are acknowledged for donating the Silicone expander material, which is the core of this work. I gratefully acknowledge Sophisticated test and Instrumentation centre, CUSAT for the help rendered in ICP-AES analysis.

I would like to thank Dr. Annie John and staff of the TEM laboratory for helping me with TEM analysis. Dr. H. K. Verma, Mr. R. Sreekumar and Mr. Suresh Babu are

sincerely acknowledged for the technical assistance in SEM and FTIR studies. I am thankful to Dr. T.V. Anilkumar for providing training in confocal microscopy.

I owe a special sense of gratitude to Dr. P.V. Mohanan and the staff at Division of toxicology for all the support in in vivo experiments and Dr. A.C. Fernandez and his team at Division of Laboratory Animal sciences for the timely provision and maintenance of the experimental animals. Dr. Anoop Kumar and lab members of Molecular medicine are acknowledged for the help in gene expression studies.

My special thanks go to Ms. Sulekha baby for teaching me the techniques in histology and to my colleagues in the lab, Dr. Sabareeswaran, Ms. Neena Issac , Mr. Joseph Sebastian and Dr. Manjula James for their whole hearted support in my studies.

I treasure the invaluable friendship of Dr.P.R. Anilkumar whose encouragement at the needy times which I could never forget.

Heartfelt thanks to my seniors, Dr. Bernedette Madathil, Dr. Asha Mathew and my friends, Ms. Bindu S, Ms. Manitha B Nair, Ms. Viji Mary Varghese, Ms. Susan Mani, Ms. Lynda Thomas, Mr. Tilak Prasad, Mr. Rojan Jose and Mr. Anwar Azad for being there for me whenever there was a need.

Remembering with a thankful heart, my family, parents, husband and daughter, for their unfathomable support and understanding and for being with me through the thick and thin.

Above all, I bow my head before God, The Almighty, for the blessings showered on me…for all things I have and I don't…for helping me to reach the shore safely and successfully…

Josna Joseph

LIST OF FIGURES

LIST OF TABLES

ABBREVIATIONS

ATR	Attenuated total reflection
αSMA	alpha Smooth muscle actin
cDNA	complimentary deoxy nucleic acid
CSF	Cerebro spinal fluid
DAB	Di amino benzidine
dNTP	deoxy nucleotide triphosphate
DPX	Di-n-butyl phthalate in Xylene
ECM	Extra cellular matrix
ED-A	Extra type III domain- A
EDTA	Ethylenediaminetetraceticacid
Erk	Extra cellular signal regulated kinase
ETO	Ethylene tetroxide
FBS	Foetal bovine serum
FDA	Food and drug administration
FN	Fibronectin
GAPDH	Glyceraldehyde 3-phosphate dehydrogenase
HPLC	High pressure liquid chromatography
HRP	Horse radish peroxidase
ICAM	Inter cellular adhesion molecule
IFNγ	Interferonγ
IL-1β	Interleukin 1 beta
IL-10	Interleukin 10
IL-1α	Interleukin 1 alpha
IL-6	Interleukin 6
ISO	International standards organization
MRI	Magnetic resonance imaging
NK cells	Natural killer cells
NMR	Nucelar magnetic resonance

PCR	Polymerase chain reaction
PDGF	Platelet derived growth factor
PGE2	Prostaglandin E2
PMA	Phorbol myristyl acetate
PVDF	Polyvinylidenefluoride
RIPA	Radioimmunoprecipitation buffer
RT	Room temperature
SDS	Sodium Dodicyl Sulphide
SE	Silicone expander
SEM	Scanning electron microscopy
TBS	Tris buffered saline
TCPS	Tissue culture poly styrene
TEM	Transmission electron microscopy
TGFβ	Transforming growth factor beta
TIMP	Tissue inhibitor of matrix metalloproteinases
TMB	Tetra methyl benzidine
TNFα	Tumor necrosis factor alpha
UHMWPE	Ultra High molecular weight polyethylene
VCAM	Vascular cell adhesion molecule
VP shunt	Ventriculo peritoneal shunt

SYNOPSIS

Silicone is a widely used material in the manufacturing of different types of implants. One of the most important field of application is mammoplasty, for both post mastectomy reconstruction and cosmetic augmentation. There have been numerous reports of excessive fibrosis around such implants leading to contracture and severe pain. Although silicone was originally regarded as being inert in the human body, its polymeric and hydrophobic characteristics make it potentially immunogenic. Recent reports indicate that the rates of localized complications and repeat surgeries following breast implantation are high and the long term effects unknown. Fibrous tissue associated failure has also been reported around hydrocephalus shunts leading to failure of shunt function. Research initiatives in finding out the cause of failure of silicone breast implants have been mainly centred around immunological reactions to the silicone gel. There are only occasional reports of investigation into the cause of the excessive fibrosis and contracture.

Chapter 1 of the thesis introduces the topic of research. An overview of different types of biomaterials used as components of medical devices is presented with a description of the synthesis and chemical properties of silicone and structure of breast implants. The chapter details out the normal biological response seen around an implant and goes on to introduce the role of physical and various biological factors like cells and cytokines in the formation of fibrous capsule around the implant.

Chapter 2 reviews the scientific literature published in relation to clinical failure following long term residence in the human body. Earlier investigations were initially centered on systemic complications that arose from silicone implants which were generally related to either silicone gel bleed from the implant or migration of low molecular weight silicones that spalliate from the surface of silicone implant to distant organs like lymph node, spleen and liver. Various techniques has been employed to detect this leaching out of silicone to distant

organs. The most frequent local complication of silicone breast implants is capsular contraction, resulting in intense pain and distortion in shape of the implants. Many physical and biological factors are responsible for this fibrous capsule formation. Histopathological examination of dissected fibrous capsule has revealed the presence of immune cells like macrophages and lymphocytes, various adhesion molecules, ECM proteins and heat shock proteins. *In vitro* experiments have revealed engulfed released silicone particles by macrophages that are pivotal immune cells involved in inflammation. These activated cells can in turn produce fibrogenic cytokines that can activate fibroblasts to a more contractile phenotype called myofibroblasts which have been found in the fibrous capsule. Data published on the role of immune cell released cytokines in myofibroblast formation have been reviewed. An account of data published on molecular studies of fibrous capsule and the signaling pathways involved in fibroblast activation has been detailed in this chapter. The review ends with an update of various antifibrotic approaches adopted to prevent the formation of fibrous capsule around silicone implants.

However, most of the studies were done on clinically retrieved prosthesis and the results were inconclusive. Experimental studies have been few and mostly related to either material characteristics or tissue response to material. There is a lack of information regarding the role of various cytokines at tissue material interface and their role in the extensive fibrosis. In the present study we aim to study over a specified time period the interrelationship between immune cells around silicone implants, formation of myofibroblasts and collagen deposition in *in vivo* models. The study would also elucidate cytokines, proteins and signaling pathways involved in the fibrosis using *in vitro* models.

Chapter 3 describes in detail the materials used and methodology adopted in this work. The methodology is broadly categorized into three major divisions:

Phase 1 : *In vivo* implantation studies in rats and rabbits

Phase II : Role of macrophage-secreted product in fibroblast activation into myofibroblast

Phase III : Silicone degradation in Psuedo extracellular fluid and the silicone extract in material leachants on fibroblast to myofibroblast transition.

Commercially available Silicone expander material with Ultra high molecular weight polyethylene as the reference material were characterized for wettability. Both materials were implanted in gluteus maximus muscle of rats for studies over 6 months and in Para vertebral muscle in rabbits for studies over one year. Tissue response was studied using light microscopy and Transmission electron microscopy. Cells and cytokines in the fibrous capsule were identified by Immunohistochemistry and were qualitatively graded. Real time PCR quantification of selected profibrotic and antifibrotic cytokines present at tissue-material interface over three different time periods was carried out. Cell adhesion to material surface was examined by Scanning Electron Microscopy. Changes in material surface characteristics before and after implantation were studied by FTIR spectroscopy.

Similar evaluation was carried out in the long term rabbit animal model. SEM-EDAX and ICP-AES studies were done to detect the presence of silicone release products in the peri-implant tissue.

Cell-material interactions were studied using the immune cells, macrophages and T lymphocytes. *In vitro* study to find out whether cytokines released from macrophages on initial contact with material have any effect on transformation of fibroblasts to myofibroblasts was carried out. U937 monocytes were differentiated to macrophages by the addition of Phorbol-Myristyl –Acetate and grown over the surface of silicone material for various time periods and the released cytokines in the culture medium were analyzed by commercially available ELISA kits. RAW adherent macrophages were also seeded on material surface and expression profile of proinflammatory and profibrotic cytokines was studied. The role of cytokines expressed in the macrophage conditioned media on fibroblast transition was assessed by quantitative evaluation of the gene and protein expression of α-SMA in L929 fibroblasts.

The effect of T lymphocyte derived cytokine, IFNγ on fibroblast modulation was also studied in human lung fibroblasts.

An *in vitro* degradation study of silicone material was done in Pseudo extra cellular fluid based on ISO 10993-13 guidelines. In addition, to evaluate the role of silicone leachants on fibroblast modulation, the silicone extract was added in various concentrations to

L929fibroblasts for 24 hour and gene expression of SMA was analyzed.

Elucidation of key signaling molecules involved in fibroblast activation pathway was assessed in an *in vitro* model by a proteomic approach. Human lung fibroblasts was cultured on surface of material in presence of macrophage conditioned media for 24 hours. The cells were lysed and protein expression of Erk molecule and α-SMA was studied by western blot techniques.

A six months implantation study was also carried out with commercially available hydrocephalus shunt material made of silicone on rat models. As above, changes in material surface characteristics before and after implantation were studied by FTIR spectroscopy. Tissue response was assessed by light microscopy and immunohistochemistry.

Chapter 4 presents the results achieved from the experiments conducted and discusses these results with regard to scientific data previously published.

Histopathological examination showed that the initial acute inflammatory response around silicone tissue expander, hydrocephalus shunt material and UHMWPE resolved with time. But there was a distinct difference in fibrous capsule thickness between silicone and UHMWPE.This was substantiated by trichrome staining for collagen. Immunohistochemistry confirmed persistence of myofibroblasts and immune cells like macrophages and T lymphocytes around silicone when compared to UHMWPE. The cytokines expressed in initial time periods were TGFβ and TNFα where as IFNγ, IL6 and IL-10 expressed in later time periods. Real time RT-PCR quantitation of cytokines in peri-implant tissue showed expression of profibrotic and antifibrotic cytokines and persistence of myofibroblasts. Ultrastructural studies by transmission electron microscopy demonstrated cells with more intracytoplasmic bundles, fibronexuses and rough endoplasmic reticulum, indicative of myofibroblast transition. Cell adhesion to silicone material was less when compared to UHMWPE at all time periods as shown by Scanning Electron Microscopy. FTIR spectroscopy revealed only shift in peaks corresponding to aliphatic hydrocarbons and there was no change in major peaks before and after implantation.

Long term studies in rabbit also showed increased fibrous capsule formation around

silicone when compared to UHMWPE. Silicone, assessed by SEM-EDAX and ICP-AES, was detected only in insignificant levels in the fibrous capsule formed around the implant.
In vitro studies revealed that cellular response and in turn cytokine release differed from material to material depending on their surface as well as bulk properties. The cytokines mostly expressed in monocytes derived macrophages on material contact were IL-1β, IL-6 and TGFβ. RAW adherent macrophages on silicone material expressed pro inflammatory cytokines, TGFβ and IL-6 the latter being significantly higher. There was a difference in expression of α-SMA in L929 fibroblasts activated by macrophage conditioned media as compared to normal cells without any treatment. A notable finding was the absence of any significant changes in αSMA expression in L929 fibroblasts activated by IFNγ.

In vitro study to detect leachants from silicone demonstrated considerable release of silicone content into the extraction vehicle, Pseudo Extra cellular fluid. Also it was noted that expression of α-smooth muscle actin was significantly high in L929 fibroblasts activated by silicone extract at a concentration of 200ppm, thus confirming the role of silicone leachants in contraction of the thick fibrous capsule around the implant.

Erk, which is a key signaling molecule involved in TGFβ and IL-6 pathway was identified in human lung fibroblasts grown in presence of macrophage conditioned media. Macrophages through the various secreted cytokines trigger Erk pathway in fibroblasts which relate to high SMA expression indicative of fibroblast to myofibroblast transition.
Tissue response to Ventriculo- peritoneal shunt was similar to that of silicone tissue expander characteristic with thick fibrous capsule, persistence of immune cells and myofibroblasts. Cytokines prominently expressed were profibrotic TGFβ and antifibrotic IFNγ.

Chapter 5 summarizes the prominent findings in this study and concludes the thesis.
Data obtained from our study indicates the importance of the silicone shell itself in formation of a thick fibrous peri-implant capsule. A differential expression of cytokines ,with a shift from proinflammatory to profibrotic cytokines around silicone implant during the different phases of wound healing was seen. Role of T lymphocytes in fibrous tissue remodeling is evident from the mounting presence of IL-10. The role of the immune cell, macrophage and

its cytokines particularly TGFβ and IL-6 on fibroblast-myofibroblast transformation has also been elucidated. Continued release of leachants from silicone implant by spalliation into the surrounding milieu, stimulates macrophages to release fibrogenic cytokines that are involved in a thick fibrous capsule formation around the implant. The absence of a role of T lymphocytes in this sequence of events was noted in the absence of any stimulatory effect of IFN γ in fibroblast to myofibroblast transition. *In vitro* studies also emphasize the salient role of IL-6 as a prominent cytokine that decides the fate of wound healing around biomaterial. The effective monitoring of this cytokine levels in an experiment model will be an indicator of normal wound healing versus a chronic inflammatory condition.

There exists a dynamic cycle of silicone release, activation of macrophages, release of cytokines and increased collagen deposition along with formation of myofibroblasts. This provides a plausible mechanism behind long term failure of silicone implants due to peri-implant contracture leading to severe pain.

To summarize, this study throws light on role of material surface and leachants in the activation of monocytes and macrophages, release of cytokines, transformation of fibroblasts to myofibroblasts and collagen deposition in the extensive fibrosis around silicone implants leading to clinical contracture and pain. It also elucidates the importance of the cytokine, IL-6 in addition to TGFβ in the transition of fibroblasts to myofibroblasts.

The chapter ends with a brief note on the future direction in relation to this work. An extensive study regarding the role that each component in silicone leachant has on fibroblast modulation needs to be addressed. The signaling pathways and key molecules involved in the fibroblast activation and the role of cytokines other than TGFβ and IL-6 in the extensive fibrosis around implants should be investigated in depth.

The formation of extensive fibrosis around silicone implants that lead to capsular contracture and implant failure is a multifaceted problem in which several factors are engaged. Identification of molecule/s involved would aid in devising newer ways to prevent the occurrence of excessive fibrosis around otherwise useful silicone implants.

Chapter 1

INTRODUCTION

1.1. Implants in the human body

Within the last decade, there has been a tremendous increase in both the variety and the number of implants and biomaterials available for use in the human body. The aseptic surgical technique developed by Dr. J. Lister in the 1860s led to the use of materials as replacements of body parts. The earliest successful implants were metal bone plates introduced in 1886 to aid in long bone fractures (Hansmann H *et al.,* 1886). 'A surgical implant may be defined as a medical device made from one or more biomaterials that is inserted into the human body, where it is intended to remain for a significant period of time to perform a specific function'(Williams DF, 2000).

Implants could be classified based on their functions:
Those that:

a. Replace a damaged, diseased or worn out part of the anatomy. e.g.: total joint replacements.
b. Simulate a congenitally absent part of anatomy. e.g.: mammary or facial prosthesis.
c. Aid in the healing process of a tissue. e.g.: orthopedic fracture plates, temporary grafts used in the treatment of burns, surgical adhesives.
d. Correct some deformity produced either congenitally, traumatically or pathologically. e.g.: spinal plates and hydrocephalus tubes.
e. Rectify the mode of operation of an organ. e.g.: heart pace makers, eye lids and penile implants.

The materials used for developing body implants or interfaces are commonly called biomaterials. Biomaterials available today can be broadly classified into: polymers, metals, ceramics, composites and natural materials. The use of different types of polymers as components of medical devices has increased over the years.

1.2. Polymers

The true beginnings of polymer science dates back to the 1930s when the first commercial polymer, nylon, was made available as a suture material. Polymers have physical properties that most closely resemble those of soft tissues and therefore this class of materials is used extensively to replace the functions of soft tissues including skin, tendons, cartilage, vessel walls, lens, breast and bladder. A number of synthetic polymers like poly olefins, poly esters, poly urethanes, poly acrylates, poly sulfones, poly ethers and silicone rubbers find applications as biomaterials.

1.3. Silicones

Silicones became commercial products in the late 1940s after perfection of the Rochow method of synthesis. Silicone polymers range from low molecular weight silicones to large polymer chains with molecular weight of 30,000 Dalton. They are inert, inorganic compounds used as both explants and implants and can be prepared in many different forms ranging from hard rubber to liquid crystal. The various medical applications of silicone is represented in Table 1.

Silicone containing polymers are derived by reaction of elemental silicon with methyl chloride. This reaction forms dimethyl chlorosilane, which when hydrolyzed with water generates polydimethyl siloxane commonly known as silicone (Figure 1). This generates a high molecular weight gum that is mixed with the reinforcing filler, silica and cross-linked to form a stable polymer. Cross-linking is achieved by introduction of vinyl derivative chains of vinyl methyl siloxane or by incorporation of peroxides to cross-link via

a free radical mechanism. Polymer, reinforcing particles and cross-linking agents are mixed using a compounding mill consisting of two metal rollers that squeeze the material into a sheet. Materials after rolling can be screened to remove large particles. The final stock is then processed into final form by compression molding, transfer molding, extrusion, calendaring, dispersion coating, and hand lay-up.

Table1. Silicone Medical devices

Catheters	Heart valves
Hydrocephalus shunts	Pace maker tubing
Rhinoplatsy	Membrane for blood oxygenator
Scribner shunt for dialysis	Abdominal wall reconstruction
Dentures	Artificial testicles
Scleral implants	Vaginal reconstruction
Joint implants	Endo tracheal tubes
Packing for thoracic cavity	Breast augmentation

Silicone rubbers are classified mainly into:

1. High temperature vulcanizing (HTV) silicones, usually in a semi-solid gum form in the uncured state. They require processing to produce finished items.
2. Room temperature vulcanizing (RTV) silicones, which usually comes as flowable liquid, used for sealants, mould making, encapsulation and potting.
3. Liquid silicone Rubbers (LSR)

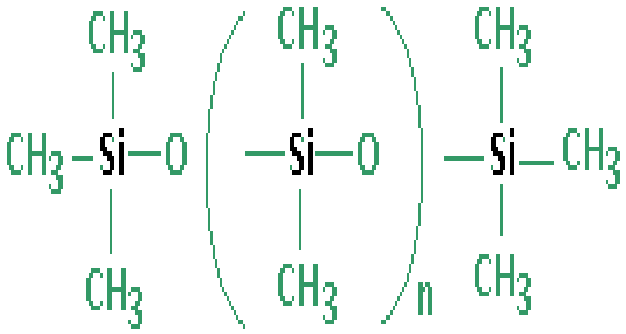

Figure 1. Polymeric backbone of poly dimethyl siloxane.

Silicone with its special properties like chemical inertness, thermal stability and resistance to oxidation, have wide applications in the biomedical field.

1.4. Silicone breast implants

In 1961, Thomas Cronin and Frank Gerow developed the first mammary prostheses by combining rubbery and liquid silicone to create a soft, firm gel that was wrapped in a silicone polymer. Breast implants are used for breast augmentation, breast reconstruction following mastectomy, or revision of an existing implant. Breast implants available today are either smooth gel-filled, textured gel-filled, polyurethane covered, saline-filled (Figure 2), of a double lumen or a permanent expander (Bondurant S *et al.*, 1999).

Figure 2.Silicone saline breast implant (www.wikipedia.org)

Silicones now represent the most widely used implantable synthetics. However, they are also the most controversial of the implantable materials. Although silicone was originally regarded as being inert in the human body, its polymeric and hydrophobic characteristics make it potentially immunogenic. Recent reports indicate that the rates of localized complications and repeat surgeries following breast implantation are high with patients developing clinical symptoms in later periods (Shanklin DR *et al.*, 1996). In addition to the local phenomena, several case reports of systemic connective tissue diseases have been published (Baldwin CM *et al.*, 1983, Brozena SJ *et al.*, 1988**).** As a result, in 1992 FDA banned gel filled implants for general use except for patients undergoing breast reconstruction after therapeutic mastectomy, until additional studies were conducted and a more definitive conclusion regarding the safety of implants was reached (Kessler DA , 1992).

Silicone breast implant complications can be divided into two categories: local chest wall complications and more generalized systemic problems. Local complications include capsular contracture or the tightening of scar capsule around the implant, mal position and rupture or leakage of the implant.

Capsular contracture is much less common and less severe with saline implants than with silicone gel implants. The causes of the capsule formation have not yet been fully explained. Various theories have been formulated, according to which, characteristics of the prosthesis, such as impurities in the polymer, hydrophobicity, contamination before implantation and gel bleed are the main responsible factors. The silicone based compounds contained in the breast implant includes silica, various silicone polymers and cyclic siloxanes. All of these materials have been implicated as potential sources of inflammation *in vivo* which ultimately lead to implant failure (Picha GJ *et al.,* 1990). In addition to these, the biological mechanisms leading to the formation of excessive fibrous tissue are also considered.

1.5. Hydrocephalus shunts

Another silicone implant which is widely used and was reported of fibrous tissue associated failure is hydrocephalus shunts (Figure 3). Hydrocephalus occurs in approximately 50 out of every 10,000 children born alive (Fernell E *et al.,* 1986). It occurs if there is a mismatch between the CSF production and the absorption. Hydrocephalus treatment is surgical. It involves the placement of a ventricular catheter into the cerebral ventricles to bypass the flow obstruction/malfunctioning arachnoidal granulations and drain the excess fluid into other body cavities like peritoneal cavity (ventriculo-peritoneal shunt) right atrium (ventriculo-atrial shunt), pleural cavity (ventriculo-pleural shunt) and gallbladder from where it can be resorbed .

Although CSF shunt systems are effective in treating hydrocephalus, shunt dysfunction is a common problem. Recent trials estimated the failure rate for all implanted shunts to be 40–50% during the first two years after surgery (Browd SR *et al*., 2006*b*).

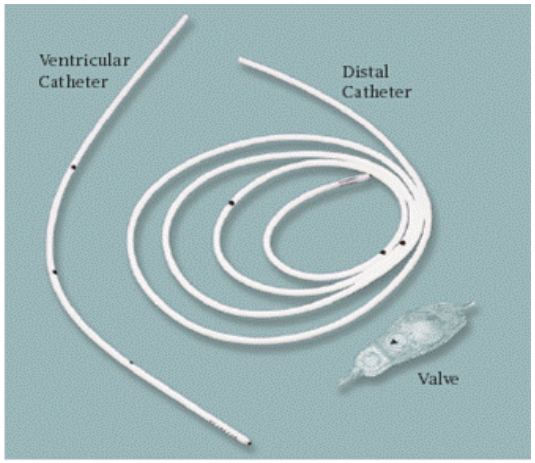

Figure 3. Hydrocephalus shunt (http://images.google.co.in.)

Complications are due to obstruction due to excessive fibrosis at the distal end, mechanical failure, infection or excess drainage (Kalousdian S *et al*., 1998; Sgouros S *et al*., 2004, Browd SR *et al*., 2006*a*). Shunt obstructions and infections often occur soon after implantation, 11 months on average, while mechanical complications can occur years later, 90 months on average (Boch AL *et al*., 1998).

1.6. Tissue - biomaterial interaction

Biomaterial science involves or encompasses surgical implants and medical devices and their interaction with the tissues they contact. Good biocompatibility is achieved when the material exists within a living body without causing adverse reactions or being affected by it. Thus biomaterials must be compatible with body tissues mechanically, chemically as well as pharmacologically. Their study therefore includes physical and chemical properties of component materials and those of tissues into which they are implanted. The form, structure, texture, rigidity or flexibility of the implant plays a fundamental role in eliciting tissue response to the material.

One of the characteristics of living tissue is its ability to respond to injury. This response is primarily one of inflammation followed by repair and is complex. Implantation of a prosthesis essentially initiates the same pathway of inflammation followed by repair. An interface is created between damaged tissue, blood and exudates which is rich in active molecules like proteins. These proteins are immediately adsorbed on to the surface of

implant and concomitantly, an inflammatory reaction is triggered off with vascular, cellular and humoral responses. Following this, aggregates of inflammatory cells like neutrophils, lymphocytes and macrophages, form at implant site. The end phase of healing around the implant is the collagen laid down by activated fibroblasts leading to the formation of a fibrous capsule around the implant. The response of tissues at implant site involves a myriad of mediators including chemotactic substances and growth factors that modulate cell function such as activation, proliferation, and protein production.

Thus the inflammatory response plays a pivotal role in the biocompatibility of a material considered as a foreign body. In addition to the initial injury induced by the introduction of material into a living system, the persistent presence of the foreign material in contact with living tissue induces an inflammatory response which can remain local, benign and short, or can become systemic, persistent and health threatening.

1.7. Fibroblast response to implants

As part of tissue response to the process of implantation of a material into the body, fibroblasts are activated. There is a transition of quiescent cells into proliferative and fibrogenic cellular elements. The early event in fibroblast cell activation is 'initiation', which includes rapid changes in gene expression and phenotype that renders the cells responsive to cytokines and other local stimuli (Petillo O *et al.,* 2002). Fibroblast invasion into granulation tissue surrounding the implant is mediated by numerous molecules including growth factor, chemotactic cytokines, and matrix components. Enzymes such as neutral proteinases, plasminogen activators, collagenases and elastases produced by macrophages may influence the fibrogenic response to polymers by regulating the extracellular environment and remodeling the connective tissue. The net balance between production of growth promoting factors and destructive proteolytic factors should be viewed as an extremely delicate balance that could favor fibrous capsule formation or degradation.

Up regulation of collagen synthesis during activation is the most striking molecular response of fibroblast to biomaterial and is mediated by several factors including TGFβ (Lin

PH *et al.*,1997). Granulation-fibrous tissue and scar tissue formation are reflective of excess collagen deposition, the biomechanical properties of which are determined by the quantity of the specific biomaterial and components of the extracellular matrix. The understanding of mechano-chemical interrelations is necessary to determine all measures providing control of implant functioning in the body. These include quantitative analysis of connective tissues like collagen, glycosaminoglycans, glycoproteins and their metabolic activity.

During resolution phase of wound healing the activated fibroblast may revert to a quiescent state under the influence of anti inflammatory cytokines like IL-10, which provides a negative fibrogenic signal to limit scar accumulation (Petillo O *et al.,* 2002). Excessive fibrosis and scar tissue formation on the other hand are end results of imbalance in the levels of pro-inflammatory and anti inflammatory cytokines.

The evaluation of the levels of fibrogenic cytokines with studies aimed at the characterization of the peri prosthetic tissue, represents the natural evolution of fibrosis around implants. The activation and cell communication can be observed utilizing *in vitro* methods such as cell culture systems.

1.8. Cytokines as master regulators

Cytokines are a group of usually short range protein mediators which have important roles in the development, function and control of cells of the immune and hematopoeitic systems. The foreign body response to implanted biomedical devices and prostheses is guided by leukocyte-derived cytokines. Adherent monocytes/macrophages secrete cytokines in response to the implant, that direct the recruitment of more leukocytes and other cell types, including fibroblasts to the tissue/material interface. The non adherent cells present within the exudates surrounding the implant such as neutrophils, monocytes and lymphocytes also secrete cytokines that direct leucocyte chemotaxis and activation as well as the activities of the biomaterial adherent leuckocyte population.

The types and levels of cytokines surrounding an implanted device initially drive the acute and chronic inflammatory reactions and later initiate the wound healing response

while inflammation resolves. When describing the foreign body response to implanted materials, cytokines are classified as being either pro-inflammatory or pro-wound healing depending on which events they promote. In addition to deciding the fate of implanted devices or prostheses by guiding the foreign body response, cytokines present in the local milieu dictate macrophage super oxide generation and fusion into Foreign Body Giant Cells (FBGC) contributing to the failure of the implant.

1.9. Myofibroblasts

The fibroblasts present in a wound area turn into specialized forms of fibroblasts termed myofibroblasts. Myofibroblasts are thought to be an intermediate cell between fibroblasts and smooth muscle cells. They are key cells for the connective tissue remodeling that takes place during wound healing and fibrosis development. Activation of fibroblast into myofibroblast is characterized by development of intra cytoplasmic stress fibers that confer to these cells the capacity of developing tension. The most important marker of fibroblast to myofibroblast phenotypic transition is the de novo expression of αSMA. The work of several laboratories has demonstrated that the induction of the myofibroblastic phenotype requires the concerted action of growth factors such as $TGF\beta_{1,}$ specialized ECM molecules such as fibronectin splice variant ED-A and a mechanically stressed environment (Desmouliere A *et al.,* 2005, Hinz B *et al.,* 2003). With return of wound site to normal architecture during the resolution phase, these myofibroblasts undergo apoptosis (Desmouliere A *et al.*, 1995). This process is lacking during the onset of fibro contractive diseases, where the persistence of cell contractile activity leads to continuous matrix remodeling and retraction. Figure 4 illustrates the various cytokines and growth factors that play a role in fibroblast modulation.

1.10. Pathobiology of fibrous capsule around silicone implants

The pathological examination of the scar capsules surrounding silicone gel implants which have been removed due to severe pain, often show macrophages filled with vacuolated or foamy material, silicone gel. This is due to gel bleed from the implant

presumed to occur to some extent in all such implants. In addition to macrophages, strong T cell responses has been observed in correlation with lymphocytic infiltration and the subsequent granuloma development. Studies have revealed that 95% of the lymphocytes in peri prosthetic capsules were T cells, and T cell memory for silicones was demonstrated in breast implant patients (Shanklin DR et al., 1999).

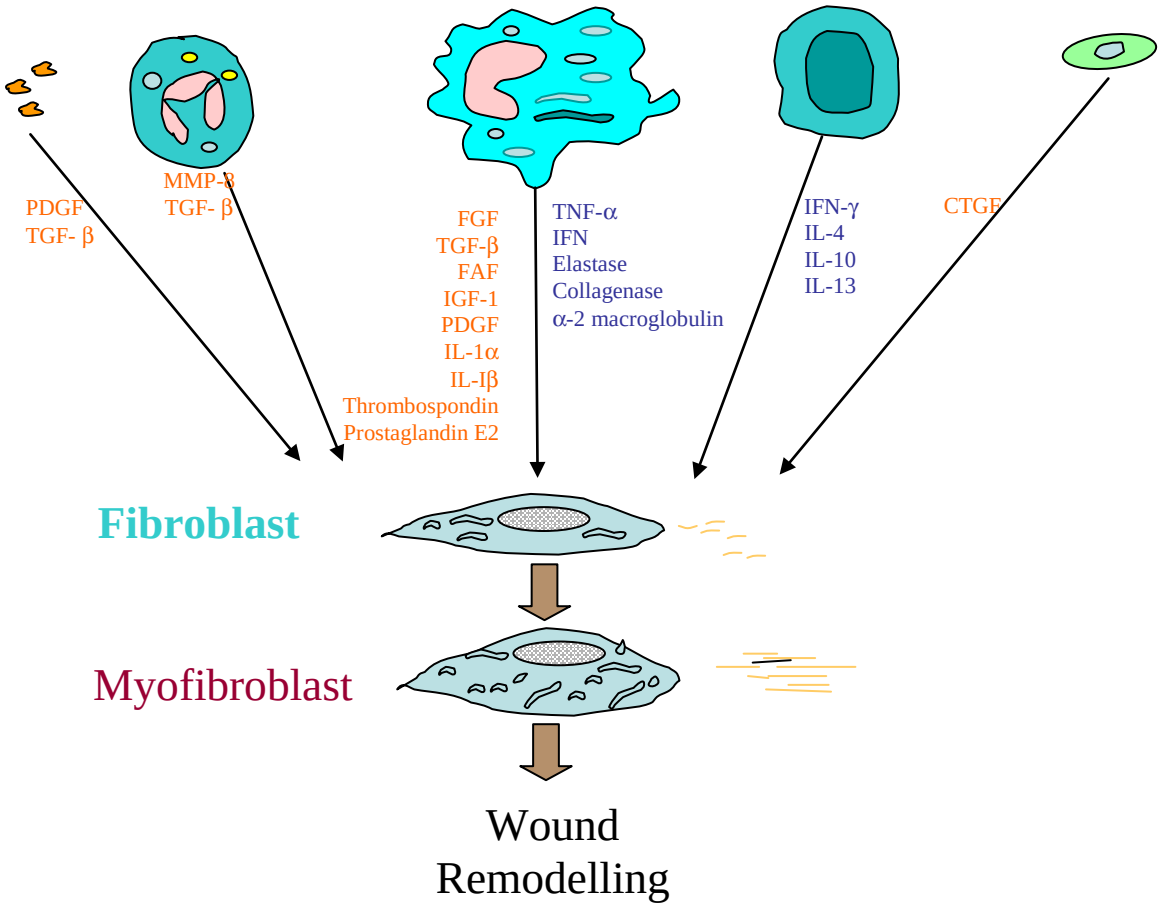

Figure 4. Growth factors and cytokines involved in fibroblast to myofibroblast transformation

The degree of fibrosis is less for silicone polymer sheath than for silicone gels. The mechanism according to which the formation of a capsule around the prosthesis occurs in 30%-50% of mammary implants is still unknown. It was hypothesized that the early stage of

capsule development was characterized by acute inflammatory reaction involving cell mediated immunity.

Silicone can diffuse through the shell of the implant and is then phagocytized by macrophages present in the surrounding tissue. The ingestion of silicone particles by the macrophages induces a state of activation leading to the release of cytokines with high fibrogenic activity. This process is thought to trigger fibroblast proliferation and capsule formation around the implant. Moreover, chronic inflammation such as a foreign body reaction and silicone granulomas will develop. Also macrophages can degrade silicone *in vivo*, and hydrolyzed silicone compounds as well as silica can be formed (Kossovsky N *et al.,* 1995). It was reported that silicone can be transported via macrophages to various organs through the blood (Flassbeck D *et al.,* 2001) and the released silicone particles from the implant can interact with the immune system possibly by linking to carrier proteins and behaving as haptens.

A major unanswered question is whether local inflammatory and hyper plastic cellular reactions are silicone-specific, ie caused by specific components, additives, degradation products unique to silicone or whether these responses reflect a non specific Foreign Body reaction (FBR). Another question that need to be addressed is can the body react to silicone shell or is it only the silicone gel associated with an immune reaction? During the 1990s, saline filled implants received less analytical attention than those filled with silicone gel. Recent studies focus on reasons of failure of these devices. Silica has been reported in the lymph nodes in saline implant patients. The silastic envelope of saline implants and tissue expanders is also a silicone polymer that may breakdown in the body into silica, possibly eliciting an immune response (Weinzweig J *et al*., 1998).

Future development of devices relies to a large extent on the in depth study of retrieved failed implants after long term residence in the human body. Such studies include detailed study of the material components of the implant and histological and molecular evaluation of adjacent tissue.

Tissue expanders made of silicone have been implanted in an animal model. The study focuses on the different type of cells and their cytokines present at the interface over a long term period of implantation. Methods of investigation include histological techniques

and immunohistochemical identification of cells and cytokines. Molecular techniques have been used to elucidate fibroblast to myofibroblast transformation and gene expression pattern of selected cytokines over specific time periods. The up regulation of signaling molecules in this transformation were studied in an *in vitro* model.

This thesis is an investigative study of cell- material interactions at the interface of silicone implants with adjacent tissue.

Chapter 2

REVIEW OF LITERATURE

Biomaterial Science is concerned with surgical implants and medical devices and the interaction with the tissues they contact (Ducheyne P *et al.,* 1984). The materials used for developing body implants or interfaces are commonly called biomaterials. The first clinical application of a "biomaterial' dates back to 1759 when Halowell united the edges of a lacerated brachial artery using a wooden peg and twisted thread (Wesolowski SA *et al.,* 1963). A biomaterial is defined as 'a material intended to interface with biological systems to evaluate, treat, augment or replace any tissue, organ or function of the body' (Williams DF, 1999). The various biomaterials used as part of medical devices is illustrated in Table 2.

Table 2: Biomaterials for use in the human body (Adapted and modified from Sujata VB, 2002)

Polymers	Metals	Ceramics	Hydrogels
Polyolefins Polyesters Polyamides Polyurethane Polyacetals Polyether Silicone Rubber	Co-Cr alloys Titanium Platinum Aluminium Nitinol Stainless steel	Alumina Zirconia Hydroxyapatite Calcium PO4	Polyvinylalcohol Poly ethylene glycol Poly hydroxy ethyl methacrylate Poly vinyl pyrrolidone

2.1. Polymeric biomaterial

The 1930's witnessed the use of polymers in a variety of reconstructive applications. Medical applications of polymers fall into three major categories: (a) extracorporeal devices such as catheters, tubings, blood and urine bags, blood oxygenators, dialysis membranes, wound dressings, artificial limbs and contact lenses, (b) implanted devices such as heart valves, pace makers, intraocular lenses, maxillo-facial and mammary prosthesis, drug delivery implants, hip and knee joints and dental devices and (c) temporary implants such as degradable sutures, polymer scaffolds for tissue engineering, temporary bone and tissue fixation devices (Dumitru S, 2002).

2.2. Silicone as a biomaterial

Silicone is a widely used material in the manufacturing of different types of implants. At the time of world war II, Silicone in liquid form was used for breast augmentation in Japan. In 1955, Holter developed a ventriculo peritoneal shunt made of silicone for drainage of excessive fluid in hydrocephalic patients. This was followed in 1959 when De Niola was credited with the first implantation of silicone when he replaced a urethra with silicone rubber tubing (Lopez GP *et al*., 1992).

In 1961, Cronin and Gerow developed the first mammary prosthesis by combining rubbery and liquid silicone to create a soft, firm gel that was wrapped in a silicone polymer. It is this elastomer form that has been further utilized in the development of tubes, catheters, valves, clips, prostheses, artificial tendons, intra ocular lenses and blood tubing (Loh IH *et al*, 1992). Silicone foam was used for mammary augmentation in 1963 by Demergeian. This was followed in 1965, when silicone rubber rods were first used as finger joint prostheses (Friedman DW *et al*., 1994). Additionally, during this period, silicone ball and cage model heart valves were introduced to market (Sefton MV e*t al*., 1987)**.**

2.3. Silicone breast implants

Silicone breast implants have been available commercially since the early 1960s. Breast implants are surgically implanted either under the breast tissue (sub glandular) or under the muscle (sub muscular) to enlarge the breast for cosmetic reasons or to reconstruct the breast after mastectomy or breast injury (Arepalli SR *et al.*, 2002). There are two primary types of breast implants: saline-filled and silicone-gel-filled implants. Saline implants have a silicone elastomer shell filled with sterile saline liquid. These implants were first manufactured in France in 1964, introduced by Arion with the goal of being surgically placed via smaller incisions (Arion HG, 1965). Silicone gel implants have a silicone shell filled with a viscous silicone gel. There have been several alternative types of breast implants that were developed, such as those filled with polypropylene string or soy oil.

2.4. Complications associated with silicone breast implants

The past decade has witnessed many controversies concerning the safety of the use of silicone gel as a filling material for breast implants. These concerns included the possibility of triggering cancer, the incidence of local complications and systemic immunological effects such as connective tissue disease. Prospective studies of saline-filled breast implants showed rupture/deflation rates of 3-5% at 3 years and 7-10% at 5 years for augmentation patients (FDA handbook, 2004). The silicone breast implant crisis led to the FDA ban of its use in 1992 (Kessler DA, 1992). Silicone breast implant complications can be divided into two categories: local chest wall complications and more generalized systemic problems.

2.4.1. Systemic effects

The majority of controversy regarding silicone implants centers around the relationship of these implants to systemic diseases. A variety of rheumatic diseases including chronic arthropathy, systemic sclerosis, rheumatoid arthritis, Systemic Lupus Erythematosus, fibromyalgia, Human adjuvant disease and Sjogren's syndrome have been reported in

patients with silicone gel breast implants (Baldwin CM *et al.,* 1983, Bronzena SJ *et al., 1988*, Endo LP *et al.,* 1987, Silver RM *et al., 1993*, Kumagai YA *et al.,* 1979, Brown SL *et al., 2002*, Celli B *et al., 1978*)**.**

There were reports stating that silicone implants could trigger humoral immunity. Kossovsky *et al.* claimed that a subpopulation of silicone breast implanted women developed antibodies to laminin and fibronectin, but this was not seen in the sera of healthy women with various rheumatic diseases (Kossovsky N *et al.,* 1994). A study of forty individuals who underwent silicone breast augmentation for more than ten years indicated abnormalities in T helper/suppressor ratio, increased autoimmunity and increased production of immune complexes (Vojdani A *et al,* 1992). Standard lymphocyte stimulation test performed on implant patients by Shanklin *et al.* showed increased T cell stimulation (Shanklin DR *et al.,* 1996). A new term, 'Siliconosis' was put forward to indicate the disease that occurs after exposure to or implantation of silicone devices. It manifests as atypical connective tissue disease with features similar to auto immune diseases but can be distinguished by specificity of cellular immune responses to silicone and silica.

On the contrary, studies by de Jong *et al.* and Bente *et al.* reported that long term exposure to silicone breast implants do not induce anti polymer antibodies in the sera (de Jong WH *et al.,* 2004, Bente J *et al.,* 2004). This finding corroborated with Holmich *et al.* who pointed out through their study that there is no association between silicone implant rupture and connective tissue disease or rheumatic conditions, except for an excess capsular contracture (Holmich LR *et al.,* 2003).

2.4.2. Local effects

Local complications associated with silicone implants include capsular contracture or tightening of scar capsule around the implant, mal position, rupture and leakage of implant. The most frequent local complication is capsular contraction, which can be seen up to 40% of patients (Friemann J *et al.,* 1997). This results in intense pain and distortion in the shape of implants. Capsular contracture is most often clinically evaluated by Baker's classification depending on the external symptoms and is depicted below in Table 3.

Table 3: Baker's Classification of breast implant failure

Grade 1	Breast normal, soft and look natural
Grade II	Breast little firm, but look natural
Grade III	Breast firm and distorted in shape
Grade IV	Breast hard and distorted. Pain and discomfort

In spite of all the various studies, the exact reason behind the development of a fibrous capsule around the implant is still an enigma.

2.5. Silicone bleed detection

Silicone from implanted breast prostheses leak through the intact membrane. Pfielderer *et al.* have revealed the presence of silicone in peri-implant capsule and in distant organs like liver and spleen in animals with silicone implants after 10-12 months of implantation (Pfielderer B *et al.*, 1995). In order to determine the exact location and to achieve a semi quantitative estimation of the amount of silicone in the surrounding tissue, a method involving scanning electron microscopy (SEM) and energy dispersive analysis of X-ray (EDAX) was used (Winding *et al.*,1988). By this method they were able to demonstrate the presence of the element silicon (Si), a polymer with a general formula (CH3 [Si (CH3)2O]n Si(CH3)3 along the inner border of vacuoles in the fibrous capsule corresponding to the light microscopic localization of silicone droplets and in macrophages. The tissue adjacent to the prostheses had a higher silicon content than the control tissue. The most specific non-invasive test to diagnose intra and extra capsular implant rupture is magnetic resonance imaging (Gorczyca DP *et al*., 1994). Also NMR spectroscopy can detect silicone presence in organs like liver (Pfleiderer B *et al*., 1995). Rudolph *et al.* have reported that even though silicone was identified by X-ray analysis in the surrounding tissue of implant, it was unrelated to clinical hardness of breast evaluated according to baker's scale (Rudolph R *et al*., 1978).

2.6. Biological response to silicone implants

In contrast to early presumption that silicone is inert, Kossovsky *et al.* suggested the bioactivity theory in 1995 which states that silicones interact with their biological environment, perturb that environment and are acted upon by that environment (Kossovsky N *et al.*, 1995). The biological response to silicone is controlled by : the chemistry of the silicone, the chemistry of additives and fillers such as silicone dioxide, the physical state of the silicone, oil, gel or rubber, specific inflammatory and immune features of a species or individual, and the chemistry and composition of the adsorbed surface film of macromolecules. The adsorption of macromolecules to silicone surface is in turn governed by three physicochemical processes: the interactions of charged groups, dehydration effects and thermal stability (Norde W *et al*., 1992). Experiments show that low energy (hydrophobic) surfaces deposit more proteins than high energy (hydrophilic) surfaces (Benesch J *et al.*, 2000). Also Spilizewski *et al.* have showed that cell adhesion was more to Poly Dimethyl Siloxane than low density polyethylene (Spilizewski KL *et al*., 1987).

The response of the host to silicone implants is similar to a Foreign Body Reaction. Intra corporally implanted medical devices will provoke the body to initiate an inflammatory reaction called Foreign body reaction. The progression of fibroblast modulation is regulated by soluble mediators such as cytokines, chemokines and matrix metalloproteinases which are locally produced by tissue cells and infiltrating inflammatory cells. The cellular processes that are involved in fibroblasts are cellular activation, angiogenesis, extravasation, migration, phagocytosis and finally fibrosis (Luttikuzhen DT *et al.*, 2006). The end stage of healing response to biomaterials is fibrosis or fibrous encapsulation which is the formation of a dense connective tissue scar. The net balance between production of growth promoting factors and destructive proteolytic factors should be viewed as an extremely delicate balance that could favour fibrous capsule formation and/or degradation. While some degree of fibroblast contraction is necessary for wound closure, excessive proliferation may lead to scar tissue formation.

2.7. Hydrocephalus shunts and shunt obstruction

Hydrocephalus is a condition in which excessive accumulation of cerebrospinal fluid (CSF) in the brain increases intracranial pressure. The most common and effective treatment of hydrocephalus is the CSF shunt system, which has been used for over 50 years (VandeVord PJ *et al*., 2004). These shunts relieve pressure by draining excess CSF from the cerebral ventricles or sub arachnoid spaces into a less constrained area of the body, such as the peritoneal cavity or the right atrium of the heart (Bayston R *et al*., 2004).

The CSF shunts typically consist of a proximal catheter, which runs from the cerebral ventricles' sub arachnoid spaces to a valve that connects to a distal catheter and regulates the drainage of CSF. The distal catheter is a long thin silicone tube that is placed subcutaneously and terminates in a distal body cavity where the CSF can be reabsorbed into the body (Garton HJ *et al.,* 2004, Browd SR *et al*. 2006*a*; de Aquino HB *et al*. 2006). CSF shunt devices are manufactured almost solely from medical grade silicone, owing to its chemical stability, minimal biological reactivity, low toxicity and non carcinogenicity (Agnew WF *et al*., 1962). The most common CSF shunt complication is obstruction, affecting 40% of shunts during the first year after implantation and 80% within 10 years (Sgouros S *et al.*, 2004). Shunt obstruction caused by tissue in growth through the drain holes has been widely reported, and choroid plexus and glial tissue account for the majority of offending tissues (Collins P *et al*. 1978; Del Bigio MR *et al.*1992). Inflammatory tissue response to implanted shunts also contributes to the catheter obstruction (Sekhar LN *et al*. 1982; Del Bigio MR 1998). The obstructed catheters are often associated with acute and chronic inflammatory cell infiltrate and multinucleate foreign body giant cells (Schmidt S *et al*., 1993).

2.8. Factors affecting capsule formation

2.8.1. Physical factors

Many factors contribute to the biological response to implanted materials that are related to the surface chemistry, size, shape, site of implantation and duration of the

implant material in humans and in animal models (Lord GH, 1986). Characteristics of the prosthesis, such as the impurities in the polymer, silicone hydrophobicity, contamination before implantation, and silicone bleed are the other main factors responsible for capsule formation (Granchi D *et al*.**,** 1995). Piccha *et al.* have showed that the polymer's molecular weight influences its migration, encapsulation, intensity of cellular response and the degree of fibrosis is less for Silicone oil than the Silicone gel and solid polymer sheath (Picha GJ *et al*., 1990).

But there was contradictory reports by Bonfield that fibrous tissue encapsulation is determined by complex interactions which occur among the polymer, protein and surrounding tissue and no predominant effect by polymer or protein is present (Bonfield TL *et al*., 1992).

Most studies have also shown a higher frequency of capsular contracture for smooth implants than for implants with textured surfaces (Coleman DJ *et al*., 1991) whereas inflammatory response was significantly high in textured implants rather than smooth silicone implants (Bucky LP *et al.***,** 1995).

The risk of implant rupture increases with implant age. Studies in animal model have shown that capsule forms in a relatively short time of two months (Picha GJ *et al*., 1990). Most of the implants rupture between the third and tenth year of implantation (Holmich LR *et al*., 2003). It was observed that the contractile ability of tissue expander implants decreased with the time since expander insertion and increased with expander exposure, peri-expander infection and clinical evidence of adverse capsular contracture (Coleman DJ et al., 1993).

2.8.2. Biological factors

Histological examination of explanted capsules vary from densely fibrotic, acellular specimens to those showing intense inflammation with activated macrophages, multinucleated giant cells and lymphocytic infiltrates (Hanlon TPO' *et al.,* 1996). Another group, Wells *et al.* have also reported that the infiltrating cells in capsular tissue were primarily macrophages and lymphocytes (Wells AF *et al.,* 1994)**.** Legrand *et al.* have carried out a detailed study regarding the structure of fibrous capsule that forms around silicone

implants (Legrand AP *et al*., 2005). They could find an:1) hypo/acellular interface layer of thick collagen fibres, 2) hyper cellular interface layer with vascularisation and an 3) outer capsule with synovial metaplasia of the interface layer. It was reported that there was a significant positive correlation between capsule thickness, presence of chronic inflammation and macrophage presence (Eltze E *et al.*, 2003) whereas Gayou *et al.* observed that capsule contracture is not directly related to capsule thickness (Gayou R *et al.*, 1979).

The silicone escaping from prosthesis was found extra cellularly as silicone droplets among collagen fibres and intra cellularly as micronized silicone in cytoplasm of foamy cells, macrophages and giant cells**.** Mancino *et al.* suggest that diffused silicone particles from implant can interact with the immune system possibly by linking to carrier proteins and behave as haptens (Mancino D *et al.*, 1984). This diffused silicone is ingested by the macrophage inducing a state of activation leading to the release of cytokines with high fibrogenic activity. Macrophages can degrade silicone *in vivo*, and hydrolysed silicone compounds as well as coordinated silicon complexes and silica can be formed (Eltze E *et al*., 2003). These macrophages can also transport silicone to various organs through the blood (Flassbeck D *et al*., 2001).

The role of T cells in immune response to silicone implants has also been studied by various groups. T cell activation around silicone implants occurs as early as 1 year after implantation and can persist for as long as nine years (Katzin WE *et al.***,** 1996**)**. Peri-implant connective tissue capsule may represent a possible site of antigen processing and presentation (Millonig G *et al.*, 2001). Granchi *et al.* observed an increase in cells with phenotype CD57+, an antigen occurring on natural killer cells and CD8 cytotoxic/suppressor T lymphocytes in patients with capsule contracture≥3 of the baker scale (Granchi D et al.,1995). The cellular and molecular composition of fibrous capsules removed from patients at various times after surgery due to breast cancer relapse or to relieve painful constrictive fibrosis have been analyzed by Dolores *et al.* (Dolores W *et al.*, 2004)**.** They found aggregates of CD25 expressing T lymphocytes in the capsular tissue, near to blood vessels and suggest the possibility of migration of these activated lymphocytes to the main blood stream and causation of systemic side effects correlated with silicone breast implants. They

concluded that activated lymphocytes possibly react with silicone itself, against composite neo epitopes, cryptic epitopes or altered self-proteins. In addition to macrophages and lymphocytes, Rudolph *et al.* found contractile fibroblast in fibrous tissue capsules around silicone breast implants (Rudolph R *et al*., 1978).

2.9. Myofibroblasts

Myofibroblasts are specialized fibroblasts that are transiently involved in wound healing process. These cells exert contractile forces to nearby ECM and deposit collagen at wound site. They are intermediate between fibroblast and smooth muscle cell (Phan SH, 2002).

Myofibroblasts, the hallmark of fibrotic diseases, contribute to pathology of fibrosis by secreting large amounts of ECM. Myofibroblast markers are αSMA, vimentin , cytokeratin, prolyl-4-hydroxylase , SM-myosin, SM22 and caldesmon. The main features for defining myofibroblast are abundant rough endoplasmic reticulum; modestly developed myofilaments with focal densities, fibronexus junctions, vimentin and αSMA staining (Eyden B, 2003). Histological features include a plump-spindle-cell morphology with an ill defined cytoplasm paler and less fibrillar than smooth muscle cells.

Fibroblasts modulate into myofibroblast through a process regulated by cytokines such as TGFβ1 and ECM molecules such as cellular fibronectin splice variant ED-A and a mechanically stressed environment. Hinz *et al.* reported that granulation tissue subjected to mechanical tension expressed αSMA more earlier than control tissue (Hinz B *et al.*, 2003). The most important marker of fibroblast to myofibroblast transition is the *de novo* expression of αSMA, which is essential for the highly contractile activity of myofibroblast. They develop complex adhesion structures with the ECM, called “Fibronexus”, which is thought to be important for the efficient transmission of contractile force to the ECM to promote wound contraction.

The occurrence, structure and contractility of myofibroblasts in the capsules around tissue expanders and static implants have been studied in the rat, pig and humans. The

capsules showed a characteristic layered structure with myofibroblasts being the predominant cell type (Coleman DJ *et al*., 1993).

Myofibroblasts disappear massively through apoptosis when the epithelial layer is reconstituted in wound area. This process is lacking during the formation of hypertrophic scars or on the onset of fibrocontractive diseases (Desmouliere A *et al.*, 1995). Laitung *et al.* observed that low capsular contracture rate around tissue expanding devices is paradoxical to the increased cellularity of myofibroblasts in the fibrous capsule around the implant. Their presumption is that these myofibroblast ungerdo modulation, once the expansion process has ceased (Laitung JK *et al*., 1987).

2.10. Role of cytokines in fibroblast to myofibroblast transition

Cytokines can be either pro-inflammatory or anti-inflammatory and act via. autocrine or paracrine function. Brodbeck *et al.* have classified cytokines as either pro/anti inflammatory/wound healing as in Table 4 (Brodbeck WG *et al.*, 2003).

Table 4: **Classification of cytokines involved in inflammation and wound healing**

Wound Healing			
	Pro	IL-1ra TGFβ IL-4 IL-13	IL-1β
	Anti	IL-10	TNFα IL-6 IL-8 IL-2
Inflammation			

Several cytokines are involved in the modulation of myofibroblasts. These include

TGFβ (Desmouliere A *et al.*, 1993), PDGF (Denel TF *et al.*, 1991), IFNγ (Desmouliere A *et al.*, 1992a), IL-6 (Gallucci RM *et al*., 2006), extracellular matrix components such as heparin, fibronectin ED-A (Dugina V *et al*., 2001, Serini D *et al*., 1998) and tenascin. These are produced mostly by macrophages and also by lymphocytes, endothelial cells and fibroblast. Fibroblasts and myofibroblasts respond differently to these cytokines according to their stage of differentiation during wound healing (Moulin V *et al*., 1998)**.**

TGFβ is a profibrotic cytokine that induces myofibroblast transition *in vivo* and *in vitro*. There is a large body of evidence indicating that myofibroblasts are induced by autocrine / paracrine TGFβ1stimulation. Up regulation of collagen synthesis during activation is among the most striking molecular responses of fibroblast to biomaterial and is mediated by both transcriptional and post transcriptional mechanisms, not all of which can be ascribed to TGFβ1 (Petillo O *et al*., 2002)**.**

IL-1 has been reported as a prominent regulatory molecule of fibroblast activity. it induces the fibroblast to synthesize collagen and also has been shown to stimulate collagenase production by cultured fibroblasts (Postlethwaite AE *et al.*, 1988). Besides its role on fibroblast proliferation, it also stimulates the helper lymphocytes to produce more cytokines, such as IL-2 and IFNγ. These functions of IL-1 implicate, its role as a regulatory factor determining the extent of fibrous hyperplasia at tissue-implant interfaces (Bonfield TL *et al.*, 1992). There is another report that activated fibroblast can revert to quiescent state and IL-1 may control this response. IL-1 cytokine down regulate inflammation and increase interstitial collagenase activity while it provides a fibrogenic negative signal to limit scar accumulation (Petillo O *et al.*, 2002).

CD4+T cells secrete IFNγ which can suppress collagen synthesis (Ghosh AK *et al*., 2001). It was reported that TGFβ and IFNγ exert opposite effects on collagen synthesis (Weng H et al., 2007)**.** In contrast to TGFβ, IL-1beta and IFNγ down regulate the expression of αSMA as well as decrease fibroblast proliferation and collagen deposition.

IL-4 is a potent inducer of collagen gene synthesis in fibroblasts (Buttner C *et al*., 2004)**.** Prakash *et al.* have reported that fibrosin, a novel heparin-binding cytokine produced by CD4T lymphocytes plays an important role in up regulating the appearance of myofibroblasts

during wound healing and in fibrotic diseases (Prakash S *et al*., 2007).

Any release of components from a biomaterial might alter cytokine regulation and therefore modify the wound healing process (Messer RLW *et al*., 2007). Semi –quantitative RT-PCR analysis has revealed that hydrophilic surfaces showed a decreased expression of pro-inflammatory cytokines like IL-6 and IL-8 and pro-wound healing cytokines like IL-10 and TGF β**.** Proteomic analysis by this same group revealed that pro inflammatory cytokines like IL-1β and IL-6 decreased with time whereas anti-inflammatory IL-10 gradually increased with time over a hydrophilic surface (Anderson JM *et al*., 2007)**.** In 2000 itself Giulietti *et al.* have put forward Real time quantitative PCR as an effective tool to quantify cytokine gene expression (Guilietti A *et al*., 2001).

2.11. Signaling Pathways involved in macrophage/fibroblast activation and cytokine secretion

Understanding the molecular pathways implicated in the process of myofibroblast activation is a critical step in developing matrix niches that can regulate the myofibroblastic phenotype and recognizing factors that inhibit or reverse this process of myofibroblast formation .

Members of the mitogen activated protein kinase family, Erk, c-Jun N-terminal kinase and stress activated protein kinase-2(p38) are central elements that transduce the signals generated by growth factors and stress agents (Su B *et al.,* 1996). Findings of Furukawa *et al.* provide direct evidence that p38 MAPK-dependent phosphorylation of smad-3, together with TGFβ 1 receptor dependent phosphorylation of Smad2, leads to fibrogenic signal in myofibroblasts during chronic liver injury (Furukawa F *et al.,* 2003). p38 and ERK MAP kinase cascades appear to be profibrotic whereas the JNK MAP kinase cascade may be generally antifibrotic (Leask A *et al*., 2004)**.**

Differential cytokine regulation indicates a sophisticated coordination of cytokine levels associated with the management of wound healing response after removal of activator/injury**.** Regulatory control of the signaling pathways for cytokines is complex, and

many diverse signaling pathways are coordinated simultaneously to direct the inflammatory process**.**

2.12. Molecular studies of fibrous capsule around silicone implants

Wolfram *et al.* have in detail carried out a study on cellular and molecular composition of fibrous capsules removed from patients(Dolores W *et al.,* 2004). They have identified immune cells like CD4+ ,CD8+ T lymphocytes, dendritic cells, CD44, CD45RO, CD45RA and CD25 expressing cells, collagenous and non collagenous ECM proteins, HSP 60 and adhesion molecules like ICAM-1, P- selectin, VCAM-1 in the fibrous capsule.

Backovic *et al.* analyzed the composition of the proteinacious film over silicone implant, the dynamics of protein deposition, and protein modifications after adsorption both *in vivo* and *in vitro*. Differential analysis of protein deposition was performed, followed by protein identification with mass spectrometry, database matching, and Western blots. They could identify thirty different proteins of which structural and extracellular matrix proteins predominated, followed by mediators of host defense, metabolism, transport, and stress related proteins. In addition, several biochemical modifications of fibronectin, vitronectin, and heat shock protein 60 were detected (Backovic A *et al*., 2007).

2.13. Antifibrotic approaches

The four major approaches involving cytokines are: inhibition of cytokine synthesis, inhibition of cytokine release, inhibition of cytokine action and inhibition of cytokine intracellular signaling pathways (Henderson B, 1995).

TGFβ, a main factor involved in myofibroblastic differentiation and some of its partners such as CTGF (Duncan MR *et al*., 1999) or endothelin-1 (Shao R *et al.,* 2003), may represent interesting tools to attenuate the "dark side" of tissue repair (Border WA *et al.*1992). It has been reported that TGFβ1 inhibitor peptide applied in a matrix with tetra

glycerol dipalmitate is effective in achieving a reduction in peri prosthetic fibrosis after placement of silicone implants, either subcutaneously or submuscularly (Ruiz-de-Erenchun RMD *et al*., 2005). TGFβ knockout mice is ultimately of the lethal phenotype (Goumans MJ *et al*., 2000). This points that this pluripotent cytokine is essential for normal health. Disrupting intracellular TGFβ /Smad signaling may provide a novel approach in controlling fibrosis.

IFNα antagonizes the TGFβ/Smad3-stimulated COL1A2 transcription *in vitro* and suppresses COL1A2 promoter activation *in vivo*, providing a molecular basis for antifibrotic effects of IFNα (Inagaki Y *et al*., 2003). Also there are reports showing that IFNα decreases αSMA expression by human hepatic stellate cells in culture (Mallat A *et al.*, 1995) and reduces liver fibrosis in non-A, non-B hepatitis (Guerret S *et al*., 1999; Manabe N *et al.*, 1993).

It was reported that prostaglandinE1 treatment decreases liver fibrosis in the bile duct ligation model (Beno DW *et al*., 1993). Angiotensin II involvement in fibrosis is suggested by data showing that angiotensin-converting enzyme inhibitors can inhibit fibrosis in the kidney (Ruiz-Ortega M *et al*., 1997). Studies with angiotensin receptor knockout animals show reduced fibrosis in experimental models of fibrosis such as ureteral obstruction (Ishidoya S *et al*., 1995). In addition to these biomolecules, there are few synthetic drugs that act as anti fibrotic, but whose action mechanism is not clearly understood.

However, most of the studies were carried out on clinically retrieved prosthesis and the results were inconclusive. Experimental studies have been few and mostly related to either material characteristics or *in vitro* response to material (Ziats NP *et al.*, 1988). There is a lack of information regarding the role of various cytokines at tissue material interface *in vivo* and their role in the extensive fibrosis. Further studies are required to directly assess the reasons for contraction around some implants and not around others. Control of capsular contracture may be achieved by controlling biochemical as well as cellular events.

HYPOTHESIS:

With this aim, we hypothesise:

- There is a persistence or reappearance of phenotypic expression of myofibroblast at the implant site due to slow release of low molecular weight silicone particles from shell.
- Silicone particles initiate an immune response that involves T cells, B cells and macrophages. Cytokines released by these cells either up regulate or downregulate the phenotypic expression of myofibroblasts.

OBJECTIVE

To study over a specified time period the interrelationship between immune cells around silicone implants, formation of myofibroblasts and collagen deposition. The study would identify cytokines, proteins and signaling pathways involved in the fibrosis around such implants.

APPROACH

Phase 1 : *In vivo* implantation studies in rats and rabbits

Phase 11 : Role of macrophage-secreted cytokines in fibroblast activation into myofibroblasts

Phase 111 : Silicone degradation in Psuedo extra cellular fluid and the role of silicone extract in fibroblast modulation.

Chapter 3

MATERIALS AND METHODS

The materials used were silicone tissue expander commercially used for breast augmentation, silicone Ventriculo-Peritoneal shunt material commercially available and an in house synthesised Ultra high molecular weight poly ethylene. The silicone tissue expander was a two component silicone elastomer and the UHMWPE used, is a known biocompatible material cited by international standards for use as an appropriate experimental control in the biological evaluation of medical devices (ISO 10993-12, 2002). *In vivo* studies were carried out in animal models: short term in rats and long term in rabbits. *In vitro* studies were done to investigate the effect of cytokines and the role of silicone leachants on fibroblast to myofibroblast transformation. The plan of investigations are outlined in Figure 5.

Phase I

3.1. Material characterisation

3.1.1 Contact angle analysis

The wettability study of different material surface was analyzed by contact angle measurements. The contact angle of Silicone expander and UHMWPE materials before implantation were studied using a digital goniometer equipped with SCA-20 software (Model OCA, Dataphysics, Germany). The materials were cut into 1 cm^2 pieces. The measurements were taken 5 times with deionised water bubble probe and the mean value was taken as the contact angle.

Figure 5. Schematic diagram of Materials & Methods

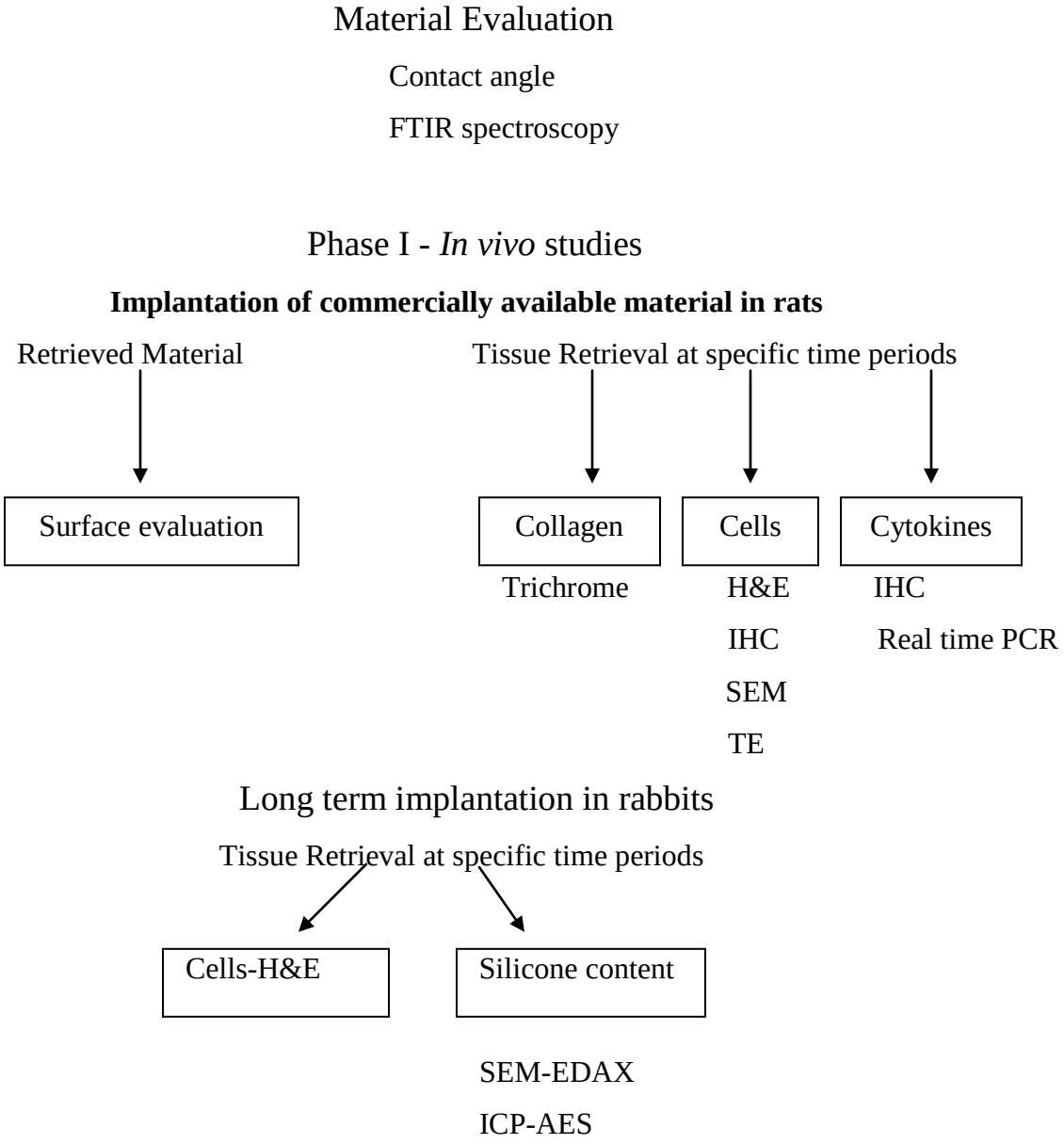

In vitro studies

Phase II -Role of macrophage-secreted product in fibroblast activation into myofibroblast

Phase III -Silicone degradation in Psuedo extracellular fluid and the role of silicone extract in fibroblast modulation.

3.1.2. Fourier transform- infrared spectroscopy

Molecular structure of material pre and 180 days post implantation was studied by a NICOLET 5700 FTIR in an ATR mode. The spectral pattern obtained was matched with known materials in Hummel polymer sample library using OMNIC-2 software. Change in spectral pattern was looked for in both samples.

3.2. *In vivo* studies

The *in vivo* studies were carried out in two animal models- Rats and Rabbits. Since the life span of rat animal model is short, an extended long term implantation was carried out in rabbits.

3.2.1 *In vivo* studies- RAT

3.2.1.1 Implantation and retrieval of Silicone expander (SE) and UHMWPE in rats

All animal experiments were conducted with prior approval of the Institute Animal Ethics Committee (IAEC). Both SE and UHMWPE were cut into pieces with dimensions of 1.5cm x 1.5cm x 1 mm, cleaned and sterilized with ethylene oxide and were implanted in gluteus muscle of young female Wistar rats as shown in Figure 6. The skeletal muscle was selected as an ideal site for implantation because in the clinical situation the silicone expander material is in contact with skeletal muscle of breast as described in section 2.3. Animals were categorized into 6 groups, of 8 animals in each group. Approval for the animal experiment was sought from Institute Animal Ethics Committee. Implantation was done aseptically after animals were anasthetised (80 mg ketamine + 5 mg xylaxine/kg body weight). The skin was swabbed with 70% alcohol and a 1.5 cm incision made in the gluteus muscle. The SE was inserted into the muscle. The wound was closed with catgut and the skin sutured externally with a nylon suture. UHMWPE was implanted in the contralateral leg. The implantation procedure was done based on ISO-10993-6 (i). Post-implantation care was given according to the guidelines of the Institutional Animal Ethics Committee and the animals were provided with food and water *ad libitum*. At the end of the study period, animals were sacrificed with an overdose administration of sodium thiopentone. Materials with surrounding tissue from each group

were retrieved respectively at 3, 7, 14, 30, 90 and 180 days post implantation. The materials were carefully removed from tissue and fixed in 3% buffered gluteraldehyde for scanning electron microscopy and in Phosphate buffered saline for FTIR spectroscopy analysis. The tissues with implant site were fixed in 10% buffered formalin for histology and snap frozen in liquid nitrogen cooled isopentane for immunohistochemistry and RNA isolation. The snap frozen samples were stored at $^{-}80^{0}$C till the downstream processing was started. The retrieved tissues were also fixed in 3% buffered gluteraldehyde for transmission electron microscopy studies.

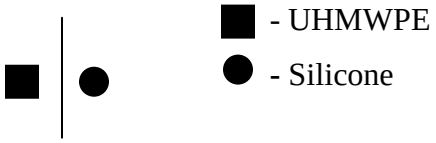

Figure 6. Schematic representation of implantation sites- Rat

3.2.1.2. Histology

Neutral buffered formalin

Disodium hydrogen phosphate anhydrous (6.5 g) (Merck, India), Sodium dihydrogen phosphate monohydrate (4 g) (Merck, India), 100 ml of formaldehyde 37-41% (Merck, India) and 900 ml distilled water. The salts were dissolved by stirring, pH of the solution was adjusted to 7 and made up to one litre.

Harris's Haematoxylin

Haematoxylin (Merck) was dissolved in absolute alcohol by stirring in a magnetic stirrer. Potasium alum (Merck) was dissolved in water by gentle heating with the help of an electric heater (Bajaj electricals, Pune). Haematoxylin solution was poured into the alum solution while it was hot and allowed to boil rapidly. This was stirred using a glass rod. Mercuric oxide and sodium iodate were slowly added to it. The reaction vessel was then plunged into a basin of cold water. Glacial acetic acid was added to the reagent and filtered.

Eosin stain

Eosin (water soluble) (Merck, India) was mixed with isopropyl alcohol in a ratio of 10:1000 (gm/ml) using a magnetic stirrer.

Acid alcohol

Seven hundred millilitres of isopropyl alcohol was made up to 1000 ml with distilled water. From this 10 ml was discarded and 10 ml of con. HCl (Merck, India) was added to it.

Scott's tap water

Potassium bicarbonate - 2 grams

Magnesium sulphate - 20 grams

Distilled water - 1 litre

Potassium bicarbonate was dissolved in a little of water. Magnesium sulphate was dissolved in water in a separate beaker. Dissolved bicarbonate was poured into the magnesium sulphate solution and mixed well. The solution was then made up to one litre with water.

Mayer's egg albumin

Egg white - 50 millilitre

Glycerin - 50 millilitre

Thymol - 100 milligrams

Egg white was made up to 100 ml with glycerin and mixed well with the help of a magnetic stirrer. Thymol was added to it and stored at 4°C.

Tissue Processing

One cm^2 cross sections of implant site from all time periods with surrounding muscle were dehydrated in isopropyl alcohol in ascending grades of dilution, cleared in chloroform and impregnated in paraffin wax. This processing was done using the Automatic Tissue processor (LEICA TP 1020). The following protocol was followed:

1. 10% Neutral buffered formalin -10 minutes
2. 80% alcohol - 2 hours
3. 95% alcohol I - 2 hours

4. 95% alcohol II - 2 hours
5. 100% alcohol I - 2 hours
6. 100% alcohol II - 1 hour
7. 100% alcohol III - 1 hour
8. 100% chloroform I - 1 hour
9. 100% chloroform II - 1 hour
10. 100% chloroform III -2 hours
11. Paraffin wax I - 2 hours
12. Paraffin wax II -2 hours

Embedding

Processed tissues were embedded into paraffin blocks using the Paraffin embedder (LEICA EG 1160).

Sectioning

5µm thick paraffin sections were taken using the Automatic Microtome (LEICA RM 2155) and collected onto glass slides coated with Meyers Egg Albumin.

Staining

Paraffin sections were stained with Harri's Heamatoxylin and Eosin using the Automatic stainer (LEICA AUTOSTAINER XL) using the following protocol:

1. Glass slides with sections were placed in slide racks and incubated in the autostainer oven for 1hour at 50°C.
2. Xylene I - 10 minutes
3. Xylene II - 5 minutes

4. 90% alcohol - 5 minutes
5. 70% alcohol - 5 minutes
6. Tap water - 5 minutes
7. Harris Haematoxylin - 5 to 30 minutes
8. Tap water - 3 minutes
9. Acid Alcohol - 10 sec to 1 minutes
10. Tap water - 5 minutes
11. Scotts tap water- 1 to 5 minutes
12. Tap water - 5 minutes
13. 1% Eosin(water soluble)- 5 to 20 minutes
14. Tap water - 15 sec
15. 70% alcohol - 2 minutes
16. 100% alcohol I - 5 minutes
17. 100% alcohol II-5 minutes
18. Xylene III - 10 minutes
19. Xylene IV - 10 minutes

Slides were air dried and mounted with Cytoseal ™ 60 and coverslipped.

Light microscopy

Histological analysis of the sections was performed via light microscopy using a trinocular microscope (Nikon Eclipse Model E600, Japan) and images captured using a digital camera (Nikon model DXM1200F, Japan) with ACT-1 software.

3.2.1.3. Trichrome staining for collagen

Bouin's fluid for Masson's trichrome staining

Saturated picric acid - 71 ml

40% Formaldehyde - 24 ml

Glacial Acetic Acid - 5 ml

Mixed saturated picric acid and formaldehyde. Glacial acetic acid was slowly added to the mixture.

Trichrome stain solution

Trichrome stain LG solution, Catalog.no. HT10-3-16(Sigma Inc.)

The paraffin sections were deparaffinised in xylene and hydrated to deionized water through descending grades of alcohol. Slides was incubated in preheated Bouin's fluid for 15 minutes at 56^0C. The slides were cooled in tapwater contained in a coplin jar and washed in running tap water to remove yellow colour from sections. Sections were stained in Harry's Heamatoxylin for 5 minutes, washed and stained with Trichrome stain solution (Accustain trichrome stain, HT-10-3-16, Sigma) for 5 minutes. Destaining was carried out in 0.5% glacial acetic acid for 1 minute. The slides were rinsed in tap water, dehydrated through ascending grades of alcohol, air dried and mounted in permanent mounting medium (Cytoseal). The stained sections were examined by bright field microscopy (Nikon eclipse E600). Collagen thickness around implant site was evaluated quantitatively by measuring the average thickness from five equidistant sites. The data obtained was analysed statistically by One –way ANOVA and represented graphically.

3.2.1.4. Immunohistochemical Analysis

Poly-L-Lysine coated slides

Poly-L-Lysine solution (0.1% w/v in water) (Sigma-Aldrich, USA) was diluted 1:10 with deionised water. This was then coated on clean microslides by smearing the solution on the slide. The slides were then kept for drying at 56°C in an incubator (M.C. Dalal & Co., India) for one hour.

Phosphate Buffered Saline (pH 7.4)

Sodium Chloride	-	8 g
Sodium phosphate, dibasic anhydrous (Na_2HPO_4)	-	1.15 g
Potassium Chloride	-	0.2 g
Potassium phosphate, monobasic anhydrous (KH_2PO_4)	-	0.2 g
Distilled water	-	1 l

The chemicals were weighed out and dissolved in distilled water, pH was adjusted to 7.4 with a pH meter, and made up to one l with distilled water.

Immunostaining Kit

UltraTech HRP (DAB) Streptavidin-Biotin Detection System PN IM2765 (Beckman Coulter, USA.)

Primary Antibodies

Mouse anti rat CD 163 (MCA 342R) purified IgG, ED2 (Serotec, UK)
Mouse anti rat CD4 (MCA 55G) purified IgG (Serotec, UK)
Anti-Actin(C-11),goat polyclonal: sc-1615(Santa Cruz Biotechnology Inc., USA)
Anti-Vimentin(C-20)goat polyclonal:sc-7557(Santa Cruz Biotechnology Inc., USA)
Anti TGF β(v),rabbit polyclonal : sc-146 (Santa Cruz Biotechnology Inc., USA)
Anti-TNFα (N-19)goat polyclonal : sc-1350 (Santa Cruz Biotechnology Inc., USA)
Anti-IL-1α(R-20)goat polyclonal : sc-1254 (Santa Cruz Biotechnology Inc., USA)
Mouse anti rat IL-1β (MCA 1397) purified IgG (Serotec, UK)
Anti-IL-6 (M-19)goat polyclonal: sc-1265 (Santa Cruz Biotechnology Inc., USA)

Anti-IL-10(M-18) goat polyclonal:sc-1783 (Santa Cruz Biotechnology Inc., USA)
Mouse anti rat IFNγ (MCA 1301) (Serotec, UK)

Tissues stored at -80°C were embedded in tissue freezing Medium (Jung Leica Microsystems) on chucks. The chuck with the tissue was then fixed on the cryostat microtome (Leica, Model CM3050 S, Germany).The temperatures set were -20^0C and -16^0C for the object and chamber respectively. Tissues were trimmed till the implant site was located. This was done by staining with toluidine blue and observing under microscope. Subsequently, 8µm cryosections were taken onto Poly-L-Lysine coated glass slides, air dried and stored at -80°C till further evaluation.

The sections were then stained for identification of Macrophages(CD 163, ED2), T helper lymphocytes (CD4) , fibroblasts (Vimentin), myofibroblasts (α-smooth muscle actin) and cyokines TGFβ, TNFα, IL-1α, IL-1β , IL-6, IL-10 and IFNγ in appropriate dilutions as in Appendix II. Specific staining was detected using the Streptavidin-Biotin Universal Detection System [UltraTech HRP (DAB), Immunotech, Beckman Coulter, France].

Immunohistochemical staining was performed using the following protocol:

1. Sections were allowed to thaw to RT in a desiccator for at least one hour.
2. Sections were fixed in cold acetone (-20°C) for ten minutes.
3. Slides were placed into a coupling jar containing PBS for ten minutes.
4. Sections were treated with 3% hydrogen peroxide for ten minutes at RT.
5. Washed in PBS buffer for two minutes.
6. Slides were removed from buffer, wiped gently around each sections and covered each section with Protein Blocking Agent (PBA). Allowed to incubate for five minutes at RT.
7. Care was taken for avoiding washing in this step.
8. PBA was poured off, wiped gently around each section and covered the section with primary antibody in appropriate dilutions (Appendix I) and incubated in a humidity chamber at RT for 60 minutes.
9. Washed in PBS buffer for two minutes.

10. Wiped gently around each section and each section was covered with biotinylated secondary antibody and incubated for ten minutes at RT.
11. Washed in PBS buffer for two minutes.
12. Wiped around sections and covered each section with Streptavidin-peroxidase reagent and incubated for ten minutes at RT.
13. Washed in PBS buffer for two minutes.
14. Wiped around each section and covered each section with freshly prepared DAB chromogen solution and incubated at RT for one minute.
15. Washed slides in distilled water for two minutes.
16. Counter stained the sections with haematoxylin (one minute).
17. Washed with tap water.
18. Bluing of haematoxylin was done with Scott's tap water.
19. Washed with tap water.
20. Air dried the sections and mounted.

A positive reaction was indicated by a coloured precipitate at sites of specific cellular antigen localization. For negative controls incubation with primary antibody was substituted with PBS alone and depicted in Appendix II. Slides were analysed via light microscopy using a trinocular microscope (Nikon Eclipse Model E600, Japan) and images captured using a digital camera (Nikon model DXM1200F, Japan) with ACT-1 software.

The Immuno positive cells were graded as few (+) and scattered; mild (++) with small collections of cells; moderate (+++) and intense (++++) sheets of cells at tissue-implant interface. The cytokines were also graded qualitatively depending on intensity of staining as mild (+) moderate (++) and intense (+++).

3.2.1.5. Transmission Electron Microscopic Analysis

Sorensen's phosphate buffer

Stock A - 0.2 M Na_2HPO_4

Stock B - 0.2 M NaH_2PO_4

Sorensen's phosphate buffer (0.1 M) was prepared by mixing 40.5 ml of stock A and 9.5 ml

of stock B.

3% buffered gluteraldehyde

The stock 8% gluteraldehyde (Polyscience, USA) was diluted to 3% using Sorensen's phosphate buffer.

Gluteraldehyde fixed tissues were cut to pieces that include tissue-implant interface. The samples were washed with cold phosphate buffer (pH 7.4), 4 changes, for 10 minutes each, with sample vials standing in an ice bath. Tissues were then placed in 1% OsO_4 for 2 hours and thereafter washed with phosphate buffer, 4 changes for 15 minutes each, in an ice bath. Tissues were then rinsed in distilled water for five minutes.

Dehydration

The tissues were dehydrated in ascending grades of acetone using the following protocol:

a. 50% acetone, 10 minutes (2 changes) in cold.
b. 70% acetone, 10 minutes in cold (stored overnight in refrigerator).
c. 70% acetone, 10 minutes at RT.
d. 90% acetone, 10 minutes (2 changes) at RT.
e. 100% acetone, 15 minutes (4 changes) at RT.
f. 100% dry acetone, 15 minutes at RT.

Infiltration

Tissues were placed in two changes of propylene oxide for five minutes each and then transferred into propylene oxide-resin mixtures of ratio 3:1 for two hours, 1:1 for two hours and finally kept overnight in vacuum in a propylene: epoxy resin mixture of ratio of 1:3. Final infiltration was carried out in pure resin prior to embedding.

Embedding

The tissues were embedded in molds containing the epoxy resin - Polybed 812 mixed with dodecenyl succinic anhydride (DDSA – Hardener), Nadic methyl anhydride (NMA – Hardener), Dimethylaminomethyl phenol (DMP – Accelerator) in appropriate ratios as per the kit instructions (Polysciences Inc, USA) and polymerized at 60°C in an oven for three days.

Sectioning

For light microscopy semithin sections (~ 1µm) were cut using a glass knife in an ultramicrotome (Leica Ultracut UCT). Once the area of interest was identified, the remaining areas of the block was trimmed off. Ultrathin sections (50-70nm) were cut using a diamond knife (Diatome®) and collected onto the shiny side of copper grids of 300 mesh size.

Staining for Light Microscopy(LM)

The semithin sections were stained with Toludine blue.

i. Sections were taken onto a few drops of water on a slide and a drop of toludine blue was added.
ii. Sections were heated on a hot plate for a few seconds.
iii. The sections were washed well in distilled water and air dried.
iv. The sections were mounted using DPX and the photographs were taken using the trinocular microscope (Nikon Eclipse Model E600, Japan) and images captured using a digital camera (Nikon model DXM1200F, Japan) with ACT-1 software.

Staining for TEM

i. All grids were made wet by dipping in distilled water.
ii. The grids were immersed in filtered Uranyl Acetate for two hours with the section side up.
iii. The grids were washed in methanol series (100%, 80%, 50%), and then washed with distilled water.
iv. The grids were placed on a filter paper to dry.
v. 0.025g of Lead Citrate were dissolved in 10ml 0.1N NaOH and centrifuged for 10 minutes.
vi. Sodium hydroxide pellets were placed in a Petri dish to eliminate carbon dioxide. The grids were then floated onto the drop of lead citrate on a parafilm placed in the carbon dioxide-free petri dish, with section side facing down and incubated for 10 minutes.
vii. The grids were washed in four changes of distilled water collected in beakers. The first two beakers contained two drops of NaOH solution.

viii. The grids were then dried and viewed under the Transmission Electron Microscope (Hitachi H-600) at an accelerating voltage of 75kV and photographs (Kodak ford film) were taken.

3.2.1.6. Analysis of surface morphology of retrieved materials

The explanted material fixed in 3% buffered gluteraldehyde were dehydrated in ascending grades of ethanol and dried in the liquid phase with iso amyl acetate. Critical point drying was carried out (Critical point dryer, Model HCP-2 Hitachi Science systems, Japan) in liquid CO2 at 150Kg/cm^2. The samples were sputter coated with gold (Ion sputter Model E101 Hitachi, Japan) and observed using a scanning electron microscope (S2400Hitachi) at an accelerating voltage of 15kV.

3.2.1.7. Gene expression studies

Qiagen kit (RNA easy fibrous tissue kit, Cat.No.74704)
Rotor stator homogenizer (Polytron system,PT-MER1600E, Switzerland)
Full velocity master mix, Stratagene, USA

RNA isolation

Total RNA was isolated from retrieved rat muscle tissue samples according to the manufacturer's description. On the day of isolation, 30 mg tissue around the implant site-tissue interface was weighed out from frozen samples without thawing and homogenized with a rotor stator homogenizer in 350µl of RPE buffer (lysis buffer). Proteinase digestion was done by incubating the sample at 55^{0}C after the addition of 10µl proteinase K, followed by ethanol precipitation after which the homogenate was applied to RNeasy mini-spin columns sitting in 2 ml collection tubes. The columns and tubes were then centrifuged for 1 min at 13000rpm, the flow-through was discarded and the columns were washed with 350 µl buffer and spun at 9500rpm for 15 seconds. The purified sample was DNAse treated with 10µl DNase I and 70 µl buffer and incubated at RT for 15 minutes. Thereafter, the columns were washed with 350µl buffer and spun at 9500 rpm for 15 seconds. The columns were subsequently washed with 500µl buffer twice with the flow through being discarded after

each centrifugation. The columns were transferred to new collection tubes and 50µl RNase freewater was applied to each column twice. The accumulated flow through was collected after the centrifugations. Yield and purity of isolated RNA was checked in nanodrop ND1000 spectrophotometer at an absorbance of 260/280 nm. The isolated RNA samples were stored in -80^{o}C till downstream analysis was carried out.

Reverse transcription

cDNA synthesis of RNA samples was carried out. Total RNA at a concentration of 1 µg was taken for each reverse transcription using Thermal cycler (Appollo Cycler,USA) at annealing temperatures of 53-58^{0}C. In 25µl total volume, 1 µl dNTP, 2.5 µl stratascript buffer, 0.5 µl RNase inhibitor, 1 µl each forward and reverse primer and 0.5 µl (50U/ µl) reverse transcriptase (Stratagene, USA) and the RNA template were added. The primer sequences were derived from cited literature and are listed in Table 5. All cDNA samples were stored at -20^{o}C until use.

Table 5: Primers used for *in vivo* gene expression studies

Name of gene	Primer Sequence	Annealing conditions	GenBank reference
α-SMA	Sense : 5'-GATCACCATCGGGAATGAACG C-3' Antisense 5'-CTTAGAAGCATTTGCGGTGGAC-3'	52.5°C/30sec	BC 158550.1
IFN γ	Sense : 5'-ATCTGGAGGAACTGGCAAAAGGACG-3' Antisense: 5'-CCTTAGGCTAGATTCTGGTGACAGC-3'	55°C/30sec	X02327.1
TGFβ	Sense: 5'-CTCACTGCTCTTGTGACAGC-3' Antisense: 5'-AGCTGCACTTGCAGGAGGGC-3'	55°C/30sec	X52498.1
IL-1 β	Sense : 5'-ATGGCAACTGTCCCTGAACTCAACT-3' Antisense:5'- CAGGACAGGTATAGATTCAACCCCTT-3'	54°C/30sec	M98820.1
IL-10	Sense: 5'-TCAGCACTGCTATGTTGCCTGCTC-3' Antisense :5'-GAGTGTCACGTAGGCTTCTATGC-3'	54.5°C/30sec	X60675.1
GAPDH	Sense : 5'-TTCTTGTGCAGTGCCAGCCTCGTC-3' Antisense: 5'-TAGGAACACGGAAGGCCATGCCAG-3'	58.5°C/30sec	XM001073242.1

Real time PCR with SYBR green dye

Real time PCR was performed to determine the mRNA expression of αSMA, TGFβ, IFNγ, IL-1β and IL-10 using chromo4 system (MJ research, USA). All reactions were carried out in a total volume of 20µl containing 10µl SYBR green master mix, 10µm forward and reverse primers and 8µl template cDNA. For each gene, quality and specificity was assessed by examining Melting curves following Real-time PCR. The cDNA copy numbers of the target gene were analyzed after normalizing with the copy number of GAPDH, the house keeping gene. The gene expression in normal skeletal muscle tissue acted as the baseline for comparison. The light cycler (MJ research, USA) run was used with the following parameters: 35 cycles, denaturation at 94^0C for 6 min, annealing temperature at 53-58.5^0C (depending on T_m of primers) for 30 seconds and elongation temperature at 72^0C for1 minute.

3.2.2. *In vivo studies*-Rabbit

3.2.2.1. Implantation and retrieval

Long term implantation study of silicone expander material and hydrocephalus shunt silicone was carried out in the para vertebral muscle of New Zealand white rabbit models. Six female rabbits were implanted with tissue expander material. Implantation was done aseptically as described in 3.2.1.1. UHMWPE was implanted in the contra lateral side. The test and control material dimensions were same as that explained in section 3.1.1. Four silicone expander pieces and four UHMWPE pieces were implanted in a single animal on dorsal side as in the schematic diagram below (Figure 7).

Figure 7. Schematic representation of implantation sites- Rabbit

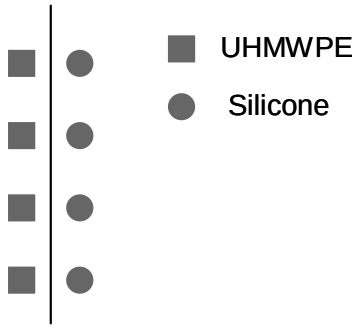

Time periods of study were 180 days, 270 days and 365 days. At the end of study, animals were euthanized with an overdose of sodium thiopentone. Material with the surrounding tissue were retrieved and fixed in 10% buffered formaldehyde for Haematoxylin &Eosin staining and in 3% buffered gluteraldehyde for Scanning Electron Microscopy-Energy Dispersive X-Ray spectroscopy (SEM-EDAX). The fibrous capsule formed around the implant was measured as described in 3.2.1.3.

3.2.2.2. Scanning electron Microscopy-Energy Dispersive X-Ray spectroscopic (SEM-EDAX) analysis

The downstream processing was done as described in 3.2.1.6. Spectrum was analysed using the program ICIC link.

3.2.2.3. Inductively coupled plasma atomic emission spectroscopic (ICP-AES)analysis

The tissue samples which were fixed in 3% buffered gluteraldehyde were washed well with deionised water, dried at 56^0 C for 2 hours. The tissues were dissolved with 5 ml HNO3 and 2 ml HClO4 and made upto 50 ml using HPLC grade water. The filtered sample was analyzed with ICP-AES system (Thermo electron IRIS Intrepid II XSP DUO).

Phase II

3.3 *In vitro* studies

3.3.1. Role of macrophage secreted cytokines on fibroblast activation into myofibroblast

In vivo, when an implant is placed into body, the circulating monocytes from the bood reach the injury site and get activated to macrophages. Both the monocytes and macrophages release a myriad of cytokines that play a pivotal role in the subsequent wound healing. An *in vitro* study to know the role of macrophage secreted cytokines in fibroblast activation was carried out by using two cell lines, monocyte derived macrophage cell line (U937) and a direct macrophage cell line(RAW 264.7).

The schematic diagram illustrated below describes the various methods adopted in this *in vitro* study.

IFNγ

↓

U937 monocytic cells------Material-----Cytokine-ELISA-----Fibroblast----- αSMA, Erk

(IL-6,IL-1 ,TNFα) (HLF) (Western blot)

RAW macrophage cells-----Material---IL-6,TGFβ ----------Fibroblast----- αSMA

(Real time PCR) (L929) (Real time PCR&

(Confocal microscopy)

3.3.1.1. Sterilisation of materials

Silicone expander material ,UHMWPE (1 cm X 1 cm)

Coverslips (1cm diameter)

The silicone expander and UHMWPE material were cut into 1 cm X 1 cm dimensions, thoroughly cleaned in detergent solution, washed and rinsed well in distilled water. The cleaned material was dried and packed for ETO sterilization which was carried out at 37^0C.

3.3.1.2. Cell line

Human monocyte cell line U-937 (ATCC Number CRL-1593.2, ATCC, Virginia, USA)

Human lung fibroblast cell line, HLF

3.3.1.3.Differentiation of monocytic cell lines to macrophages and their adherence to the material

Phorbol-myristyl-acetate (Sigma Inc.)

Human monocyte cell line U-937 were cultured in RPMI 1640 medium (GIBCO) supplemented with L-glutamine, and adjusted to contain 10% Foetal bovine serum(GIBCO) and 1% Penicillin-streptomycin(GIBCO). 1 x 10^6 cells seeded on pre-sterilised silicone expander material. 3ng PMA was used for differentiation of monocytes into macrophages. Cells were treated with PMA for 72hours and the morphology change was noted.

3.3.1.4. Study of cytokines from monocyte derived macrophages by ELISA

Primary and secondary antibodies

IL-6-BD opt EIA: Biotin anti-human

Capture antibody: 51-26451E

Detection antibody: 51-26452E

IL-1 β : Biotin anti-human

Capture antibody **:** 51-26871E

Detection antibody : 51-26872E

TNF α: Biotin anti-human

Capture antibody : 51-26371E

Detection antibody : 51-26372 E

Elisa coating buffer

Sodium bicarbonate - 0.42g

Dissolved in 50 ml water.

Phosphate- citrate buffer

Disodium Hydrogen phosphate - 3.65 g

Citric acid - 2.33 g

Distilled water - 500 ml

One TMB (3,3,5',5'-Tetra methyl benzidine, T-3405) tablet was dissolved in 10 ml phosphate citrate buffer to which 2µl 30%H_2O_2 was added.

Cytokines released byU937 derived macrophages (MDM)grown on material for 4,24, 48 and 72 hours were studied by doing Elisa of cell culture supernatants with BD Biosciences kit. Controls used were cells grown on coverslips. At the end of incubation periods, supernatant was collected, centrifuged at 13,000 rpm at 4^0C and stored at -20^0C. Cytokines investigated were IL-1β, IL-6 and TNF-alpha. 96 well Elisa plates were coated with 20 µl primary antibody diluted 1:100 in sodium bicarbonate buffer and kept overnight in refrigerator. The plates were washed twice with wash buffer (0.05%PBS-Tween) and blocked with 100 µl of 10%FBS-PBS for 2 hours.

At the end of blocking time, the plates were washed twice and 50 µl of serially diluted samples were added to the wells and incubated for 2 hour at RT. This was followed by secondary antibody incubation for 1 hour which is conjugated with Avidin-Horse radish peroxidase. 100 µl Tetramethylbenzidine substrate (Sigma) was added and incubated till colour developed. Depending on the blue colour intensity, the reaction was stopped by adding100 µl 1M H_2SO4. The absorbance was measured at 450nm and 570nm using a micro plate reader.

Positive control used were U937 cells which were primed with IFNγ (5 microl/ml) for 18 hours .The primed cells were then treated with 5 micromolar PMA for 10 min.

3.3.1.5. Quantitation of macrophage secreted cytokines

Cell lines and culture medium

Mouse macrophage cell line RAW 264.7 (NCTC clone ,NCTC, Pune, India)

The cells were cultured in MEM (Sigma) supplemented with L-Glutamine, and adjusted to contain 10%Fetal Bovine Serum (GIBCO) and 1% Penicillin-streptomycin (GIBCO).
TRI reagent, TR-118, Molecular Research Centre, Inc.

$1x10^4$ RAW cells were seeded onto silicone expander material and incubated for 24h, 48h and 72 h in a 24 well plate. At the end of each incubation period, supernatant was discarded and cells were lysed with TRI reagent for isolating RNA. Yield and purity of isolated RNA was checked in nanodrop ND1000 spectrophotometer at an absorbance of 260/280 nm. The isolated RNA samples were stored in -20^oC till downstream analysis was carried out. Real time PCR quantitation of TGFβ and IL-6 was carried out. RAW cells alone was taken as control. The cDNA copy numbers of the target gene were analyzed after normalizing with the copy number of GAPDH, the house keeping gene.

3.3.1.6. Cytokine expression levels between silicone expander, UHMWPE and TCPS

Macrophage cells were seeded over silicone expander, UHMWPE and TCPS at a density of $1x10^4$ and incubated for 24hour. The RNA was isolated and gene expression was analysed from cells as described in 3.3.1.5.

3.3.1.7. α SMA expression: RNA and protein expression study

Mouse fibroblast cell line L929 (NCTC clone 929, NCTC, Pune, India).
The cell line was cultured in MEM (Sigma) supplemented with L-Glutamine, and adjusted to contain 10%Fetal Bovine Serum (GIBCO) and 1% Penicillin-streptomycin (GIBCO).
TRI reagent, TR-118, Molecular Research Centre, Inc.

Conditioned media from experiment 3.3.1.6.was added to L929 fibroblast cells and seeded onto 24 well plated, incubated for 24 hours. RNA was isolated from cells as described in 3.3.1.5. and analysed for α-SMA, which is a marker for myofibroblast expression.

Table 6 ***: Primers used for in vitro gene expression studies***

TGF β	Sense: 5'- GCT AAT GGT GGA CCG CAA CAA CG-3' Anti sense: 5'- CTT GCT GTA CTG TGT GTC CAG GC-3'
IL-6	Sense: 5'-GAC AAA GCC AGA GTC CTT CAG AGAG-3' Antisense : 5'-CTA GGT TTG CCG AGT AGA TCT C-3'
α-SMA	Sense : 5'-CTG GAG AAG AGC TAC GAA CTG C-3' Anti sense:5'-CTG ATC CAC ATC TGC TGG AAG G-3'

α-SMA protein expression was analysed by immunofluorescent staining and visualised by Confocal Laser Scanning Microscopy (LSM 510 META) in HeNe laser at 543nm.Mean fluorescence intensity from 5 different fields was calculated using the software (LSM 510) and plotted graphically.

Immunofluorescence Antibodies

Primary

Mouse monoclonal α-Smooth Muscle Actin: A-5228(Sigma Aldrich)

Secondary

Goat antimouse IgG TRITC conjugate : T-5393(Sigma Aldrich)

The staining was carried out by the following steps:

Fixation

1. Cells grown over material were fixed by adding 0.5ml of 3.7% buffered formaldehyde.
2. Incubated overnight at 4^0C.
3. Washed thrice in PBS for 5 minutes each.

Permeabilisation

1. Washed with 200µl of PBS with 2% Triton-X100 for three times 5 minutes each.

Blocking

1. 10%BSA was added onto the cells and incubated for 10 minutes at RT

Probing with Primary antibody

1. Antibody was diluted in 1:100 dilution in PBS.
2. Added 100µl of primary antibody onto each sample.
3. Incubated for 2 hours.
4. Washed thrice with 0.5 ml of PBS for 5 minutes each.

Probing with Secondary antibody

1. Antibody was diluted to 1:100 times in PBS.
2. Added 100 µl of secondary antibody onto each sample.
3. Incubated for 1hour in dark.
4. Washed thrice with 0.5 ml of PBS for 5 minutes each.

Mounting

After the spot of cells were partially dried, mounted with permanent mountant (Fluorosave Reagent) and observed under confocal microscope (LSM 510 Meta).

3.3.1.8. Key signaling molecules involved in fibroblast to myofibroblast transition

3.3.1.8.1. Effect of monocyte conditioned media on fibroblasts

Human lung fibroblast cell line was maintained in Minimum Essential Medium (MEM 5650, Sigma) supplemented with 15% Foetal Bovine Serum (GIBCO), 2% L-Glutamine (GIBCO), 1% MEM Non essential amino acid (GIBCO) and 1% Penicillin-streptomycin (GIBCO).

These Fibroblasts were grown for 24 hours over silicone expander and UHMWPE at a density of 1 x 10^4/ml. Conditioned media from U937monocytes grown over silicone expander and UHMWPE, conditioned media from monocyte derived macrophages grown over silicone expander was collected and added to this fibroblast culture and incubated for 24 hours. At the end of incubation period, cells were harvested, centrifuged at 1000 rpm and the medium discarded. Cells were washed twice in PBS and lysed with RIPA buffer for western blot analysis. The cells alone without conditioned media addition served as the control.

3.3.1.8.2. Interferon gamma role on fibroblasts(HLF) grown on silicone, UHMWPE and Coverslip

To evaluate the role of T lymphocyte secreted cytokine, IFNγ on fibroblast to myofibroblast transition, Human lung fibroblasts were grown over silicone expander, UHMWPE and coverslip at a density of 1 x 10^4 and in a medium that contained IFN γ at a concentration of 200μg/l. At the end of 24 hours, the cells were scraped off gently from surfaces and lysed with RIPA buffer for western blot analysis. The cells alone without IFNγ addition served as control.

3.3.1.8.3. Cell lysis with RIPA buffer

Tris base - 0.79 g

Sodium chloride – 0.9 g

Deionised water – 75 ml

The pH was adjusted to 7.4. Added 10 ml of 10% NP-40 and 2.5 ml of sodium-deoxycholate and stirred till solution was clear. 1 ml of 100 mM EDTA was added and final volume was adjusted to 100 ml.

Cells were scraped out with a cell scraper and lysed with RIPA buffer containing, 50mMTris-HCl(pH 7.4), NP-40(non-ionic detergent), 0.25% Na-deoxycholate, 150mM NaCl, 1mM EDTA,1mM PMSF(Phenylmethylsulfonylflouride),1μg/ml protinin,Leupeptin,and pepstatin,1 mM sodium orthovanadate and 1mM Sodium Fluoride. The cell pellet obtained after trypsinisation was washed twice with non-sterile PBS. 150μl RIPA buffer was added to the cell pellet and briefly vortexed for 5 seconds. Repeated vortexing was carried out in cold room for 30 minutes. The extract was centrifuged at 13,000 rpm for 5 minutes at 4^0C to remove cellular fragments. Supernatant obtained was aliquoted and stored at −20°C until analysis.

3.3.1.8.4. Bradford analysis and Sample preparation

Amount of protein in the samples were estimated using the Bradford Assay.

1. Samples were thawed from −20°C to RT.
2. Diluted the samples by adding 1µl to 9µl of sterile distilled water. Triplicates of each sample was run. 10 µl Sterile distilled water alone served as the blank.
3. To each well added 200 µl Bradford reagent and incubated for 5 minutes.
4. Absorbance was read at 595nm using a microplate reader, Spectraflour(TECAN, Austria).
5. Protein Concentration was calculated.
6. Prepared samples was kept at 4^0C till stacking gel prepared.

3.3.1.8.5. Western blot

PVDF membrane, Exposure and detecting reagents

PVDF Millipore Power TL immobilion transfer membrane

Supersignal West Pico Chemi luminescent substrate (Pierce #34080)

Precision plus protein standards, Kaleidoscope (Biorad #61-0375)

Autoradiogram cassette (8"X10", Scientific company, California, #SQX-1118)

X-ray film (CL-Xposure film, Pierce,#34090)

Primary and secondary antibodies

Rabbit polyclonal, Erk 1:K-23 clone : sc-94(Santacruz Biotechnology Inc, USA)

Mouse monoclonal p44/42 : #9106 (Cell signaling)

Mouse monoclonal GAPDH : 6C5: sc-32233(Santacruz Biotechnology Inc, USA)

Goat anti mouse HRP IgG : A4416 (Sigma Aldrich)

Goat antimouse IgG2a-HRP : sc-2061(Santacruz Biotechnology)

Sample loading buffer

0.5 M Tris HCl - 15 ml

SDS - 3 g

Bromophenol blue - 0.15 g

Glycerol - 15 ml

Deionised water was added to make up to 50 ml.

Tris HCl for resolving gel

Tris base - 45.4 g

Tris base was dissolved in deionised water and pH adjusted to 8.8 using con. HCl. Deionised water was added to make up to a final volume of 250 ml.

Tris HCl for stacking gel

Tris Base - 30.3 g

Tris base was dissolved in deionised water and pH adjusted to 6.8 using con. HCl. Deionised water was added to make up to a final volume of 250 ml.

Running buffer-TBS (10X)

Tris Base - 24.2 g

Sodium chloride - 80 g

Both were dissolved in deionised water, pH was adjusted with HCl to 7.6.

Transfer buffer (10X)

Tris - 30.3 g

Glycine - 144 g

10% SDS - 100 ml

Methanol - 200 ml

Dissolved in deionised water and pH was adjusted to 8.3.

Washing buffer (TBST)

10X TBS - 100 ml
Deionised water - 900 ml

Tween 20 - 1 ml

The samples were run on 10% SDS - polyacrylamide gel at 75V for 10 min (stacking gel), 150 V for 1 hour (resolving gel). After samples run out, stopped the run, removed gel while soaking in transfer buffer and cut unused wells. Equilibrated gel in transfer buffer for 15 minutes.

Immunoblotting

1. Activated the Immobilion transfer PVDF membrane (Millipore) by soaking in 100% Methanol for 15 seconds, distilled water for 2 minutes and in transfer buffer for 15 minutes.
2. Soaked sponges and filter papers in transfer buffer.
3. The gel and PVDF membrane is sand witched in between filter paper and sponge pads. Caution was taken to avoid trapping of air bubbles in between the layers.
4. Transfer was carried out at 100V for one hour in a Mini trans-Blot cell (Bio-Rad).
5. After transferring, retrieved membrane and made markings on protein ladder.
6. Air dried the membrane and stored at −20°C till staining.

Staining with Antibodies

1. Prepared 1:100 dilution of primary and secondary antibodies in 1% non-fat milk in washing buffer.
2. Probed with primary antibodies overnight in cold room.
3. Washed thrice with washing buffer.
4. Probed with secondary antibodies for 2 hours at RT.
5. Washed thrice with washing buffer.
6. The membrane was placed in an autoradiogram cassette. Added 1 ml of chemi luminescent substrate to the membrane for 1 minute.
7. An X-ray film was placed over the membrane and exposed in dark room.

Phase III

3.3.2. Silicone degradation in Pseudo extra cellular fluid

3.3.2.1. *In vitro* leaching of silicone into Psuedo Extra Cellular Fluid (PECF)

Psuedo Extra cellular fluid (Homsy CA *et al.*,1969)

Sodium bi carbonate - 0.252 g

Sodium chloride - 0.413 g

Potassium chloride - 0.224 g

Dipotasium hydrogen phosphate - 0.1361 g

Dissolved in 100 ml deionised water. Mixed well by stirring and autoclaved.

In vitro degradation study was carried out based on ISO 10993-13(1998). Silicone expander material was cut into 1cm^2 pieces, cleaned thoroughly and ETO sterilized. This material was then immersed in 5 ml PECF taken in a screw capped material and incubated for 2 months at 37^{0}C in ordinary incubator (Memmert Co., Germany). At the end of incubation period the sample was analysed for silicon element by ICP-AES (Thermo electron IRIS Intrepid II XSP DUO).PECF alone was taken as the blank.

3.3.2.2. Effect of silicone leachants on fibroblast differentiation

Extraction of silicone was carried out in sterile PECF for 60 days at 37^{0}C and the extract was added to fibroblasts (1x10^4) in 5 ppb, 50ppb, 100ppb, 200ppb and 400ppb concentrations. Incubated for 24 hours and cells were analysed for αSMA expression. L929 Fibroblasts alone acted as the control.

3.4. Tissue responses to VP shunt material

3.4.1. Materials

Commercially available hydrocephalus shunt tubing made of silicone and Ultra heigh molecular weight polyethylene were used in the study. Ethylene Oxide sterilized materials of 1.5 mm ID x 2.5mm OD size.

3.4.2. Implantation and retrieval

The ETO sterilized materials were implanted in gluteus maximus muscle of wistar rats. The implantation procedure is same as that described in section 3.2.1.1.

3.4.3. FTIR spectroscopy

FTIR spectral analysis of VP shunt surface before and after 180 days of implantation was carried out as in 3.1.2.

3.4.4. Histology

Cellular response to the shunt material as well as to UHMWPE was studied by histological techniques as described in section 3.2.1.2

3.4.5.Collagen staining

The thickness of collagenous capsule formed around the VP shunt was evaluated by methods explained in 3.2.1.3.

3.4.6. Immunohistochemistry

Immunohistochemical techniques in cryosections was used for specific identification of immune cells and cytokines present at implant tissue interface.

Primary antibodies

Mouse anti rat CD 163 (MCA 342R) purified IgG, ED2 (Serotec, UK)

Mouse anti rat CD4 (MCA 55G) purified IgG, (Serotec, UK)

Anti-Actin(C-11),goat polyclonal: sc-1615(Santa Cruz Biotechnology Inc., USA)

Anti-Vimentin(C-20)goat polyclonal:sc-7557(Santa Cruz Biotechnology Inc., USA)

Anti TGF β(v),rabbit polyclonal : sc-146 (Santa Cruz Biotechnology Inc., USA)

Anti-TNFα (N-19)goat polyclonal : sc-1350 (Santa Cruz Biotechnology Inc., USA)

Anti-IL-1α(R-20)goat polyclonal : sc-1254 (Santa Cruz Biotechnology Inc., USA)

Mouse anti rat IFNγ (MCA 1301) (Serotec, UK)

The protocol followed was similar to that in part 3.2.1.4.

Chapter 4

RESULTS AND DISCUSSION

Phase I

4.1. Retrieved material analysis

4.1.1. Contact angle analysis

The SE was hydrophobic with a contact angle of 110.24 ± 1.34^0 in comparison to the UHMWPE which was hydrophilic with a contact angle of 77.28 ± 2.1^0 as shown in Figure 8.

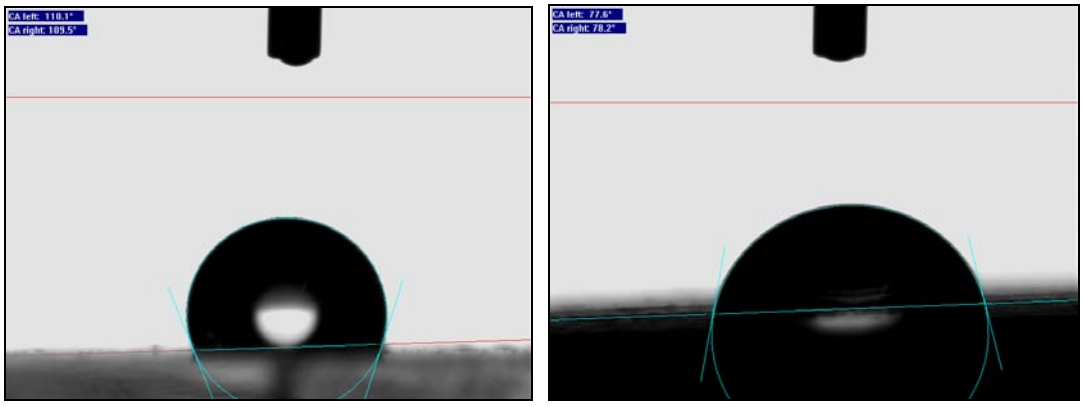

A B

Figure 8. Contact angle measurement of SE (A) and UHMWPE (B).

4.1.2. Fourier Transform-Infrared spectroscopy analysis

The spectral pattern obtained for SE pre-implantation showed peaks matching with spectrum of standard, poly dimethyl siloxane (Figure 9).

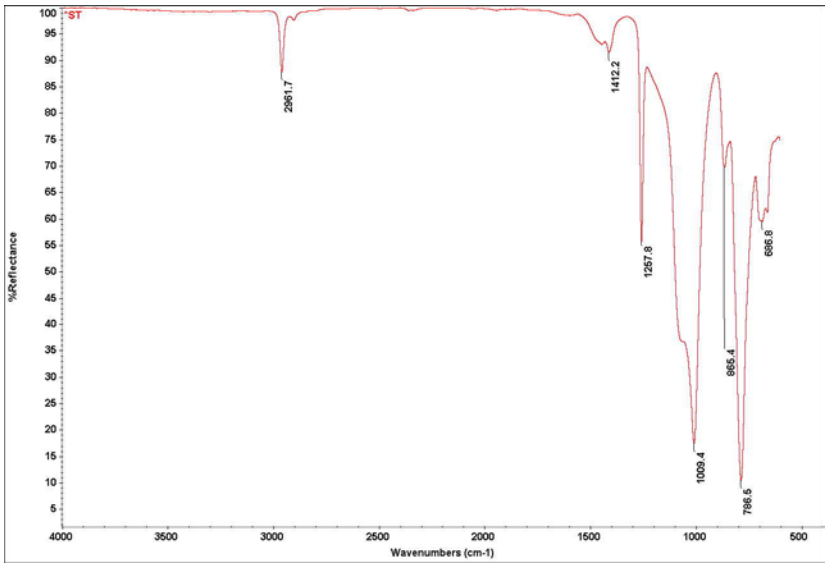

Figure 9. FTIR spectrum of SE material pre-implantation

. *In vivo* studies – Rat

. Histology

The initial severe inflammatory response at 3 days and 7 days (Figure 10A, 10C and 11B, 11D) post implantation was similar around both SE and UHMWPE implants. The implant infiltrate was composed of neutrophils, macrophages and occasional fibroblast and is similar to that reported by Anderson JM, 2001. A reduction of inflammatory cells was seen at 30 (Figure 11B) and 60 days around UHMWPE with complete absence at 180 days (Figure11L). A thick collagenous capsule observed at 30 days gradually reduced in thickness by 180 days. However at the SE-tissue interface, inflammation though reduced, persisted at 30, 60 and 180 days (Figure 11A, C and E) with the formation of a thick fibrotic capsule at 180 days (Figure 11E).

The tissue response around an implant is similar to that following an injury i.e. inflammation followed by repair with the formation of a thin fibrous capsule around the implant. In this study, initial infiltration of macrophages and lymphocytes along with fibroblasts around both silicone and UHMWPE also is similar to that observed in the

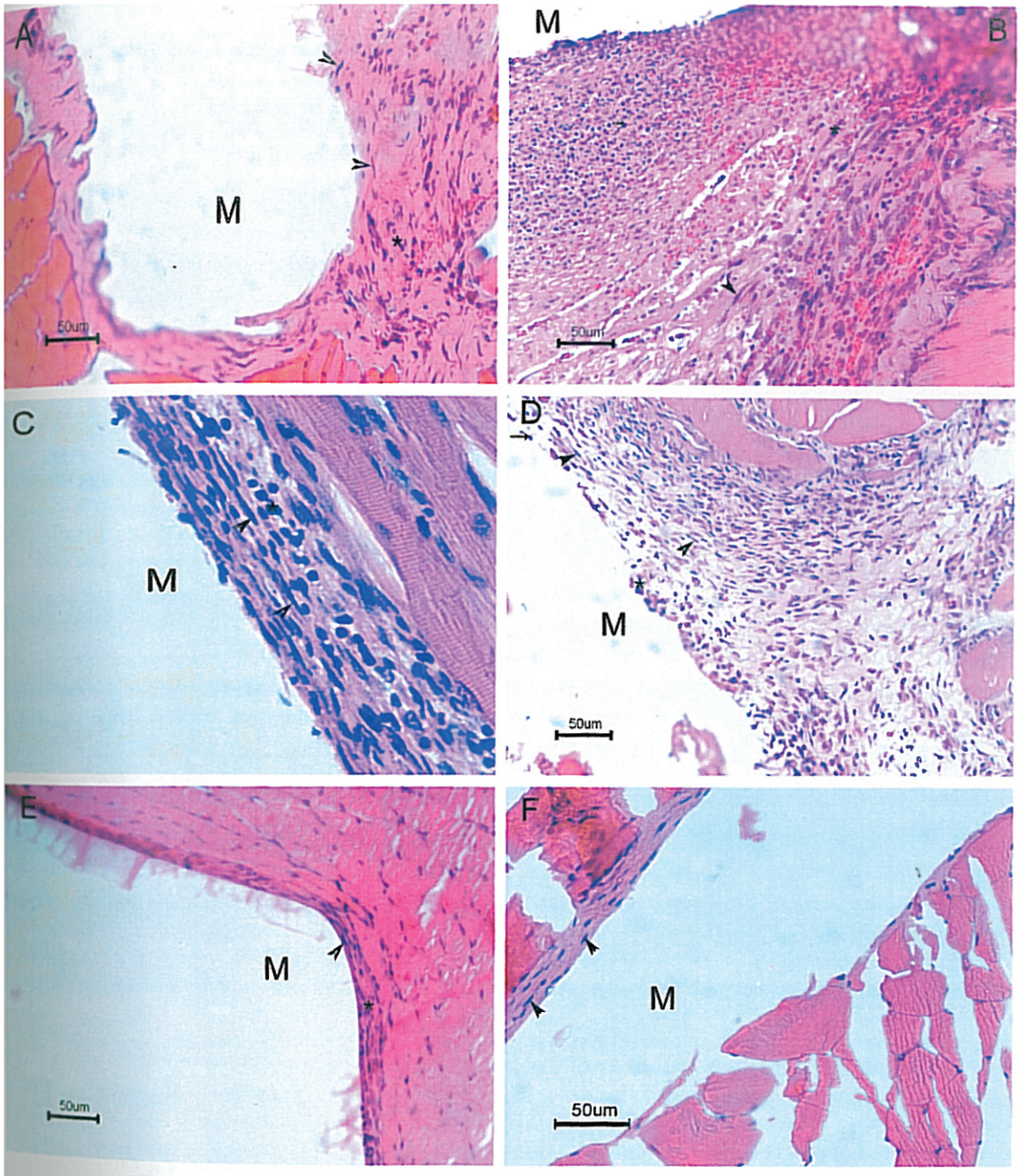

Figure 10: Light micrographs of Haematoxylin & Eosin stained sections of muscle around **Silicone expander**: 3days; 7days; 14days (A, C, E) and **UHMWPE** : 3days; 7days; 14days (B, D, F).
(M -Implant site, ➤ - Fibroblast, * - Macrophage)

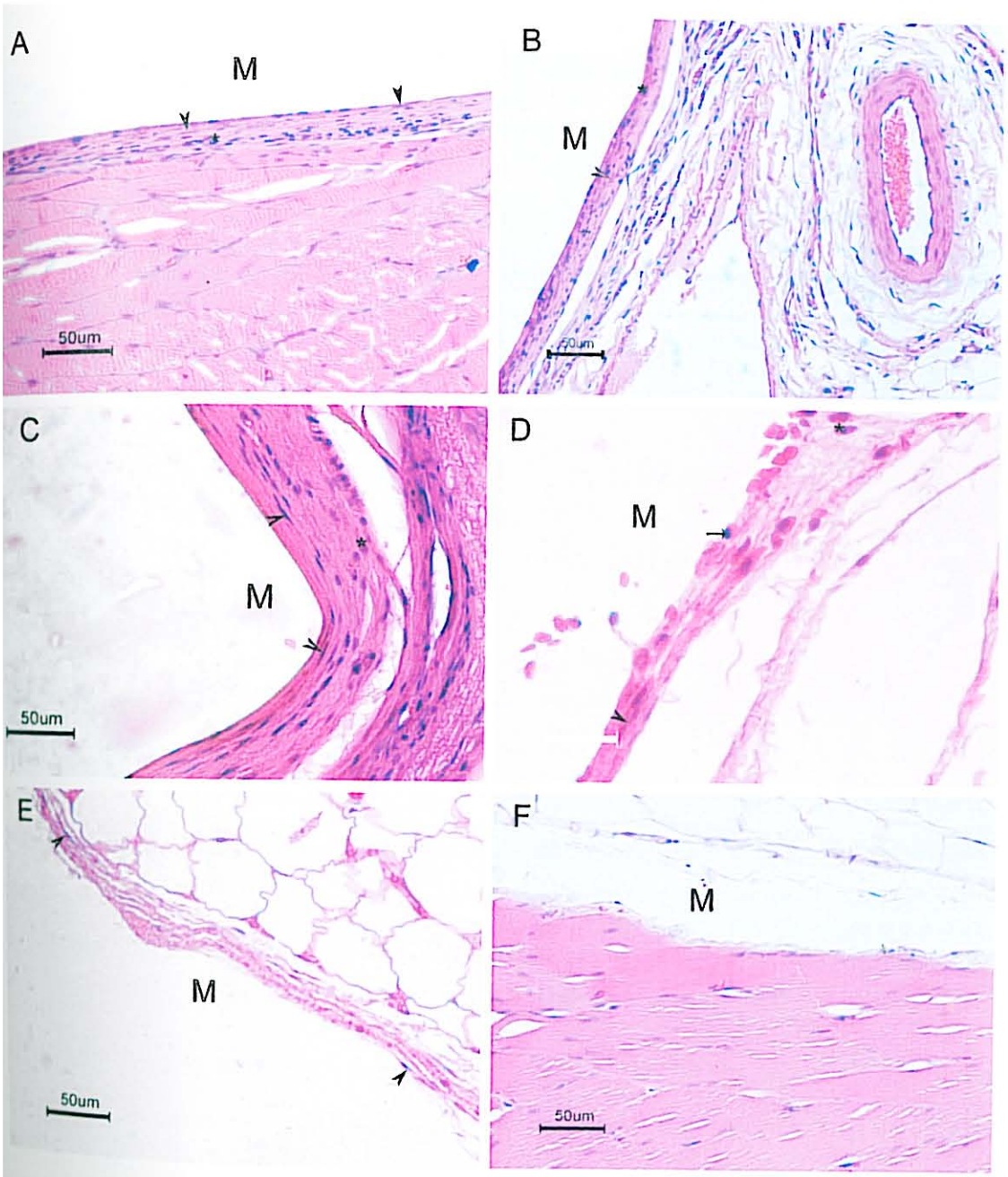

Figure 11: Light micrographs of Haematoxylin & Eosin stained sections of muscle around **Silicone expander**: 30days; 90days; 180days (A, C, E) and **UHMWPE**: 30 days; 90days; 180days (B, D, F)
(M - Implant site, ⮜ - Fibroblast, * - Macrophage, ↑ - Lymphocyte)

progress of healing of an incision by first intention. The difference in the healing phase around both materials is notable with the persistence of few macrophages and lymphocytes in the thick collagenous capsule around the silicone elastomer at 180 days post implantation. In contrast there is an absence of these cells in the thin fibrous capsule around UHMWPE at the same time period. Fibrosis is the response of fibroblasts to stimulation by cytokines, typically produced in chronic inflammation. The main cell types in fibrotic tissue are fibroblasts and myofibroblasts and in chronic inflammation contributes to walling off of the infected area or foreign body (Majno *et al.,* 1996).

The fate of the implant in host is determined by both the physico-chemical properties of the implant as well as the various biological components to which the implant is exposed to in the body. Inflammatory cells and various cytokines have been identified in the fibrous capsule around failed breast prosthesis. The foreign body response has been attributed to the silicone droplets also seen in the tissue due to silicone gel seepage or following degradation of the silicone shell. In our study, no silicone was identified in the adjacent tissue. However, microscopic examination is not enough for identification of silicone particles. Experimental studies in rats have dealt with study of the tissue response around SE. However, these studies have been short termed and are related to the tumorogenic potential of this material (Abbondanzo SL *et al***.,** 1999)**.**

4.2.2. Trichrome staining for collagen

Trichrome staining revealed deposition of collagen around both implants at 30days (Figure 12A, 12B) following implantation. There was a gradual increase over time with a thick capsule of collagen being present at 90 days (Figure 12C) which reduced at 180 days (Figure 12E) around the SE. On the other hand scant collagen was observed at the UHMWPE interface at all time periods (Figure 12B, D, E). The fibrous capsule thickness quantitated from five different areas is represented graphically in Figure13.

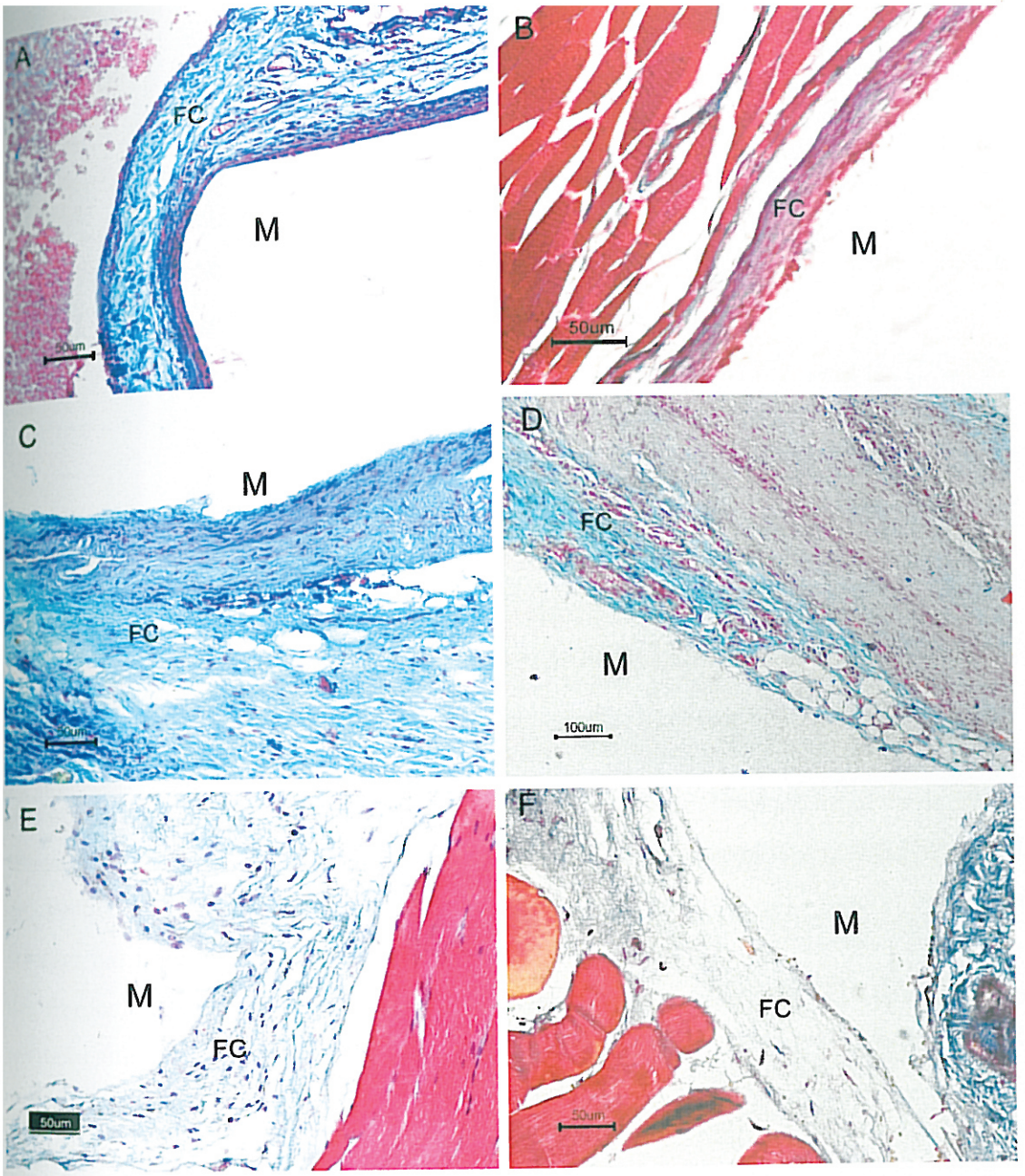

Figure 12: Light micrographs of Masson's trichrome stained sections of muscle around **Silicone expander**: 30 days; 90 days; 180 days (A, C, E) and **UHMWPE**: 30 days; 90 days; 180 days (B, D, F)
(M - Implant site, FC - Fibrous capsule)

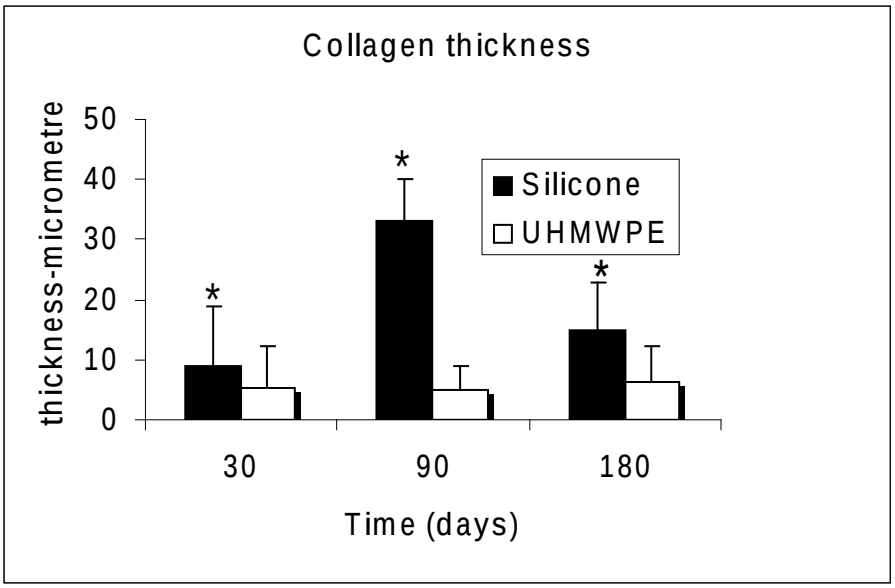

Figure 13: Quantitative evaluation of collagen deposition around silicone and UHMWPE.

Measurement of fibrous capsule thickness in Masson's trichrome stained tissue sections is a reliable method for collagen quantitation. It has been reported earlier that the fibrous capsule forms around implant usually within a short time of two months (Picha GJ *et al.,* 1990). We could observe that the thickness of collagen capsule increased to maximum at 90 days but resolved at 180 days (Figure 13). There was statistically significant difference in the fibrous capsule thickness between both the implants. Earlier studies have reported that textured silicone implants are more effective in preventing scar contracture (Pollock H *et al.,* 1993). How ever the material used in this study was smooth surfaced as evident from SEM images (Figure 27 and Figure 28).

4.2.3. Immunohistochemical identification of cells and cytokines in peri-implant tissue

Cells:

Immunophenotyping of different cells present at the tissue material interface showed an initial large number of macrophages around both implants at 30 days (Figure 14A, B). *Macrophage* infiltration remained intense around SE at 90 days (Figure 14C) with a gradual

decrease to a few cells at 180 days (Figure 14E). The number was slightly less around UHMWPE at 90 days (Figure 14D) and absent at 180days (Figure 5F) whereas they were persistent around silicone even at 180 days (Figure 14E).

T Helper cells were intensely expressed around SE at 30 days (Figure 15A) with a gradual reduction to moderate numbers at 90 days (Figure 15C) and remained mild at 180 days (Figure15E). Cells were absent around UHMWPE at 180 days (Figure 15F).

Fibroblasts were few at the SE -tissue interface at 30 days (Figure16A) which increased mildly at 90 days (Figure 16C) and reduced to few at 180days (Figure16E). The increase at 90 days is concomitant with increase in collagen too and decrease at 180 days is also concomitant with slight reduction in collagen (Figure 13). A similar trend was noted around UHMWPE (Figure 16B, D, F).

At 30 days few *Myofibroblasts* were present around SE (Figure 17A) but occasional around UHMWPE (Figure 17B). An increase to moderate levels was noted at 90 days (Figure 17C) which remained steady at 180 days (Figure 17E). On the other hand myofibroblasts were fewer around UHMWPE at early time periods and absent at 180 days (Figure 17 B, D, F). The qualitative evaluation data is summarized in table 7.

Table 7: Qualitative evaluation of immune cells at peri-implant tissue

Cells	**Antibody**	**30 days**	**30 days**	**90 days**	**90 days**	**180days**	**180 days**
		UHMWPE	**SE**	**UHMWPE**	**SE**	**UHMWPE**	**SE**
Fibroblasts	**Vimentin**	+	+	+++	++++	++	++
Myofibroblasts	**αSMA**	+	++	++	++++	nil	++++
Macrophages	**ED2**	**++++**	++++	++	+++	nil	+
T_H Lymphocytes	**CD4**	**++++**	++++	nil	+++	nil	+++

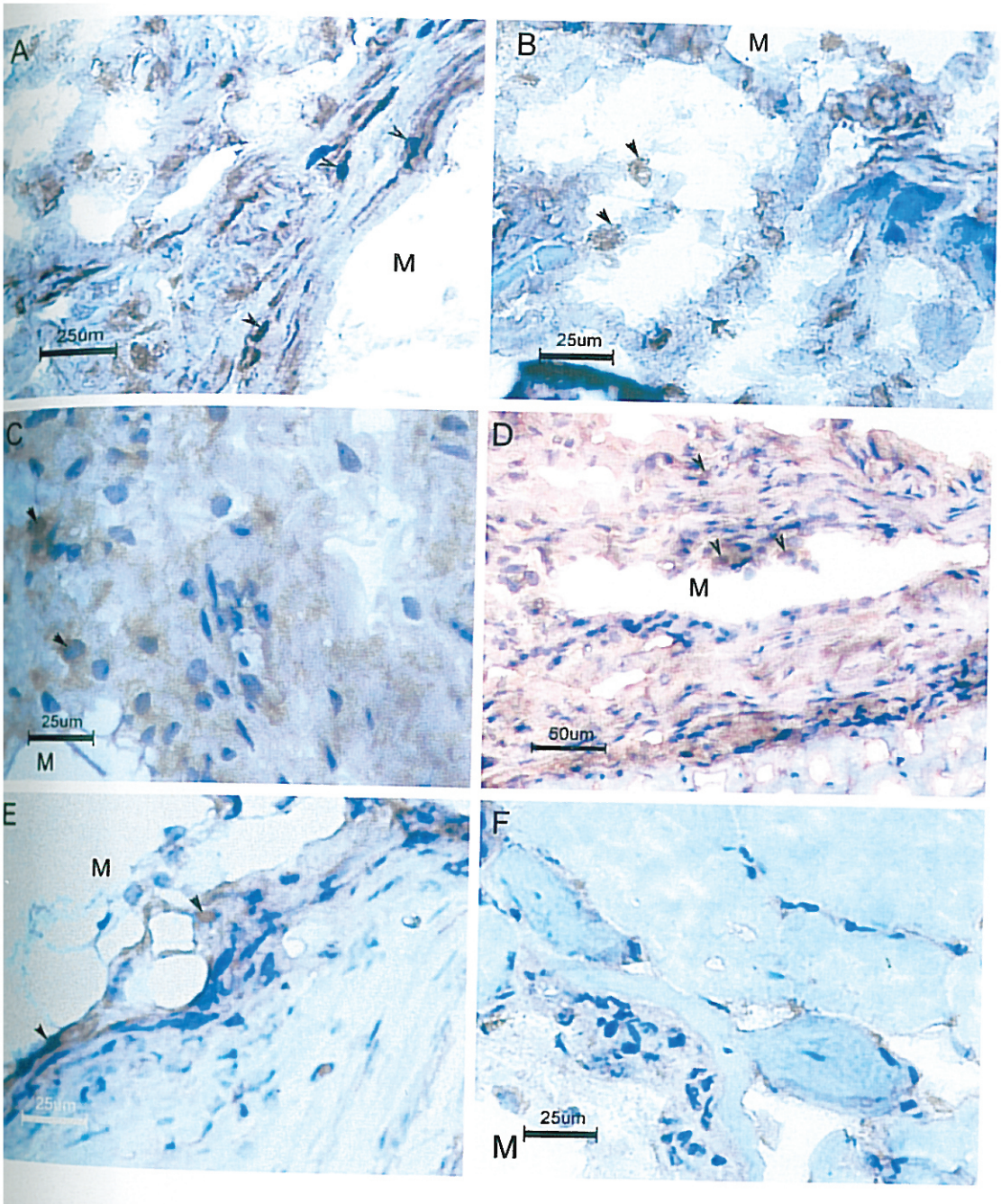

Figure 14: Light micrographs of immunohistochemical staining for ED2 (macrophages) in sections of peri implant tissue around **Silicone expander**: 30 days; 90 days; 180 days (A, C, E) and **UHMWPE** : 30 days; 90 days; 180 days (B, D, F). (M - implant site, ▲ - immuno positive cells)

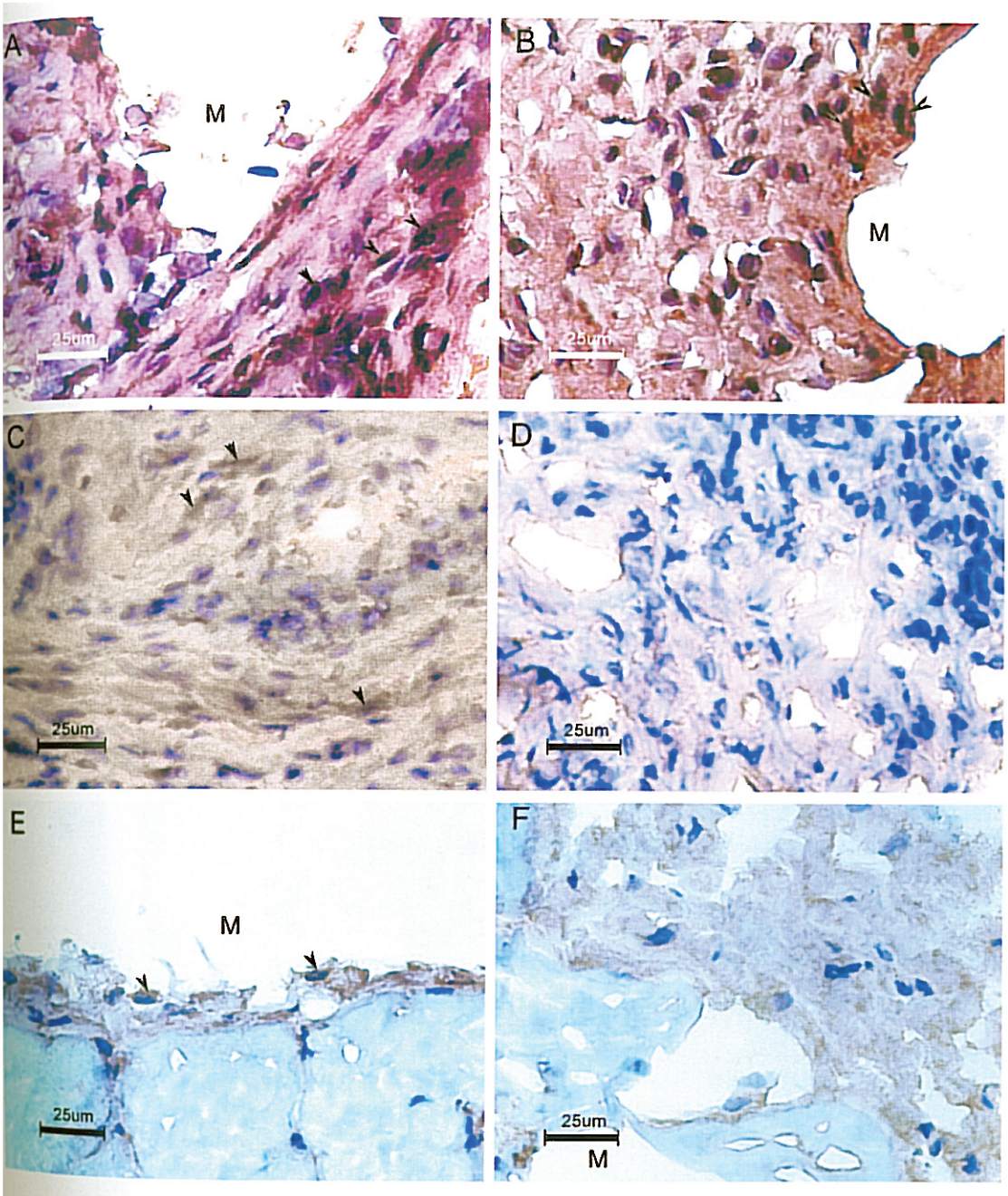

Figure 15: Light micrographs of immunohistochemical staining for CD4 (T lymphocytes) in sections of peri implant tissue around **Silicone expander**: 30 days; 90 days; 180 days (A, C, E) and **UHMWPE**: 30 days; 90 days; 180 days (B, D, F).
(M - implant site, ▲ - immuno positive cells)

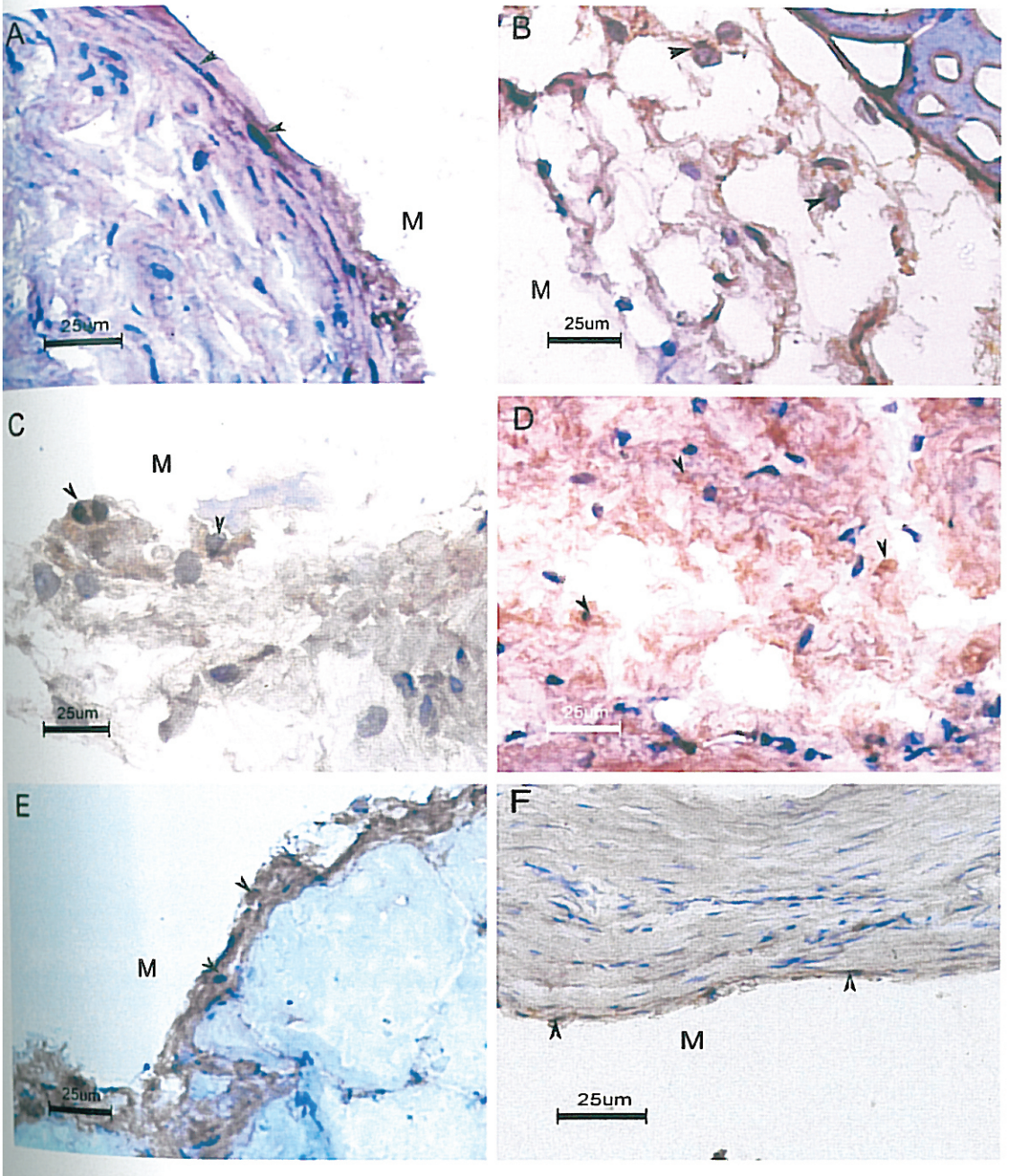

Figure 16: Light micrographs of immunohistochemical staining for vimentin (fibroblasts) in sections of peri implant tissue around **Silicone expander**: 30 days; 90 days; 180 days (A, C, E) and **UHMWPE**: 30 days; 90 days; 180 days (B, D, F). (M - implant site, ⮝ - immuno positive cells)

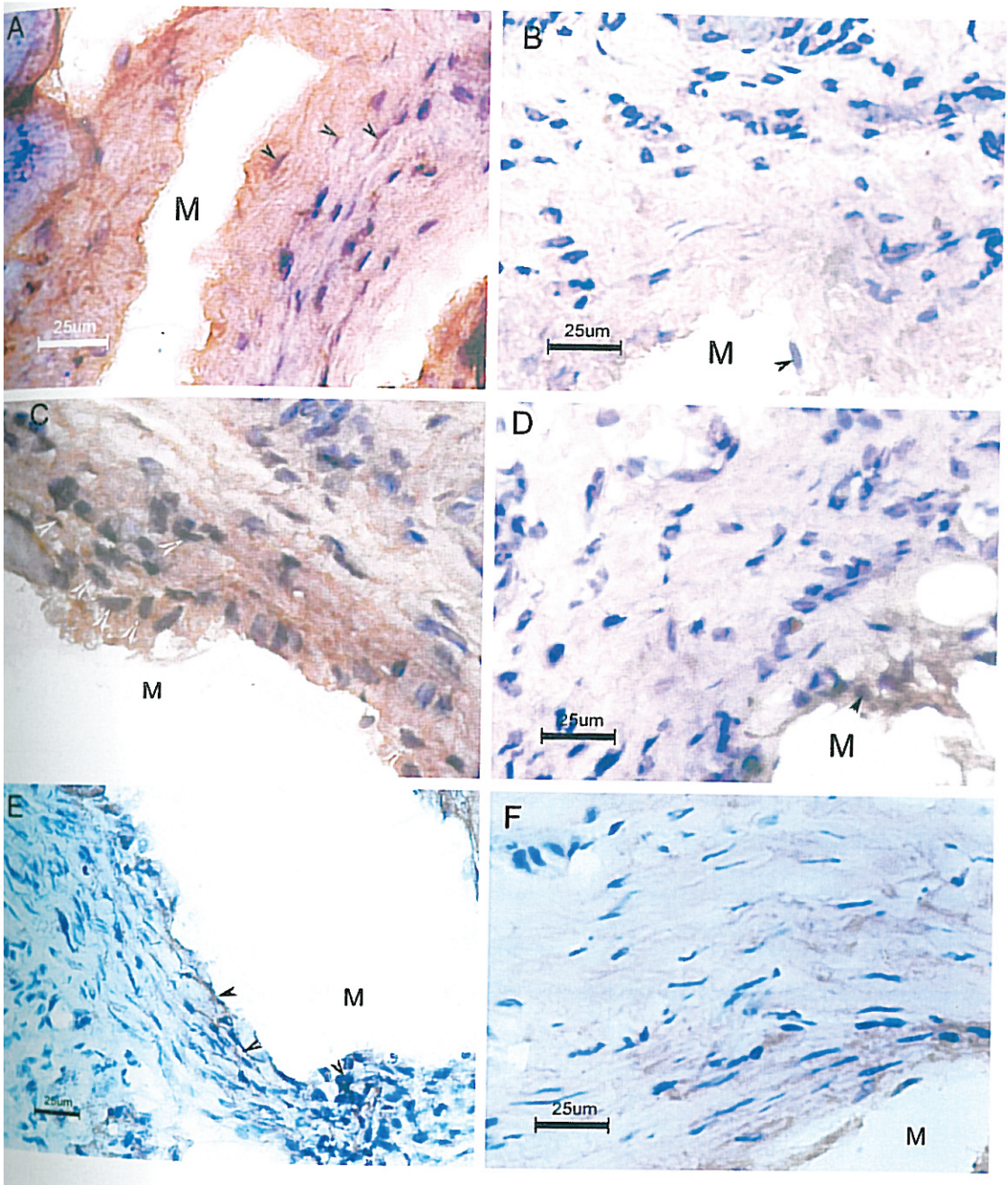

Figure 17: Light micrographs of immunohistochemical staining for αSMA (myofibroblasts) in sections of peri implant tissue around **Silicone expander**: 30 days; 90 days; 180 days (A, C, E) and **UHMWPE**: 30 days; 90 days; 180 days(B, D, F).
M - implant site, ⋀ - immuno positive cells)

Numerous studies have related the inflammation and activation of macrophages with release of cytokines, to individual chemical components of the silicone shell (Tavazzani F *et al.,* 2005). Subpopulations of macrophages were phenotyped using antibodies to ED2.CD 163 or ED2 is a cell surface glycoprotein of 175KD. It is expressed by approximately 50% of peritoneal macrophages, a subset of splenic macrophages and by resident mature macrophages in most other tissues and not expressed by monocytes. Our results are in corroboration with findings of Mancino *et al.* that macrophage plays an important role in the wound healing around silicone implants and they do persist even at long term (Mancino D *et al.*,1984).The immunohistochemical results supported the data from Hematoxylin& eosin staining.

T lymphocytes were identified by using specific antibody that recognizes CD4 cell surface glycoprotein of helper T cells. It was reported that Strong T cell immune response was noted in immunohistochemical studies of retrieved capsule tissue from patients (Dolores W *et al.,* 2004). Flow cytometric studies of patient samples revealed that 89% of implant associated lymphocytes were T cells (Katzin WE *et al.,* 1996). T cell receptors were also identified in capsular tissue (Hanlon TPO' *et al.,* 1996). It is possible that silicone implant either directly or indirectly induces a specific T-cell dependant immune response and the sensitization of the lymphocytes with the foreign material silicone, might proceed locally in the capsular tissue (Dolores W *et al.,* 2004).

Fibrosis is the response of fibroblasts to stimulation by cytokines; typically produced in chronic inflammation. The main cell types in fibrotic tissue are fibroblasts and myofibroblasts and in chronic inflammation contributes to walling off of the infected area or foreign body (Majno *et al.,*1996). Fibroblasts in the capsular tissue were identified by specific antibody against vimentin. It was observed that the number of fibroblasts were decreasing over time. This may be indicative of cells undergoing apoptosis as in normal wound healing or transformation of fibroblasts to phenotypically different cells, myofibroblasts.

Myofibroblasts of wound tissue have been assumed to originate from local recruitment of fibroblasts in the surrounding dermis and subcutaneous tissue (Ross R

et al., 1970)**.** Another possible source being pericytes or vascular smooth muscle cells around vessels in the granulation tissue. Circulating precursor cells, called fibrocytes, will migrate to wound and contribute to the formation of the myofibroblastic population of granulation tissue (Gabbiani G *et al.,* 1998). The most prominent marker of fibroblast to myofibroblast transition is αSMA (Desmouliere A *et al.,* 1992). The expression of myofibroblasts was increasing around SE over time in comparison with UHMWPE as shown in Table 7. Normally in wound healing, myofibroblasts disappear by apoptosis in later stages (Darby I *et al*., 1990). Inappropriate delay of apoptosis, and thus increased survival of activated myofibroblasts during the healing process, may be a factor which leads to excessive scarring in fibrosis (Desmouliere A *et al*., 1995*)*. Thus it is evident that the fibrogenic cytokines released by macrophages are playing a prominent role in survival of the myofibroblasts in the peri-implant tissue.

Cytokines:

TGFβ was intensely expressed at tissue-SE interface at 30 days (Figure 18A) which decreased to moderate levels at 90 days (Figure 18C) and was mild at 180 days (Figure 18E). The cytokine was mild around UHMWPE at 90 days (Figure 18D) and absent at 180 days (Figure 18F). The pro-inflammatory cytokine TNFα was moderately expressed at 30 days around SE (Figure 19A), with gradual reduction over 90 days (Figure 19C) being present in focal areas and mild at 180 days(Figure 19E). The cytokine was much less around UHMWPE at 90 days (Figure 19D) and absent at 180 days (Figure 19F). IL-1α was expressed at similar levels of TGFβ at 90 days around SE (Figure 20C) with mild expression at180 days (Figure 20E). The cytokine was intensely expressed around UHMWPE at 30 days (Figure 20B), moderately at 90 days (Figure 20D) and was absent at 180 days (Figure 20F). IL-1β was moderately expressed around SE at 90 days (Figure 21C) and was mild at 180 days (Figure 21E). The expression was intense around UHMWPE at 90 days (Figure 21D) and remained steady at moderate levels at 180 days (Figure 21F).

The collagenase stimulating cytokine IFNγ was intensely expressed around SE at 30 days (Figure 22A) reduced to mild at 90 days (Figure 22C) but increased to moderate at 180days

(Figure 22 E). It was expressed moderately around UHMWPE at 90 days (Figure 22D) but reduced to mild at 180 days (Figure 22F). IL-6 was moderately expressed at 90 days around SE (Figure 23C) with expression being slightly more around UHMWPE (Figure 23D).Expression reduced but persisted around SE at 180days mildly(Figure 23E) but was absent around UHMWPE (Figure 23F). Moderate expression of IL-10 was there around SE at 90 and 180 days (Figure 24 C, 24 E) with no reduction in expression where as around UHMWPE it reduced from mild at 90 days (Figure 24D) to nil at 180 days (Figure 24 F). The results are summarized in table 8**.**

Table 8: **Qualitative evaluation of cytokines in the peri-implant tissue**

Cytokines	**SE**			**UHMWPE**		
	30 days	**90 days**	**180 days**	**30 days**	**90 days**	**180 days**
TGFβ	+++	+++	+	++	+	nil
TNFα	+++	++	+	++	+	nil
IL-1α	+++	+++	++	++	++	nil
IL-1β	++	++	+	+++	+++	++
IFNγ	+++	+	++	++	++	+
IL-6		++	+		+++	nil
IL-10		+++	+++		+	nil

Cytokines released by inflammatory cells are involved through their effect on fibroblasts, in modulation of collagen deposition in the repair phase. **TGFβ** which is profibrotic, is initially very high but gradually reduces to mild levels at 180 days. This appears contradictory, but actually it is concomitant with the amount of collagen deposited. A similar trend is observed around UHMWPE where it is lesser at 90 days and absent at 180 days.

This is also corroborated with the mild presence of **TNFα** which is profibrotic. Thus TNFα

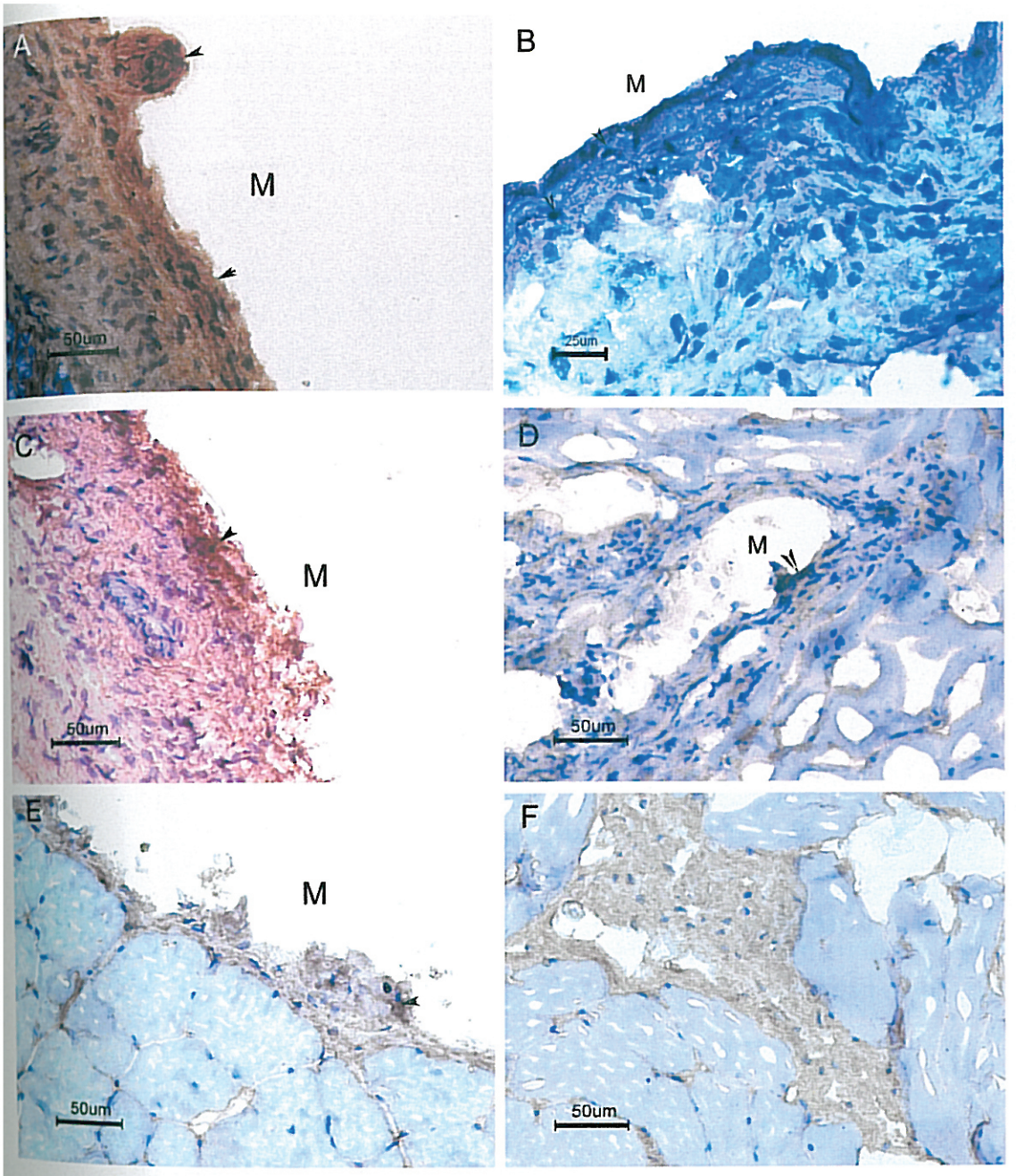

Figure 18: Light micrographs of immunohistochemical staining for TGFβ in sections of peri implant tissue around **Silicone expander**: 30 days; 90 days; 180 days (A, C, E) and **UHMWPE**: 30 days; 90 days; 180 days (B, D, F)
(M - implant site, ⮝ - positive staining)

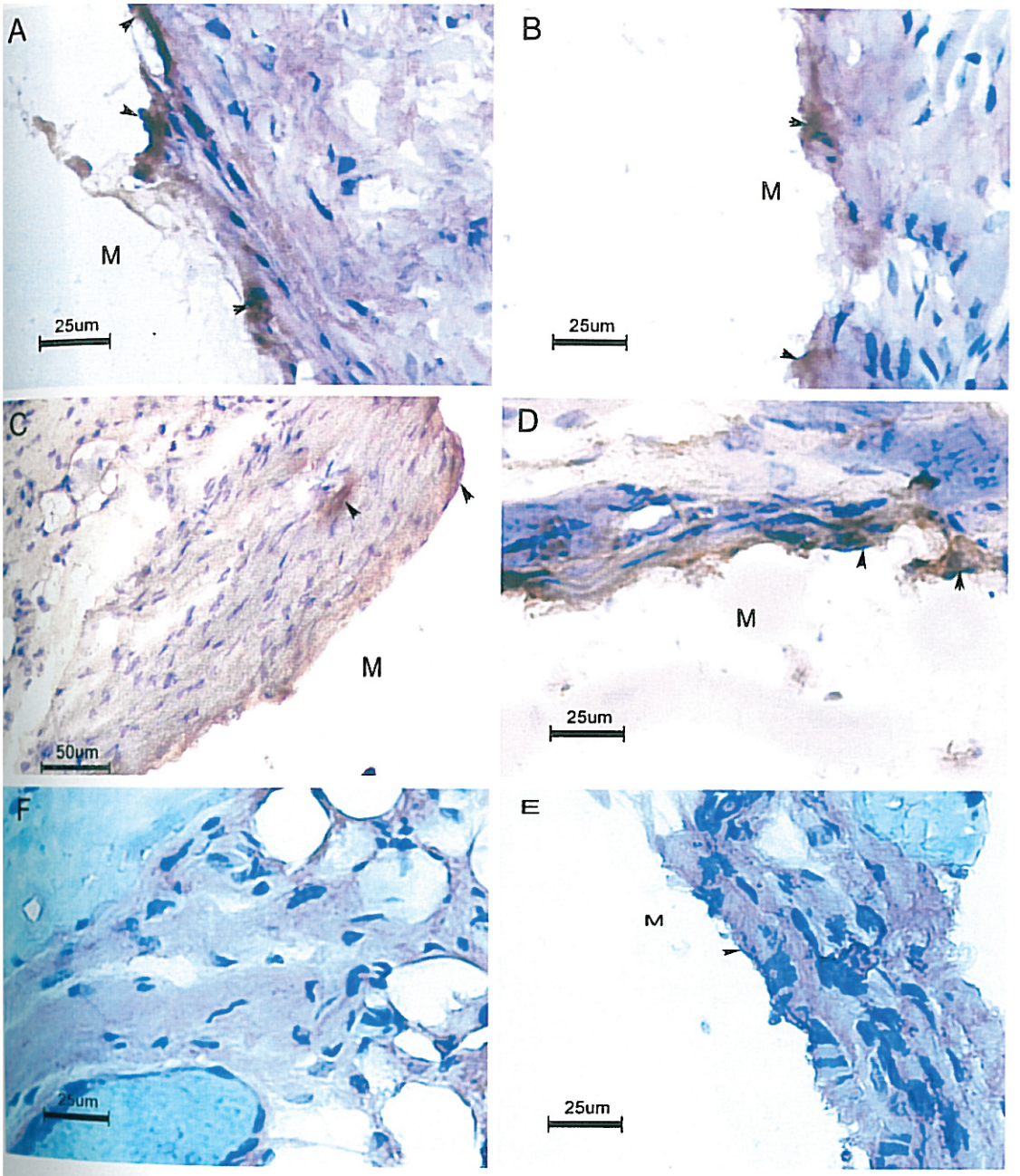

Figure 19: Light micrographs of immunohistochemical staining for TNFα in sections of peri implant tissue around **Silicone expander**: 30 days; 90 days; 180 days (A, C, E) and **UHMWPE**: 30 days; 90 days; 180 days (B, D, F)
(M - implant site, ▲ - positive staining)

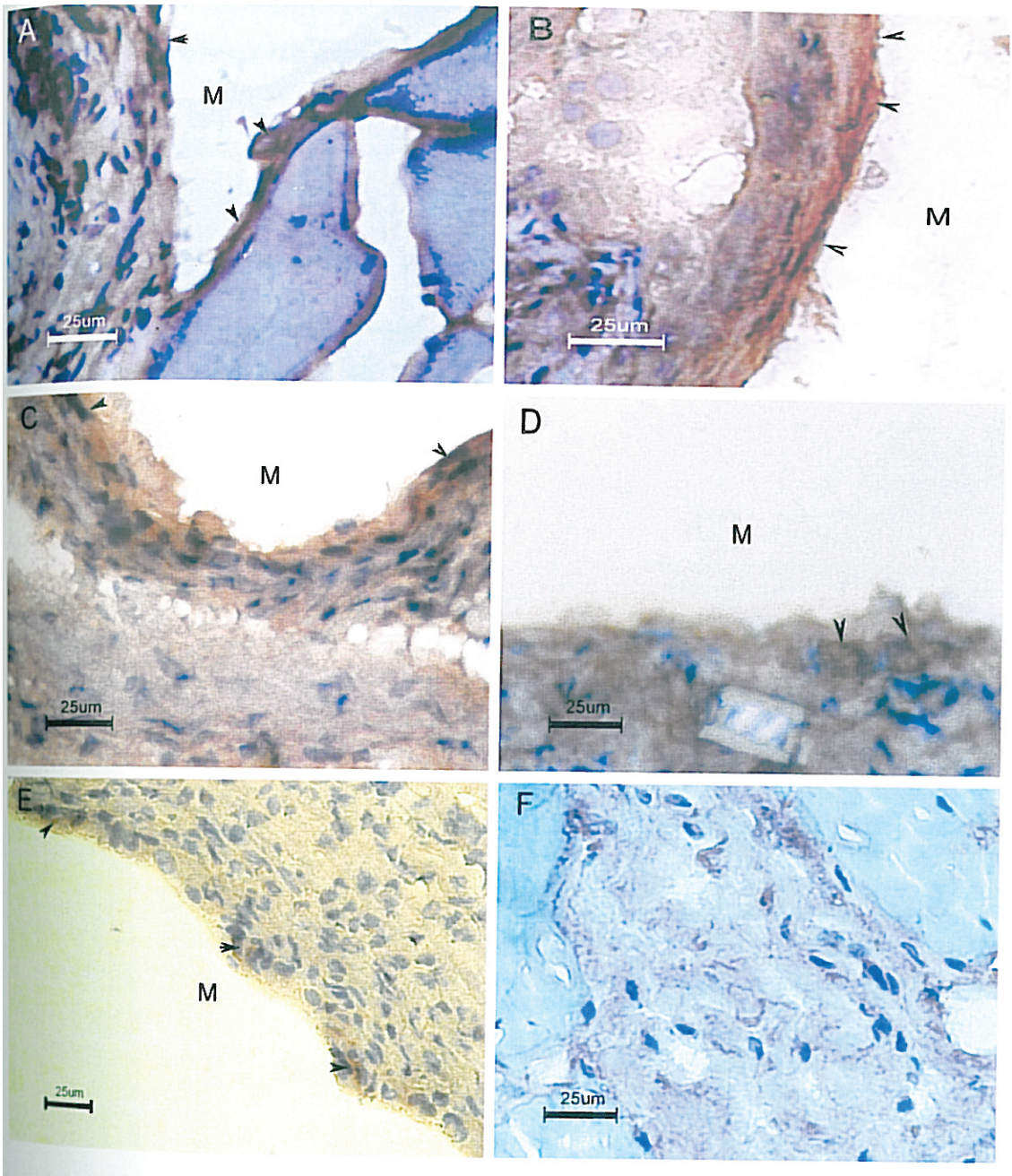

Figure 20: Light micrographs of immunohistochemical staining for IL-1α in sections of peri implant tissue around **Silicone expander**: 30 days; 90 days; 180 days (A, C, E) and **UHMWPE**: 30 days; 90 days; 180 days (B, D, F)
(M - implant site, ⮝ - positive staining)

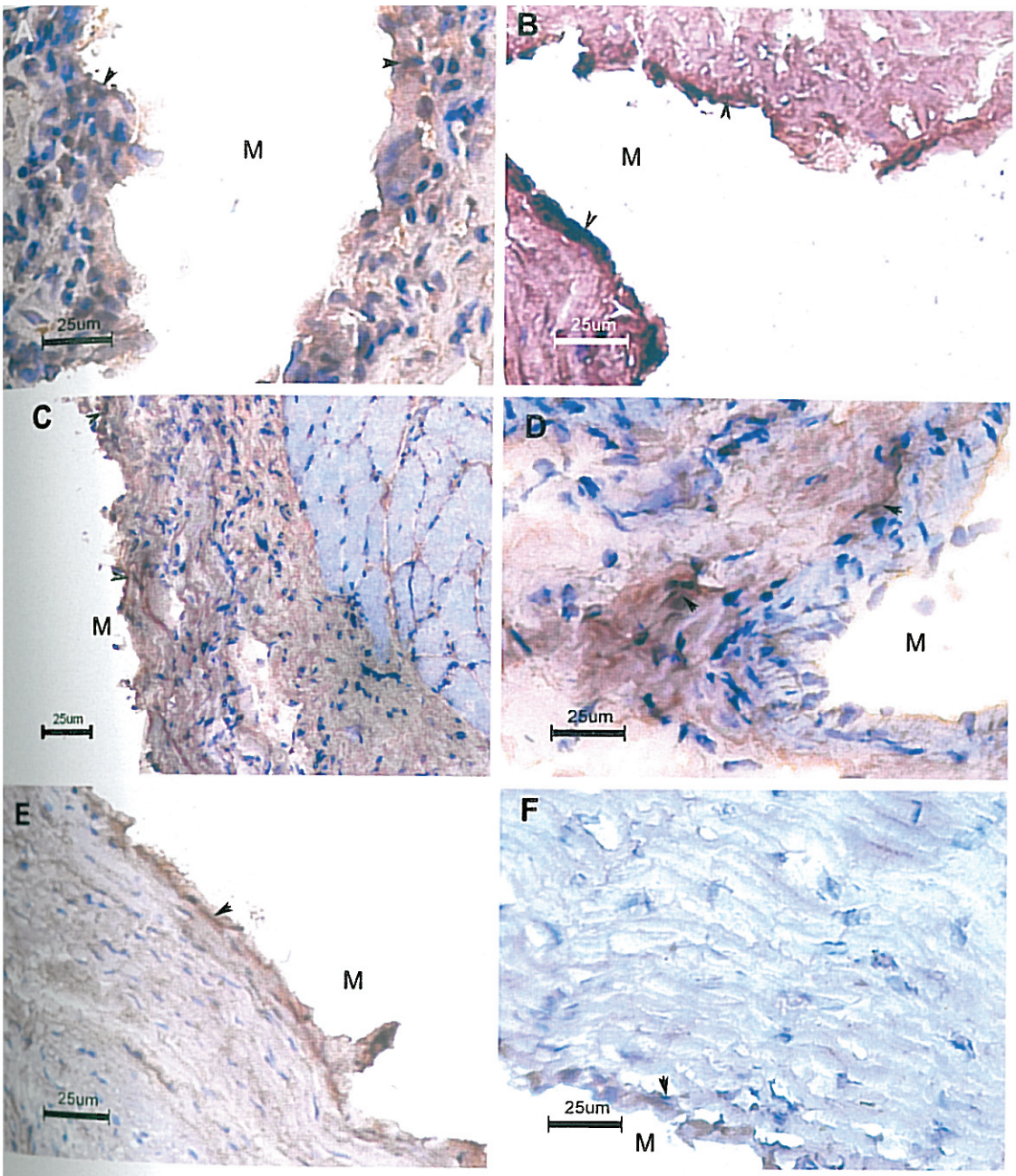

Figure 21: Light micrographs of immunohistochemical staining for IL-1β in sections of peri implant tissue around **Silicone expander**: 30 days; 90 days; 180 days (A, C, E) and **UHMWPE**: 30 days; 90 days; 180 days (B, D, F)
(M - implant site, ⮜ - positive staining)

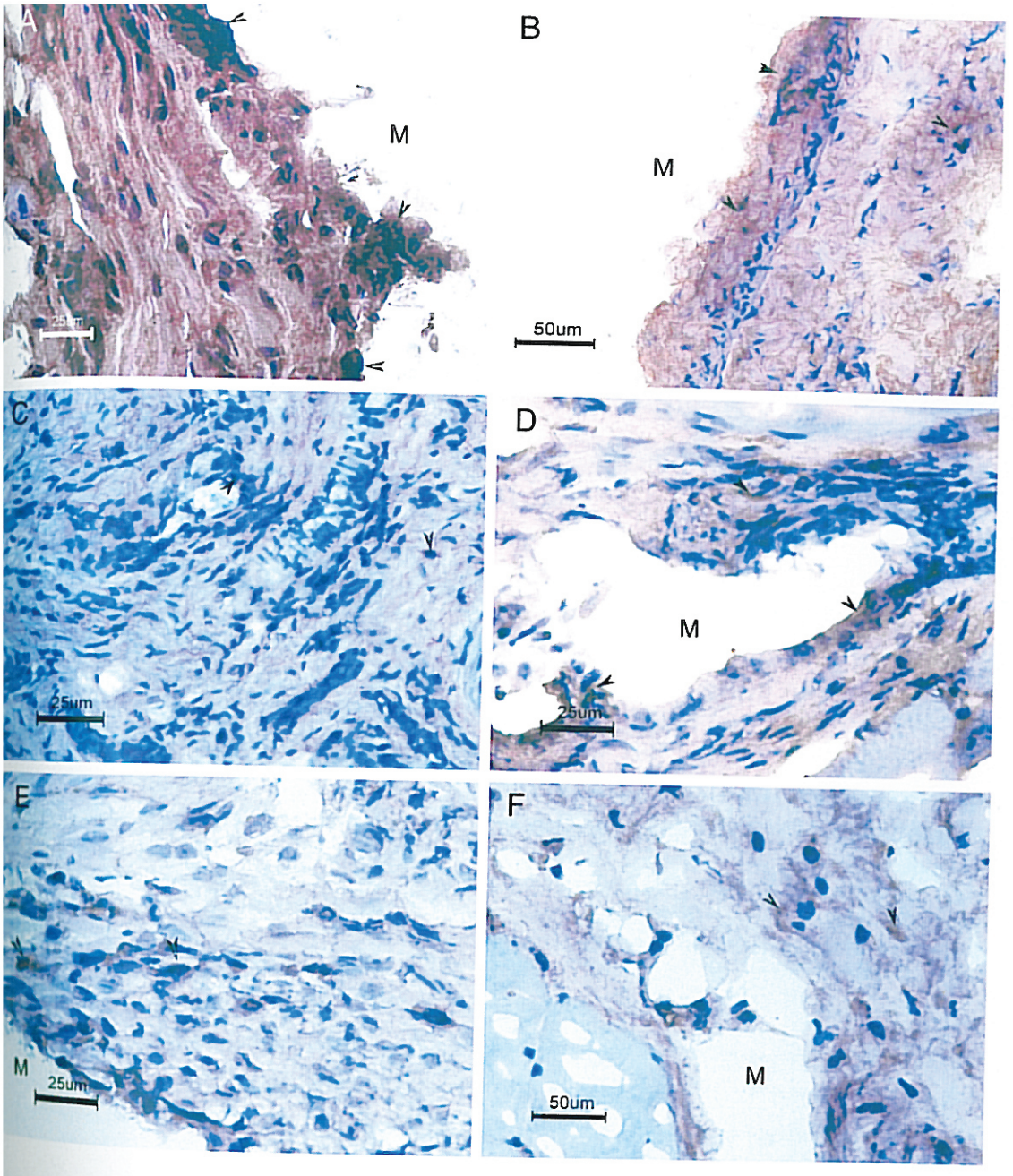

Figure 22: Light micrographs of immunohistochemical staining for IFNγ in sections of peri implant tissue around **Silicone expander**: 30 days; 90 days; 180 days (A, C, E) and **UHMWPE**: 30 days; 90 days;180 days (B, D, F)
(M - implant site, ▲ - positive staining)

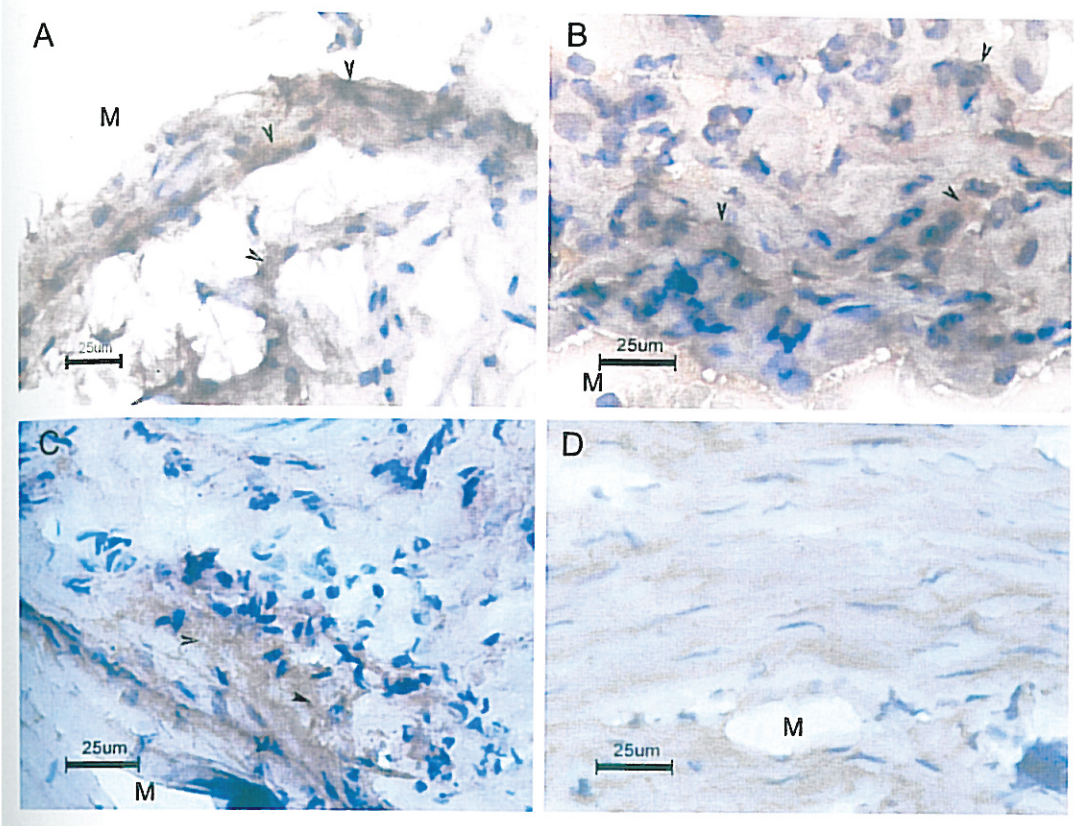

Figure 23: Light micrographs of immunohistochemical staining for IL-6 in sections of peri implant tissue around **Silicone expander**: 90 days; 180 days (A, C) and **UHMWPE**: 90 days; 180 days (B, D)
(M - implant site, ⋏ - positive staining)

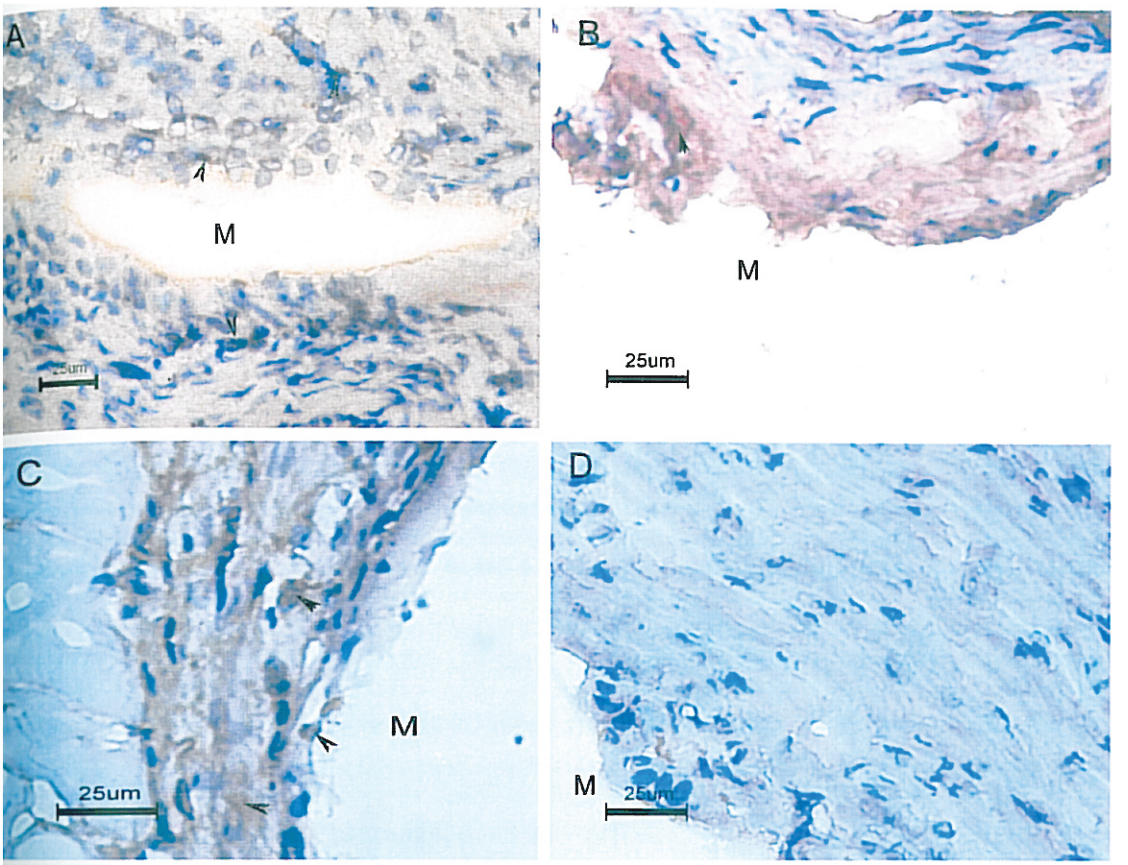

Figure 24: Light micrographs of immunohistochemical staining for IL-10 in sections of peri implant tissue around **Silicone expander**: 90 days; 180 days (A, C) and **UHMWPE**: 90 days; 180 days (B, D)
(M - implant site, ⮝ - positive staining)

and TGFβ are both responsible for modulating the collagen thickness around silicone implant. But Desmouliere *et al.* reported that TGFβ1 induces αSMA expression in granulation tissue myofibroblasts and in quiescent and growing cultured fibroblasts and other cytokines like PDGF AND TNFα, despite their pro fibrotic activity, do not induce αSMA in myofibroblasts (Desmouliere A *et al.*, 1992). Around UHMWPE, both are absent which was reflected in the thin collagen layer around the implant.

TGFβ and IFNγ exert opposite effects on collagen synthesis (Weng H *et al.*, 2007). **IFNγ** which has the capacity to decrease collagen content in wounds (Ghosh AK, 2001) and reduce myofibroblasts also appears to be concomitant with the collagen and myofibroblasts around SE. Its mild presence at 90 days and moderate levels at 180 days is concomitant with increase in collagen at 90 days and reduction at 180 days. Similar features were also noted around UHMWPE. The increase at 90 days and decrease at 180 days is concomitant with decrease of collagen at 90 days and steady at 180 days. $CD4^+$ cells which are present at 90 and 180 days have been established as the primary source of IFNγ in wound healing (Kampfer H *et al.*, 2000). However, the mild presence of IFNγ, absence of CD4 cells and thin capsule around UHMWPE appears to be contradictory.

At 180 days **IL1α** is present and **IL1β** is absent around SE. Earlier reports support the notion that IL-1 α and β may both modulate the degradation of collagen at sites of tissue injury by virtue of their ability to stimulate collagenase and PGE2 production by fibroblasts (Ziats NP *et al.*, 1988). Both cytokines might also direct reparative functions of fibroblasts by stimulating their proliferation and synthesis of collagen and TIMP (Postlethwaithe AE *et al.*, 1988). The collagen thickness around both silicon expander and UHMWPE reflect the expression of both cytokines. Also in case of IL1β around SE there is concomitance with collagen with a steady level being maintained around UHMWPE at 180 days.

Furthermore, the source of IL1 being mononuclear phagocytes, the few macrophages seen around SE at 180 days may be responsible for the presence of IL1α at 180 days. But, though macrophages are absent around UHMWPE, there is a presence of IL1β around UHMWPE, whereas it is opposite in SE. This may be due to the presence of other cells like fibroblasts in the peri implant tissue which can produce IL1 (Mauviel A *et al.*, 1999).

The probability of IL-6 having direct, crucial roles in proliferation and remodeling phases of wound healing by promoting collagen deposition and angiogenesis, has been reported earlier(Lin Z *et al.*, 2003). This appears to be corroborated in case of SE, with IL6 being present along with collagen deposition at 180days and absent around UHMWPE.

High expression of IL-10 was found in regions of infiltrating lymphocytes. IL-10 is mainly produced by the T_H2 subset of $CD4^+$ helper cells and the presence of CD4 cells as well as IL-10 at 180 days around SE and absence around UHMWPE is noted. Wells *et al.* have reported similar findings in capsular tissue around silicone implants. It was reported that anti inflammatory cytokines like IL-10 can modulate the effects of pro-inflammatory cytokines by inhibiting cytokine production and / or block cell receptor binding (de Waal MR *et al*., 1991).

4.2.4. Transmission electron microscopy

Understanding the relationship between biological response and biomaterial characteristics requires quantitative evaluation of the cells at the interface of the material. Ultra structural features of these cells are also important in understanding their physiology and functions (BehlingCA *etal*., 1986). Data obtained from transmission electron microscopic studies substantiated the results obtained from light microscopy.

The excessive fibrosis observed via light microscopy at longer time periods of 90 and 180 days, was confirmed via TEM. The electron micrographs revealed the presence of large amounts of collagen arranged in parallel bundles (Figure 25C, D and Figure 26.E, F). The characteristic banding pattern of collagen bundles were visible. Presence of both fibroblasts and myofibroblasts adjacent to the collagen bundles were observed around SE (Figure 25 D,E).

While normal fibroblasts contain a well developed rough endoplasmic reticulum with dilated cisternae and oval nucleus, myofibroblasts in addition to an abundant rough endoplasmic reticulum, neo express bundles of microfilaments with dense bodies(Desmouliere A *et al.*, 2004). Cells with intra cytoplasmic actin bundles and fibronexuses which are characteristics of myofibroblasts were noted at 180 days (Figure 25E,

25 F). The cells and the collagen bundles appeared to be arranged parallel to each other. Most of the fibroblasts were in synthetic stage with numerous large mitochondria and rough endoplasmic reticulum fibres (Figure 25 B, D). Numerous Rough endoplasmic reticulum and mitochondria, indicative of active state of cells were observed. Our results are in agreement with the observations of Eyden *et al.*, that the main ultra structural features for defining the myofibroblasts are abundant and prominent rough endoplasmic reticulum, modestly developed myofilaments with focal densities (stress fibres) and fibronexus junctions (Eyden B, 2003).

4.2.5. Analysis of surface morphology of retrieved materials

Scanning electron microscopy revealed the surface of SE to be smooth. Minimal to nil cell adhesion was noted on the surface at all time periods indicating the hydrophobic nature of the material. Occasional clumps of cells having a morphology resembling lymphocytes and macrophages (Figure 27E, 28A) and spindled cells with morphology of fibroblasts (Figure 27C) were noted at later time periods. Contact angle studies also showed the SE surface to be more hydrophobic than UHMWPE. It has been reported earlier that fibroblast attachment was more on hydrophilic surfaces as compared to hydrophobic surfaces (Webb K *et al.*, 1998). In our study we could observe that the cellular attachment was less at silicone surface at all time periods than over the more hydrophilic UHMWPE. This less adherence *in vivo* could be a factor in the formation of a compact fibrous layer around implant. Our studies are in agreement with Anderson *et al.* in that even though cell adhesion was less in hydrophobic silicone material, cellular activation with cytokine secretion was more on the SE than UHMWPE (Anderson JM, 2001).

4.2.6. Fourier transform- infrared spectroscopy

There was similarity between spectral peaks in pre and post implantation periods, except a change in the aliphatic hydrocarbon groups at 1460cm-1. FTIR studies were carried out to detect any change in surface functional moieties. There were no significant changes in surface moieties on SE after 180 days post implantation (Figure 29).

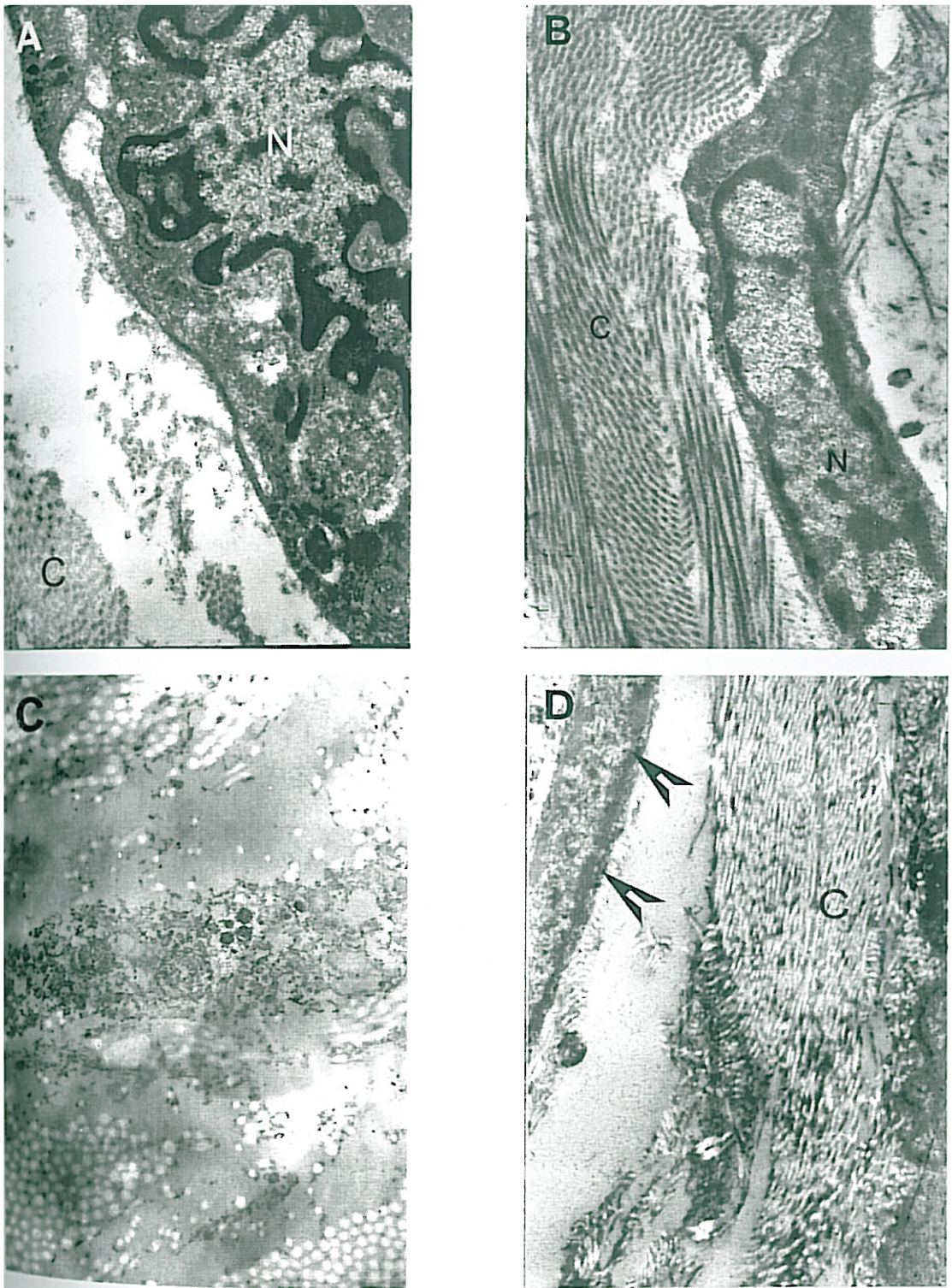

Figure 25: Transmission electron micrographs of ultra thin sections of peri implant tissue around **Silicone expander**: 30 days (A, B, C); 90 days (D) and 180 days (E, F). (C-Collagen, **N**-Nucleus, ⋀ - Fibronexuses)

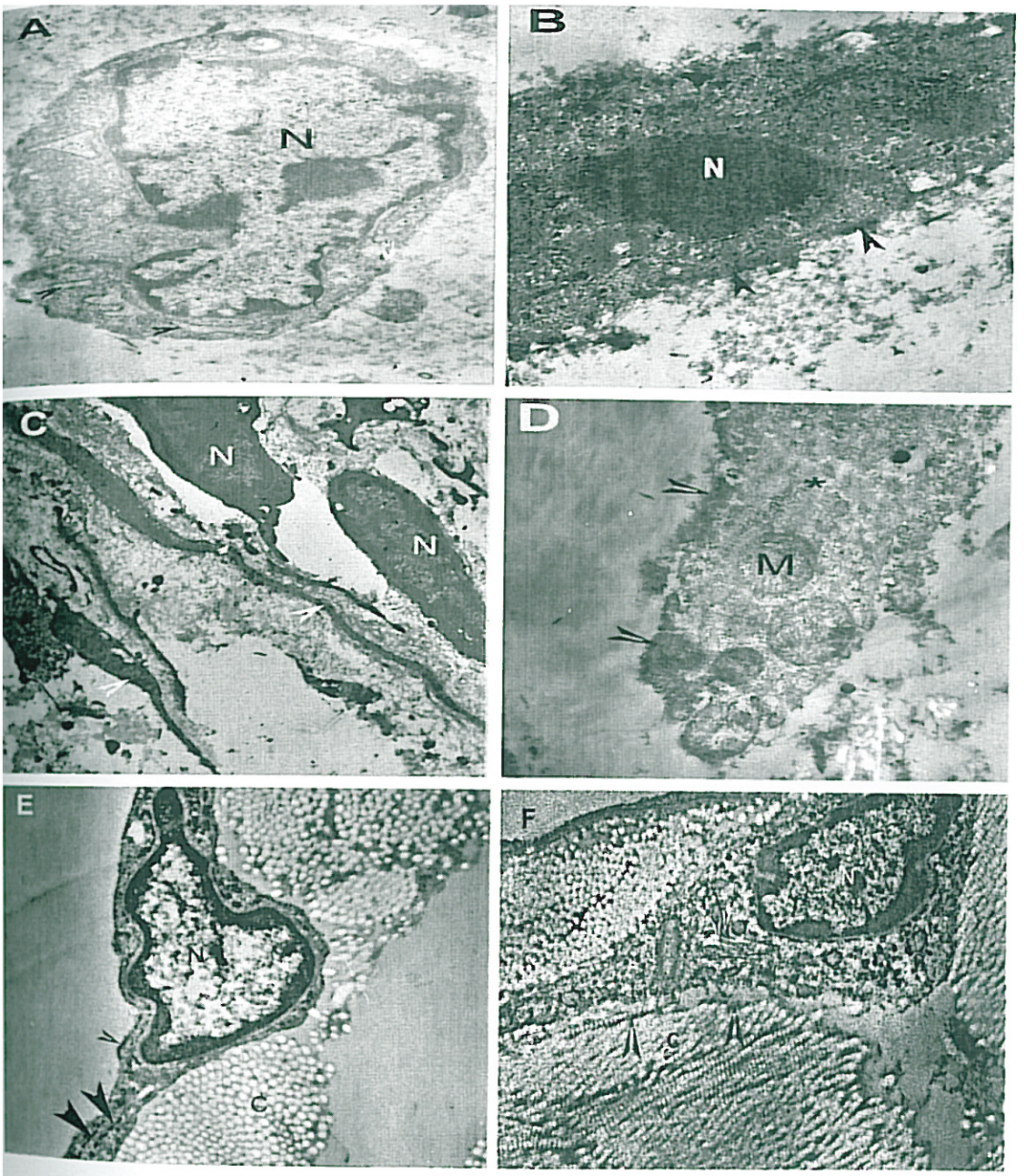

Figure 26: Transmission electron micrographs of ultra thin sections of peri implant tissue around **UHMWPE**: 30 days (A, B); 90 days (C) and 180 days (D).
(C- collagen, N-nucleus, M-mitochondria, ⮜ - Fibronexuses and intracytoplasmic bundles)

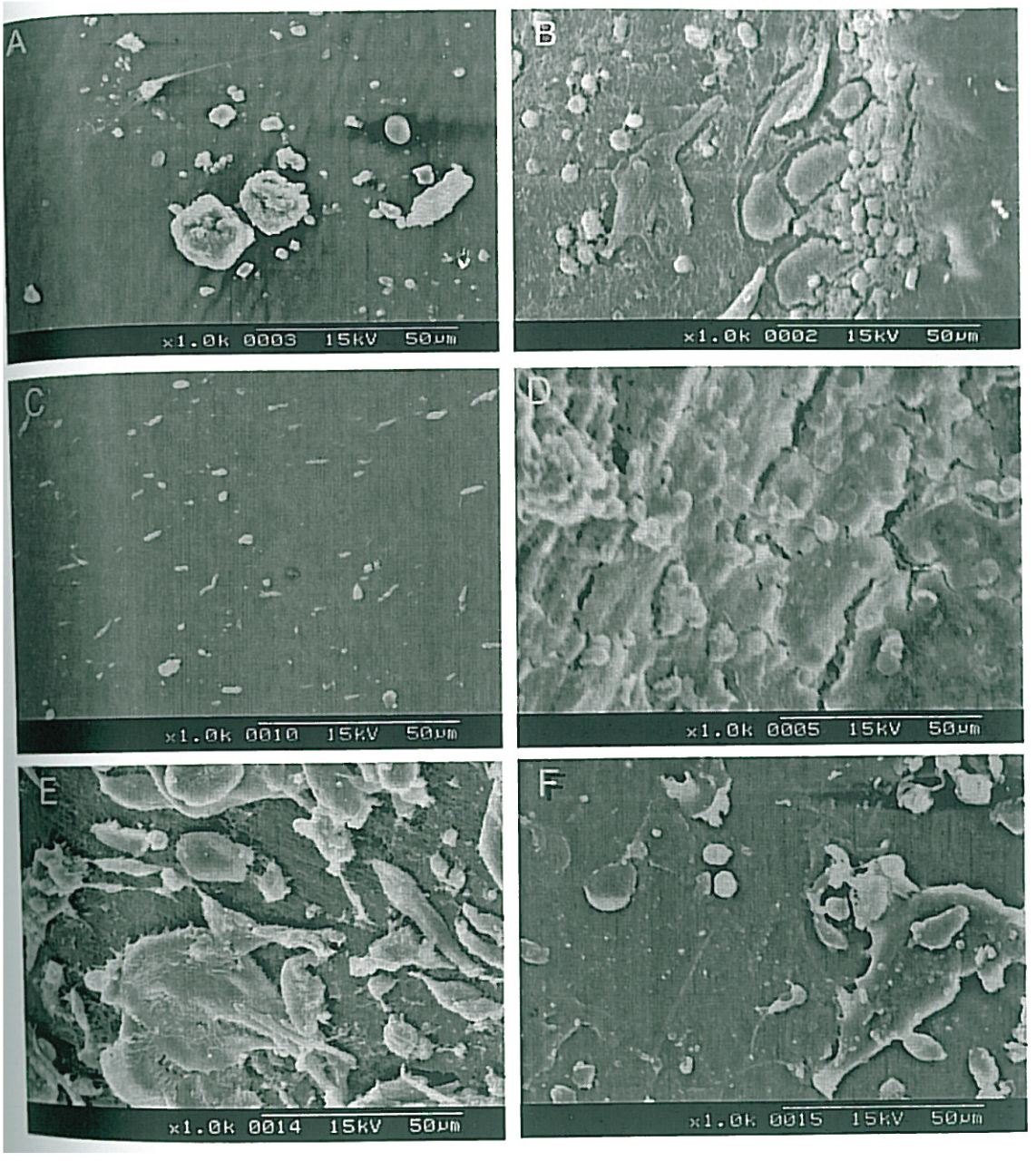

Figure 27: Scanning electron micrographs of surface of retrieved **Silicone expander**: 3days (A), 7days (C), 14days (E) and **UHMWPE**: 3days (B), 7 days (D), 14days (F)

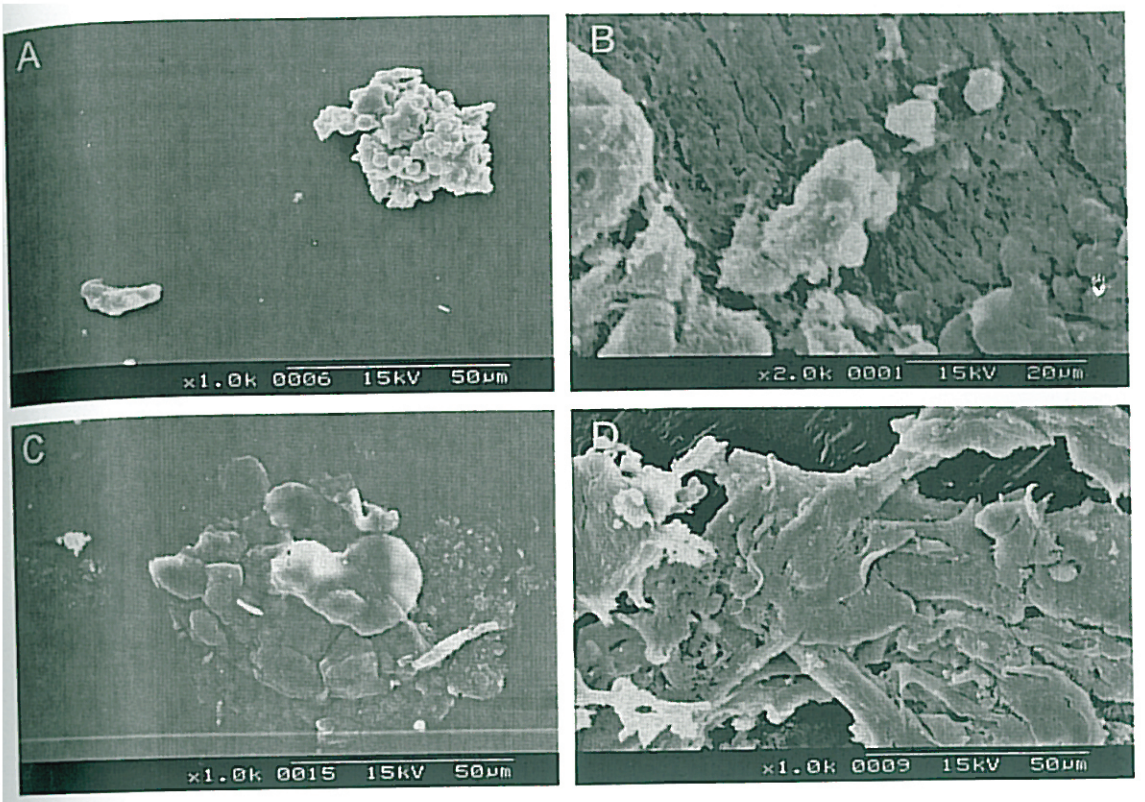

Figure 28: Scanning electron micrographs of surface of retrieved **Silicone expander:** 90days (A), 180 days (C) and **UHMWPE**: 90days (B), 180 days (D)

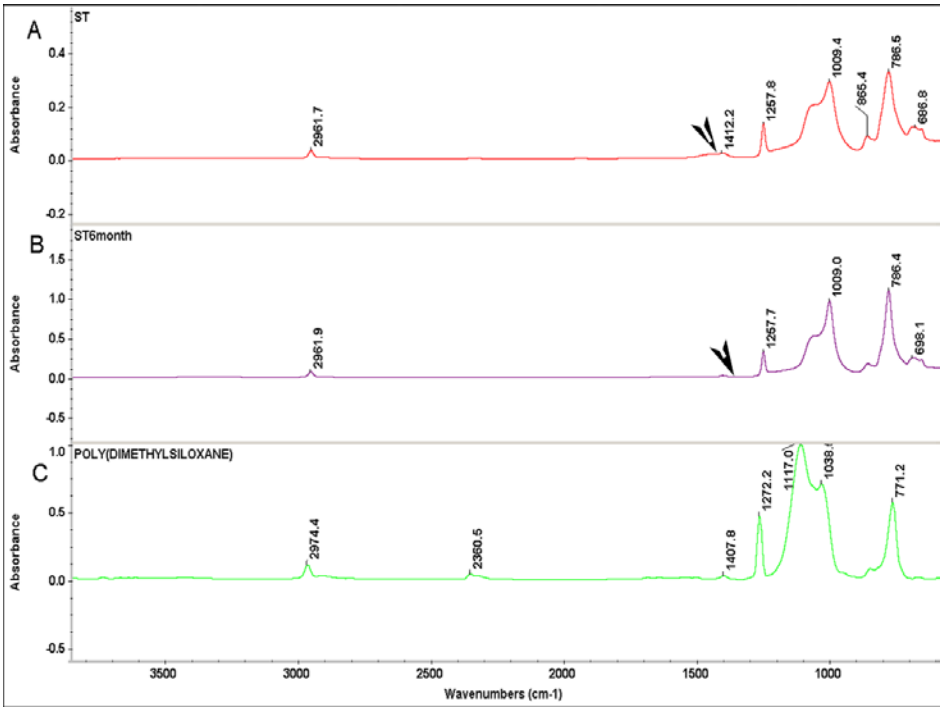

Figure 29: FTIR Spectrum of SE material before implantation and 180 days post-implantation

4.2.7. Gene expression studies

Numerous studies have related the inflammation and activation of cells with release of cytokines, to individual chemical components of the silicone shell (Wells AF *et a*l., 1994). Experimental studies in rats have dealt with study of the tissue response around silicone elastomer (Bal BT *et al*., 2009). Cytokines released by activated cells play a major role in inflammation and repair. The termination of the acute events with the formation of a fibrous capsule is the result of the delicate balance between pro and anti fibrotic proteins. These include pro fibrotic cytokines, transforming growth factor, connective tissue growth factor and anti fibrotic ones like TNFα and interferon-γ. Transforming growth factorß$_1$ (TGFß$_1$) induces αSMA and collagen synthesis in fibroblast both *in vivo* and *in vitro* and plays a significant role in tissue repair and the development of fibrosis (Desmouliere A *et al.*, 1993). They are involved through their effect on fibroblasts, in modulation of collagen deposition in the repair phase.

Real time PCR quantitation of cytokines provided new insights into the progress of wound healing around silicone elastomer and UHMWPE. The expression of cytokines like TGFβ, IFNγ , IL-10, IL-1β and myofibroblast marker, αSMA were selected for the important role they are known to play in wound healing, particularly in the repair phase.

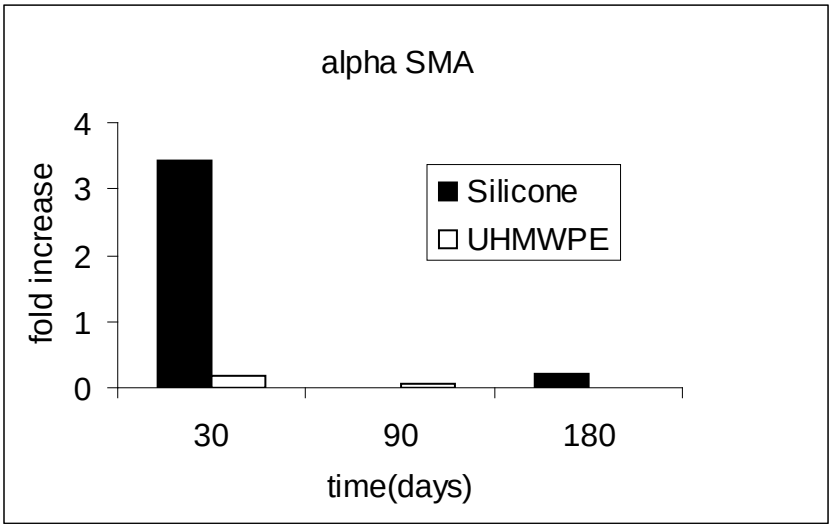

Figure 30: αSMA expression at tissue material interface around SE and UHMWPE.

As repair progresses, fibroblasts display increased expression levels of adhesion molecules and assume a myofibroblast phenotype, mediated in part by TGFβ and PDGF-A and -B, to facilitate wound contraction (Grinnell F, 1994). Identification of myofibroblasts was carried out in this study to find out if there is a difference in presence of myofibroblasts at the interface with silicone elastomer and UHMWPE. The most important marker of the fibroblast to myofibroblast phenotypic transition is the de novo expression of αSMA. αSMA is suggested as the most significant marker of myofibroblastic cells (Sappino AP *et al.*, 1990).

A difference in change in phenotypic tranformation to myofibroblasts was noted in this study at the tissue material interfaces around SE and UHMWPE with very low initial level of expression of αSMA around UHMWPE, gradually decreasing over 90 days and not being expressed at 180 days. In contrast, the cytokine was expressed at very high levels around Silicone at 30 days, being nil at 90 days and again being expressed at 180 days post implantation (Figure 30).

.

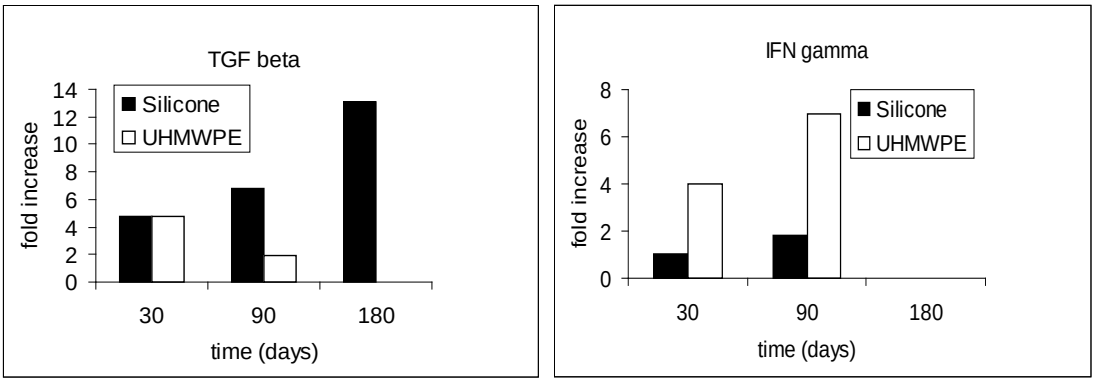

A B

Figure 31: Cytokine expression at tissue material interface around silicone and UHMWPE. A. TGF beta and B. IFN gamma.

The profibrotic cytokine TGFβ was found to increase in expression around SE at all time periods when compared to the UHMWPE (Figure 31A). TGFβ induces fibroblasts to synthesize extracellular matrix (Leask A *et al.,* 2004). TGFβ1 and β2 appear to exert a powerful stimulating activity in αSMA synthesis in cultured fibroblasts. If one considers that TGFβ is known since a long time to exert a pro fibrotic activity and specifically to stimulate collagen type I synthesis, one can conclude that this cytokine is probably the most critical for the development of scarring and fibrosis **(**Gabbiani G *et al*., 1998). In this study, the pro fibrotic action of the steadily increasing expression of the cytokine TGFβ around SE is evident in the formation of a gradual thickening of the collagenous capsule. The trend is opposite around UHMWPE with a gradual decrease, to a scant layer of collagen at the same time period.

In contrast, the antifibrotic cytokine IFNγ was more expressed around UHMWPE than SE at all time periods (Figure 31B). CD_4 T cells secrete IFNγ which suppresses collagen synthesis (Ghosh AK *et al.,* 2001). IFNγ strongly blocked the generation of myofibroblasts and moderately inhibited the production of αSMA in TGFβ1 promoted myofibroblasts (Tanaka K *et al*., 2003). Cornelissen *et al.* found a strong indication that IFNγ has the capacity to reduce the number of myofibroblasts and the collagen content during palatal wound healing (Cornelissen AMH *et al.,* 2000). The anti-fibrotic role of IFNγ in

decreasing collagen deposition and modulation of wound healing around SE in contrast to the thin capsule around UHMWPE is noted in the increasing levels of expression of the cytokine around UHMWPE and lower steady level at the silicone - material interface.

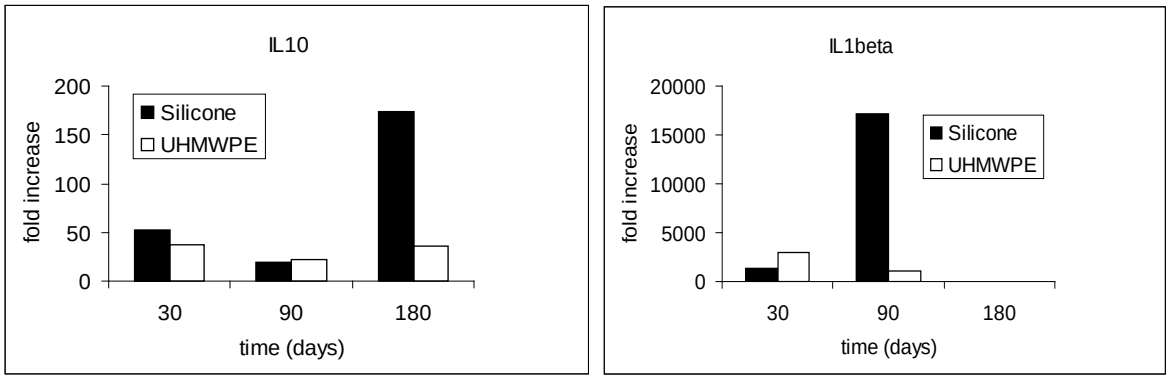

A B

Figure 32: Cytokine expression at tissue material interface around silicone and UHMWPE. A. IL10 and B. IL-1beta

IL-10 produced by $CD4^{+}$T cells is an immunomodulatory cytokine with potent anti-inflammatory effects, suppressing most facets of innate and T-cell-mediated inflammation. IL-10 may be considered anti-fibrotic via its anti-inflammatory activities (Akdis CA *et al.*, 2001). In a murine wound healing model Eming *et al.*, found that the increased matrix deposition during later stages of repair, which could be attributable to abundant TGFβ1 producing macrophages may be further amplified by the lack of direct suppressive effects of IL-10 on matrix synthesis and deposition by fibroblasts (Eming AS *et al.*, 2007). It has been reported that the addition of IL10 to fibroblasts *in vitro* has lessened the expression of type 1 collagen, the production of which is stimulated by transforming growth factor-ß (Arai T *et al*., 2000). Taking into account the anti fibrotic role of IL10, the high level of anti fibrotic IL10 observed at tissue material interface of SE may play a role in the collagen decrease (Figure 32A).

IL-1β with its pro fibrotic and anti fibrotic functions is the most highly expressed cytokine at peri implant tissue. There was a steady increase of expression of IL-1β at the SE-tissue interface (Figure 32B) which appears to corroborate with the thicker collagen, in comparison to the low level of expression and thin collagen capsule around UHMWPE.

Around SE all pro inflammatory cytokines were found to decrease over time except TGFβ level of which increased. The levels of regulatory cytokines from T cells, IL-10 and αSMA marker of myofibroblasts also increased. One potential explanation of this down regulation of pro inflammatory cytokines arises in the resolution of inflammation that occurs naturally with time. Change in cytokine levels shows a transition from inflammatory to reparative stage. Macrophages at the implant interface at early time periods, may secrete chemokines that attract T lymphocytes to the site. T lymphocytes get activated in presence of silicone particles as well as in response to cytokines from macrophages. These activated lymphocytes secrete IFNγ and IL-10 which are the prominent cytokines involved in collagen deposition and fibrous capsule modulation around the implants.

Even though macrophage level decreased over time TGFβ levels continues to increase. Autocrine function of TGFβ continues to activate fibroblast cells to Myofibroblasts as repoted earlier by Tredget EE *et al.,* 2004.

The results of this study agrees with the findings of Jones *et al.* that material surface chemistry can differentially affect cytokine /chemokine profiles produced by biomaterial-adherent macrophages (Jones JA *et al.,* 2007). The interaction between expression of TGFβ, IFN γ, IL10 and αSMA was observed in this study. After tissue injury, fibroblasts differentiate into contractile and secretory myofibroblasts that contribute to tissue repair during wound healing, but that can severely impair organ function when contraction and extracellular matrix (ECM) protein secretion become excessive (Hinz B *et al.,* 2003). In 1978 itself, Rudolph *et al.* reported contractile fibroblast in fibrous tissue capsules around silicone breast implants (Rudolph R *et al.,* 1978). The study by Kamel *et al.* suggested the fibrocyte and histiocyte recruitment and their activation in capsule may be a possible source of pain and contracture in long term implants (Kamel M *et al.,* 2001).

Upon retrieval at 365days post implantation, both the implants were deeply embedded in extra cellular matrix (Figure 34).The stereo microscopic images showed that the matrix deposition was thicker around SE (Figure 34A) when compared to UHMWPE (Figure 34B). These results correlate well with Hematoxylin &Eosin staining which showed a thick fibrous

4.3. *In vivo* experiments- Rabbit

4.3.1 Animal implantation

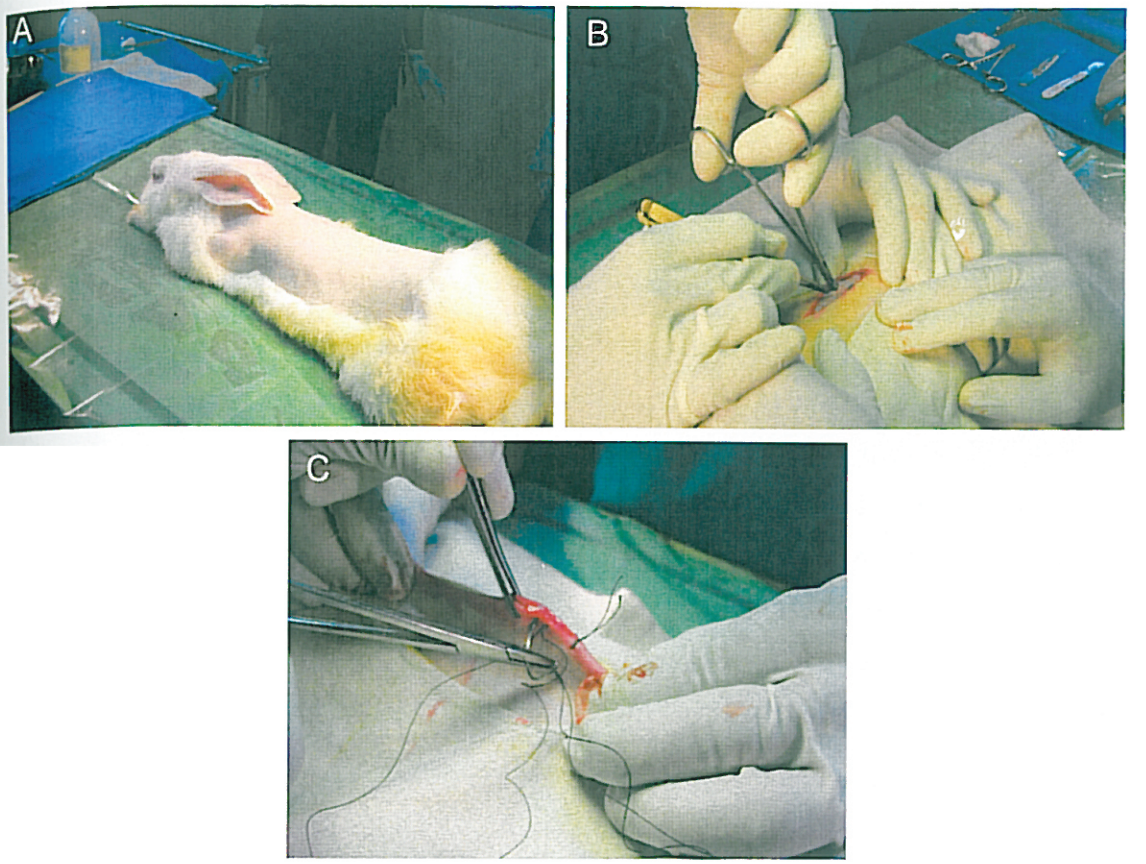

Figure 33: Animal implantation in progress.

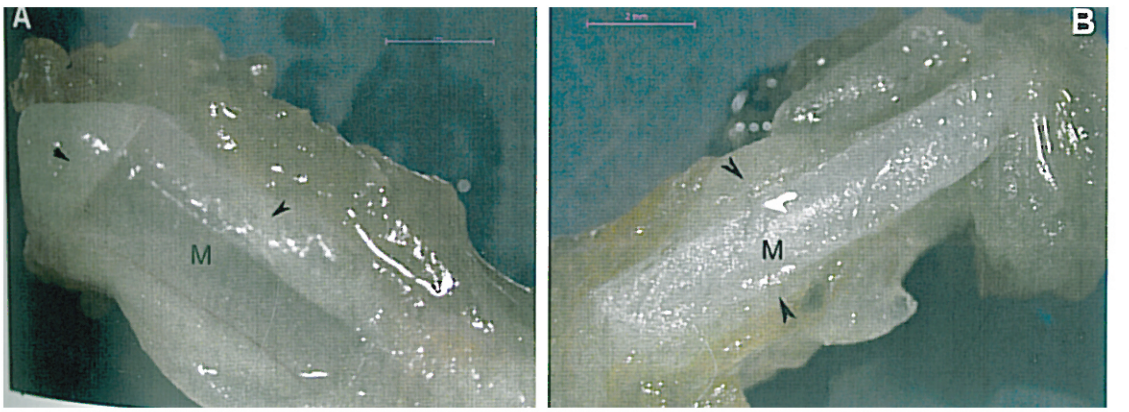

Figure 34: Extra cellular matrix deposition at 365 days post implantation around **silicone expander** (A) and **UHMWPE** (B). (**M** –Material, ⋏- ECM)

capsule formation around silicone implants (Figure 35).

4.3.2. Histomorphometric analysis of fibrous capsule around the retrieved implant

Thick fibrous capsule formation and persistence around SE even at end of 365days was observed by Hematoxylin &Eosin staining as compared to the UHMWPE (Figure 35). These results corroborated well with *in vivo* studies in rat. The inflammatory response at 180 days resolved to fibrous encapsulation at 365 days around both implants (Figure 35E and 35F)). There was significant difference in the thickness of fibrous capsule between the two materials, silicone and UHMWPE (Figure 36). The fibrous capsule formation around SE showed an increasing trend over time, whereas around UHMWPE there was a decrease at 365 days (Figure35F). Thus it is evident that cellular and tissular response varies from material to material and is dependant on surface as well as bulk properties.

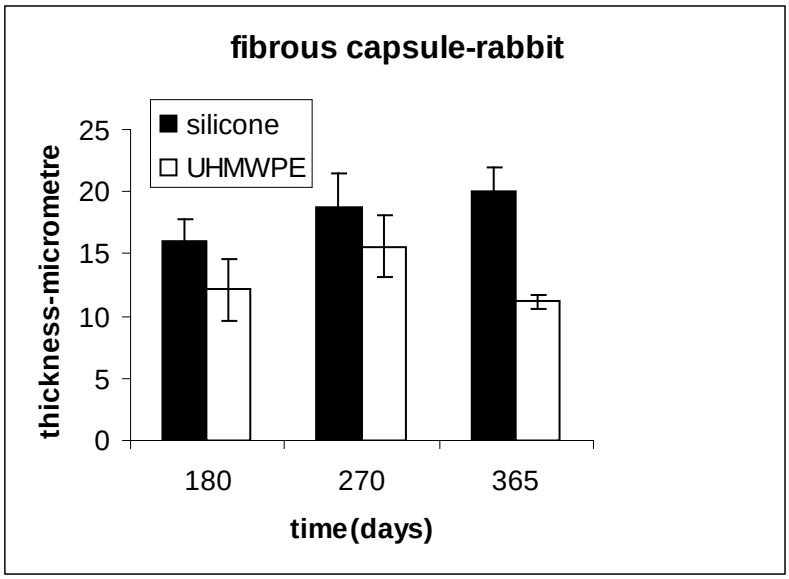

Figure 36: Collagen deposition at tissue material interface around SE and UHMWPE.

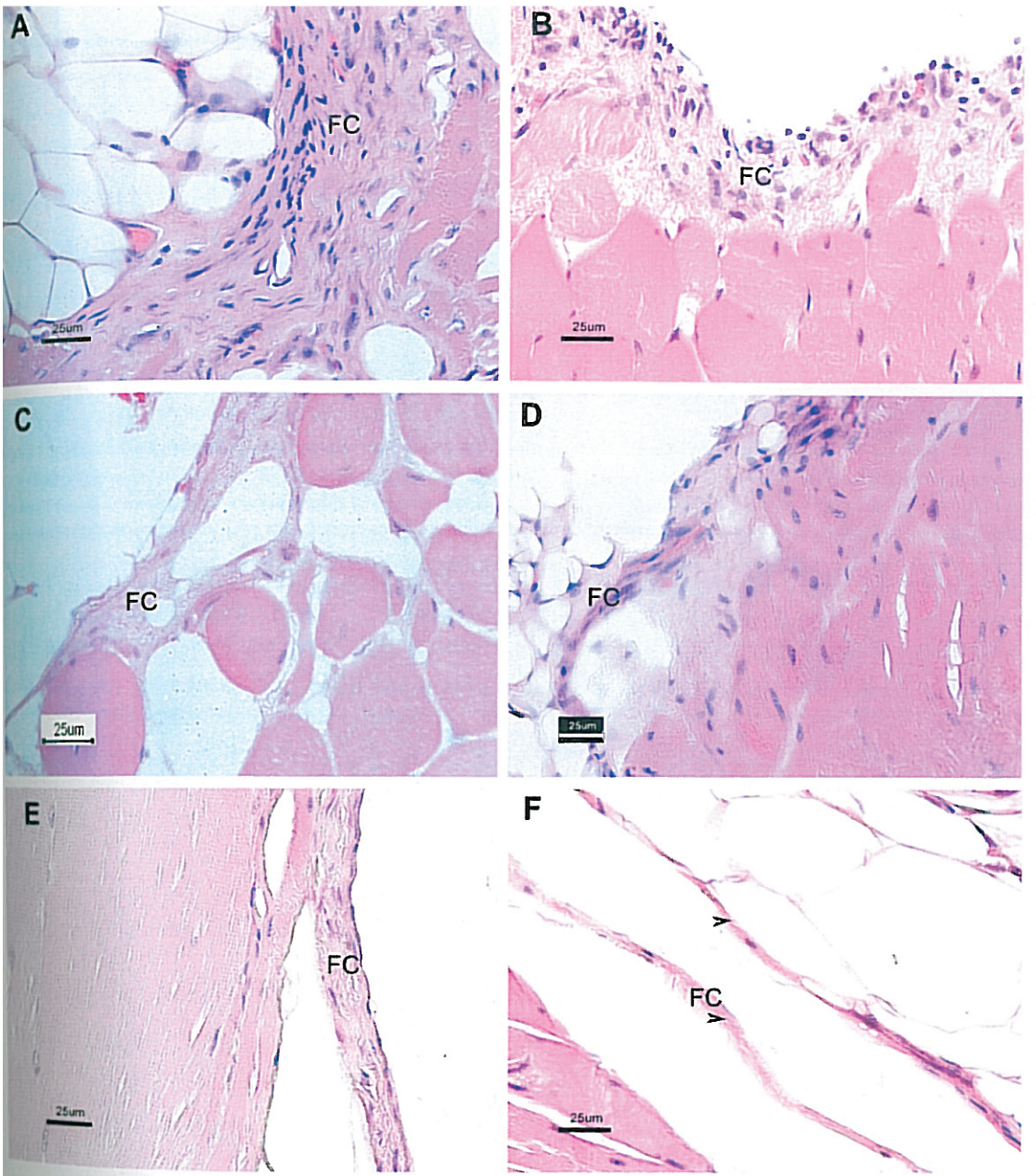

Figure 35: Light micrographs of Haematoxylin & Eosin staining in sections of peri implant tissue around **Silicone expander:** 180 days; 270 days; 365 days (A, C, E) and **UHMWPE**: 180 days; 270 days; 365 days (B, D, F)

(M -Implant site, ⮜ - Fibroblast, * - Macrophage)

4.3.3. SEM – EDAX analysis of retrieved peri implant tissue

Results from this study showed only negligible amounts of silicone content in peri – implant tissue both at 180 days and 365 days post implantation (Figure 37A and B). This may be due to extra capsular migration of silicone to distant organs. These results are in agreement with Barnard *et al.,* 1997 stating that solid silicone elastomer implants shed particulate material through fatigue and surface abrasion and such particles can be transported to remote sites (Barnard JJ *et al.,* 1997, Hunt J *et al.,* 1989)**.**

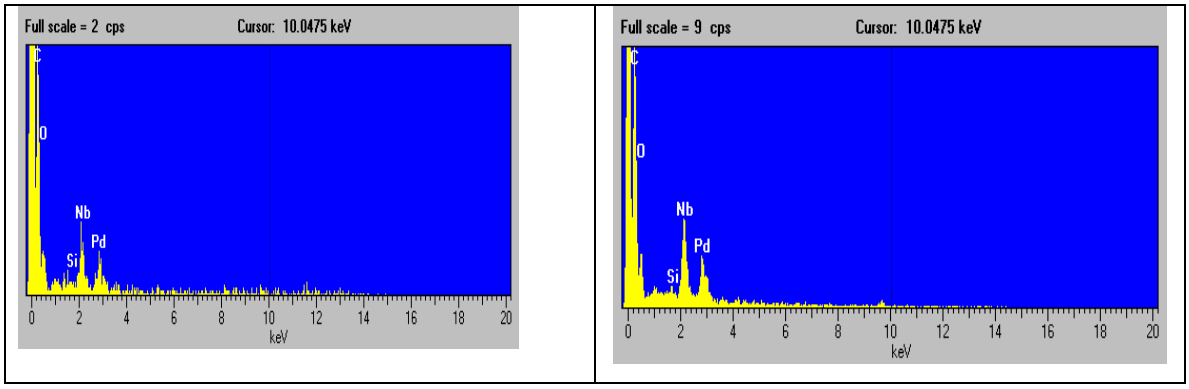

A **B**

Figure 37: Elemental distribution of silicone at peri implant tissue at 180 days (A) and 365 days (B) post implantation.

4.3.4. ICP –AES of retrieved tissue for silicone content

ICP-AES analysis of silicone in peri-implant tissue long term corroborated with SEM-EDAX results. It has been reported that ICP –AES detects precise amount of silicon in body fluids and tissues and they are more sensitive than NMR measurements (Peters W *et al.,* 1999). No difference was observed in the silicone content of peri-implant tissue between 180 day and 365 day samples (Table 9).

Table 9: **Silicone distribution in peri-implant tissue**

Time period	SE (ppm)
180 days	0.05
365 days	0.05

Phase II

4.4. *In vitro* experiments

Fibroblasts are key cells in the wound repair process. They participate in the immune response by producing and responding to cytokines and chemokines produced by other cells like macrophages and T lymphocytes.

4.4.1. Differentiation of monocytic cell line to macrophages and their adhesion to the material

This study aimed at differentiation of monocytes to macrophages, showed that within 24hrs of addition of PMA, monocytic suspension cell line became adherent to culture surface. They aggregated into adherent clumps, increased in size and showed morphology resembling macrophages by 72 hours (Figure 38.A, C, E). The morphological change was clearly evident when compared to control cells without any PMA addition (Figure 38 B, D, F).

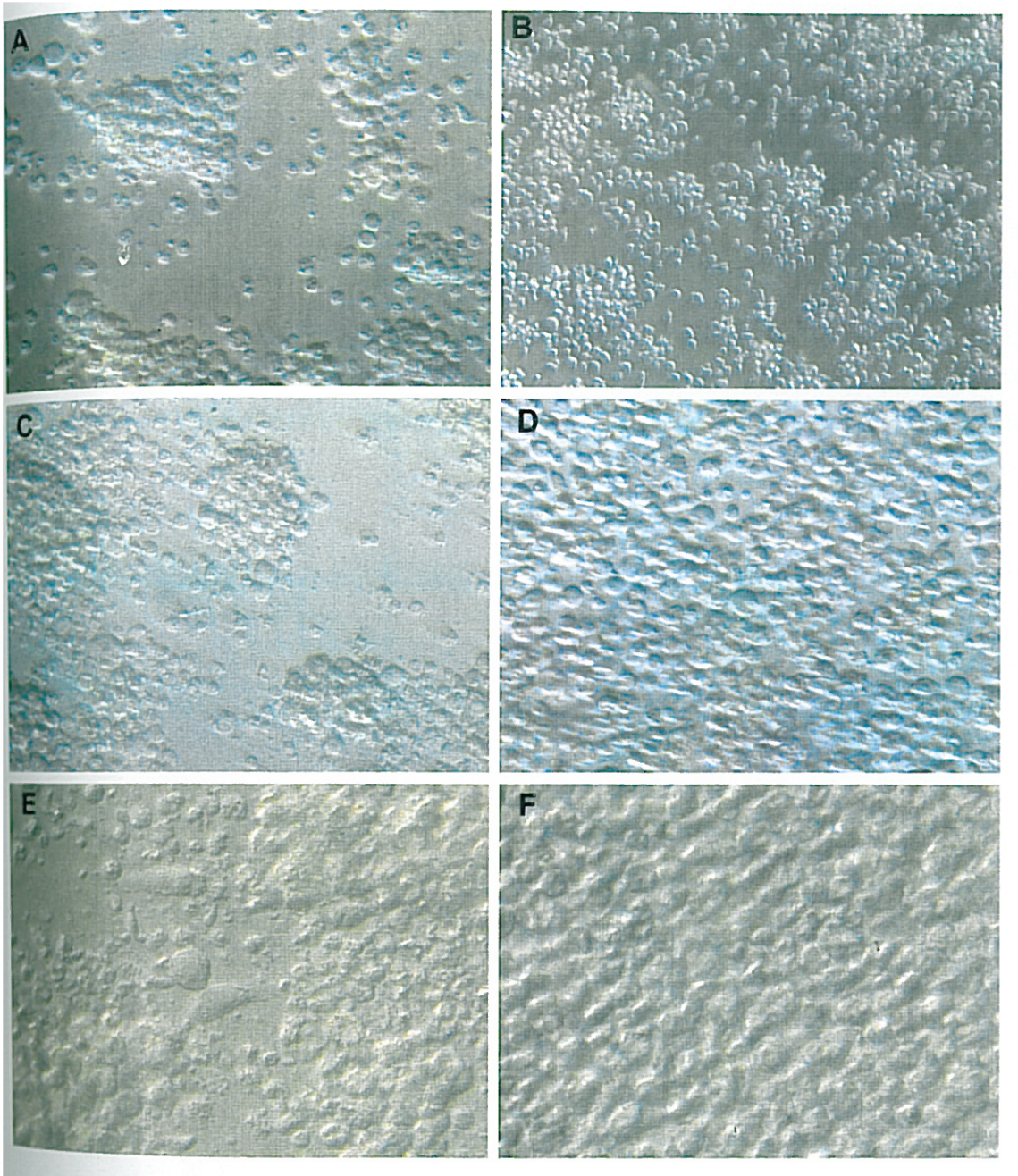

Figure 38: U937 monocytic cell line with Phorbol-Myristyl-Acetate treatment: 24h, 48h, 72h (A, C, E) and control cells without treatment 24h, 48h, 72h (B, D, F)

4.4.2. Study of cytokines from monocyte derived macrophages by ELISA

Pro inflammatory cytokines like IL-6, IL-1β and TNFα were produced by monocyte derived macrophages. In control U937 cells without any PMA addition, except IL-6 the other two cytokines were expressed. All the cytokine levels were high for cells treated with PMA alone in all time periods (Figure 39-41) and this was reported earlier by Garcia JEL *et al.*, 2000. PMA may be inducing additional cytokine secretion and initiating signalling pathways. Addition of PMA resembles a wound injury *in vivo* where numerous chemokines and cytokines are released to the wound site for the resolution of wound.

Since the PMA induced cytokine secretion was maximum, there was no significant difference in cytokine release from cells seeded on SE and other research groups, namely Tavazzani *et al.* have used a model of human monocyte derived macrophages (MDMs) to study silicone induced inflammation (Tavazzani F *et al.*, 2005).

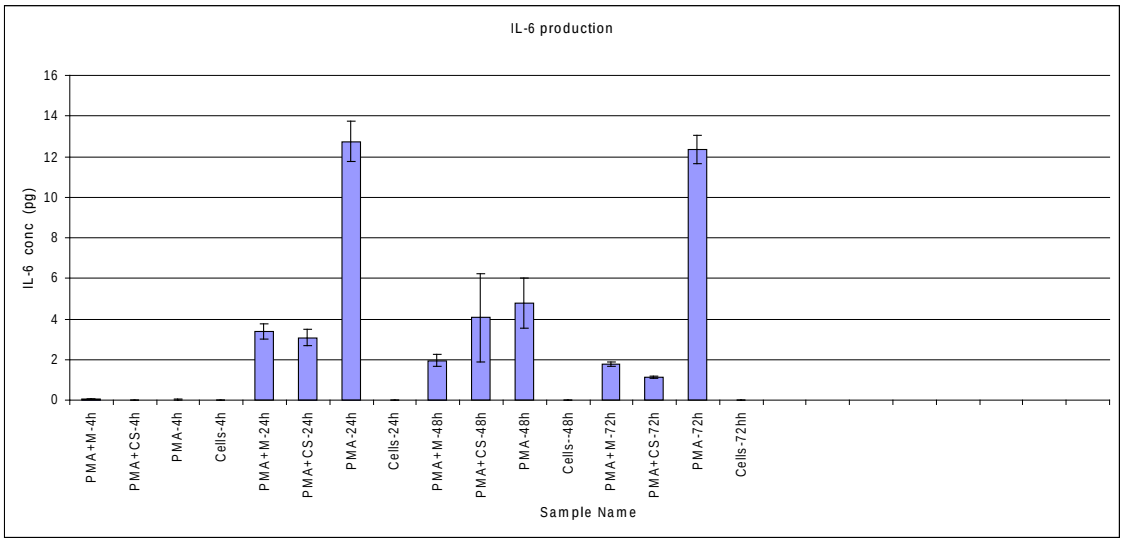

Figure 39. IL-6 production by U937 cells seeded on SE and coverslip with Phorbol-myristyl- acetate addition at 4h-72h.

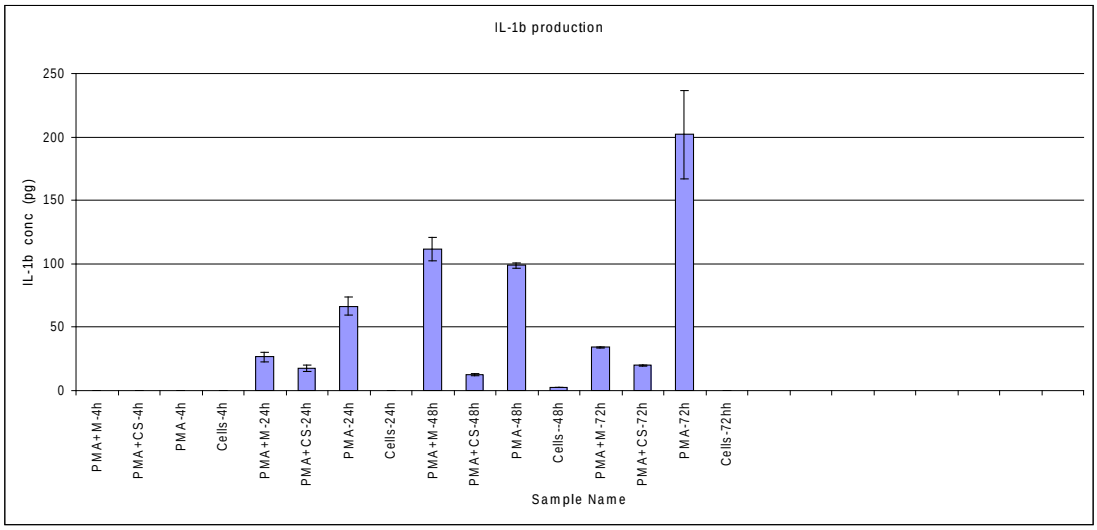

Figure 40. IL-1β production by U937 cells seeded on SE and coverslip with Phorbol-myristyl-acetate addition at 4h-72h.

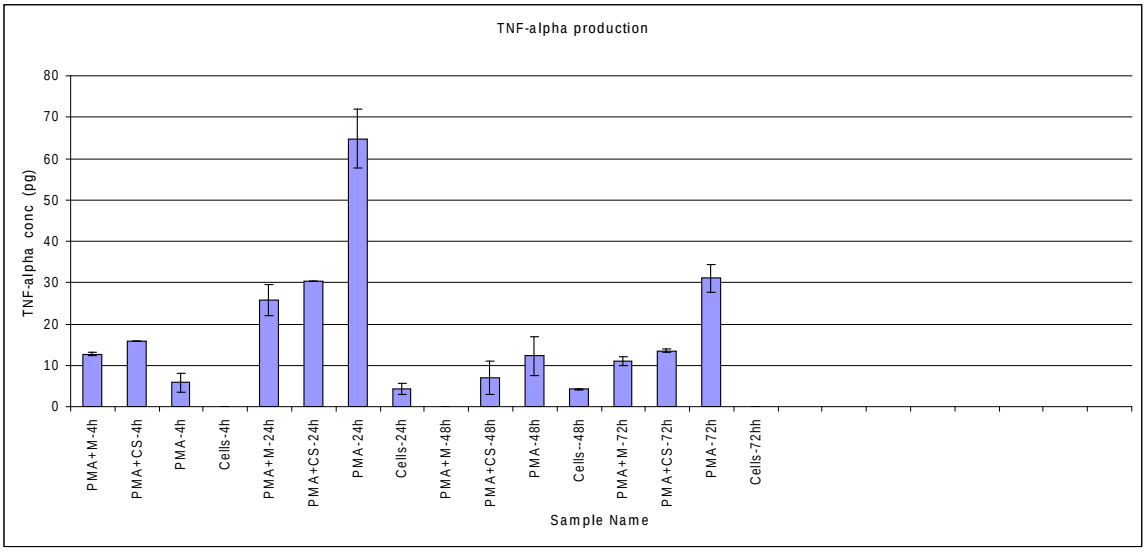

Figure 41. TNFα production by U937 cells seeded on SE and coverslip with Phorbol-myristyl-acetate addition at 4h-72h.

4.4.3. Quantitation of macrophage secreted cytokines

When grown over different material surface, the expression of pro fibrotic cytokine, TGFβ showed fold decrease in comparison to control RAW 267.9 cells alone (Figure 42A). Whereas IL-6, a pro inflammatory and pro fibrotic cytokine levels was up regulated in macrophages seeded over SE than over UHMWPE and TCPS seeded cells (Figure 42B). IL-6 expression was 3 fold higher than TGFβ. IL-6 may play a role in mediating the inflammatory response to silicones as reported by Naim JO *et al.*, 2000.

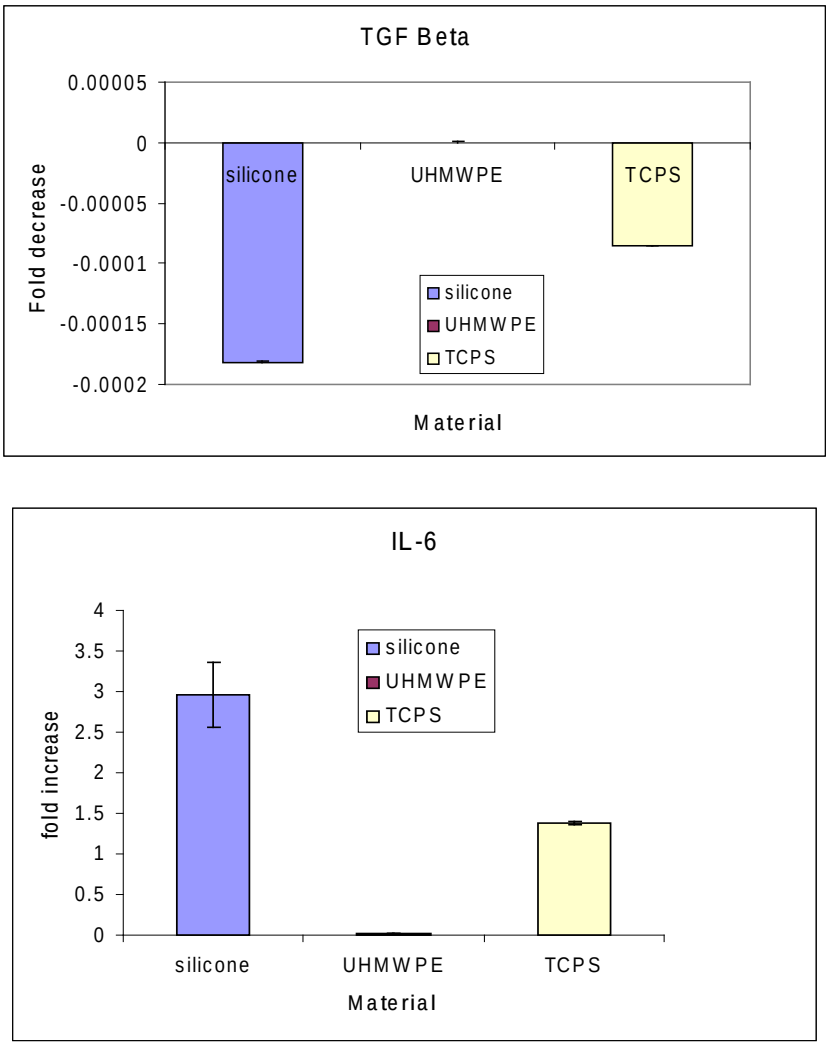

Figure 42. Gene expression levels of TGF β (A) and IL6 (B) in RAW macrophages grown over silicone as compared to UHMWPE and TCPS

4.4.4. αSMA expression : gene and protein expression study

αSMA expression in L929 fibroblasts showed a similar pattern to that of IL-6 expression levels in macrophages. The expression was high in fibroblast added with conditioned media from RAW macrophages seeded over SE. It can be assumed that cytokines from macrophage conditioned media activated L929 fibroblasts to acquire new phenotype with more actin stress fibers, characteristic of myofibroblasts. Of these cytokines the role of IL-6 is specific (Galluci RM *et al.*, 2006).

A

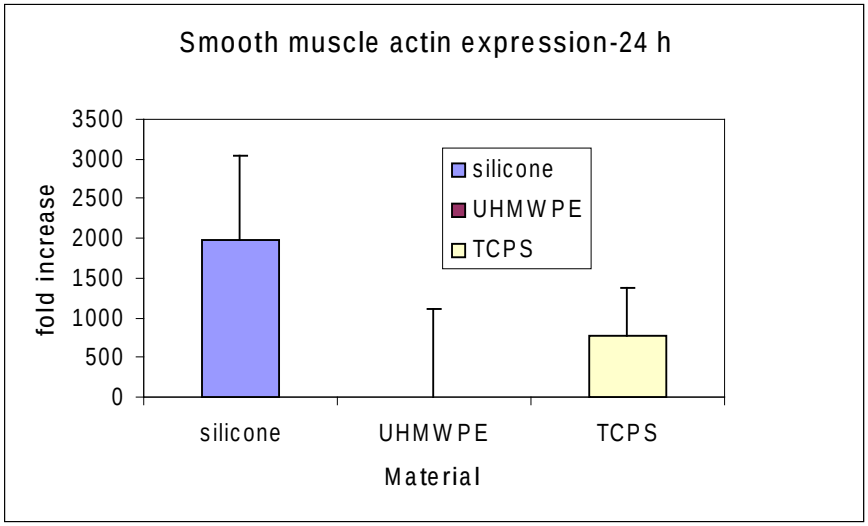

B

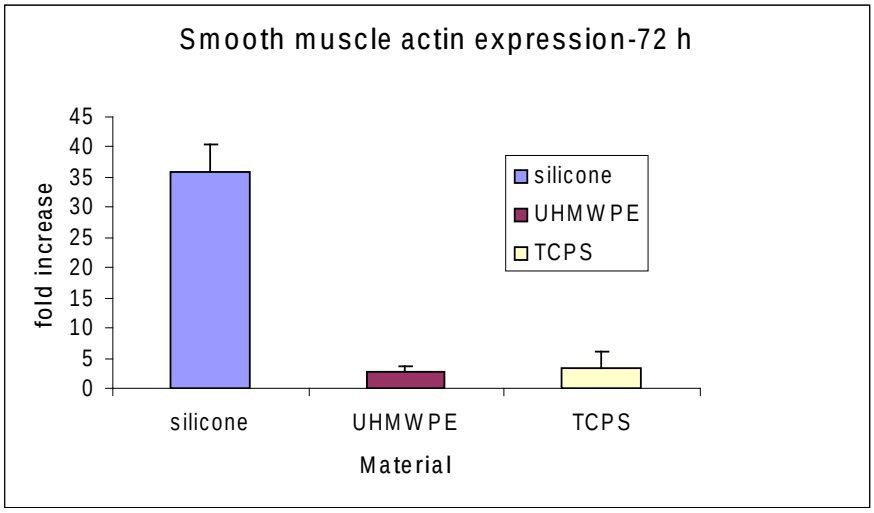

Figure 43. Gene expression levels of αSMA by fibroblasts grown for 24h (A) and 72h (B) in conditioned media of RAW macrophage grown on silicone, UHMWPE and TCPS.

The αSMA gene expression decreased with time, from 24 to 72 hours (Figure 43 A and B) and this results are not corroborated to *in vivo* observations. It can be inferred that this change is due to the absence of stimulating factors from conditioned media and increased cell death over time. *In vitro* culture conditions could not exactly mimic the *in vivo* situations. The critical limiting factors are the short life span of cells *in vitro* and variable concentration of constituents in culture media.

Protein expression study also correlated with gene expression analysis.αSMA levels were higher over conditioned media added cells seeded on SE surfaces (Figure 44B, E) than UHMWPE, TCPS (Figure 44A&C,D&F) seeded cells as well as with control L929cells (Figure 44G&H).

It is now well known that when fibroblasts become adapted to culture, they adhere to the substratum through specialized areas of membrane known as ‘adhesion plaques’ or ‘focal adhesions’ (Rees *et al.*). Numerous focal adhesion points in adherent fibroblasts were observed especially at 72 hours (Figure 44 D, E, F). The fluorescence intensity plot also demonstrated the role of silicone material in eliciting αSMA expression in fibroblasts (Figure 45).

4.4.5. Key signaling molecules involved in fibroblast to myofibroblast transition

4.4.5.1. Macrophage conditioned media effect on fibroblasts (HLF)

It was observed that αSMA was expressed only in cells added with conditioned media from monocyte derived macrophages grown on SE and in cell control (Figure 46A and 46 D). Erk expression also showed a similar trend. From this data it is evident that Erk has a profound role in αSMA expression. Growth factors, through receptor tyrosine kinases like Erk, recruit a large network of signaling proteins to execute their cellular programs. One of the four mitogen-activated protein kinase (MAPK) signaling pathways, the Erk phosphorylation cascade's importance in intracellular signaling has been compared to the role of the Krebs cycle in energy metabolism (Pages *et al*, 1999). The Erk cascade functions in cellular proliferation, differentiation, and survival. These findings suggest that cellular cytokines, especially IL-6 from macrophage cells trigerred and maintained Erk which is a key molecule in fibroblast activation pathway.

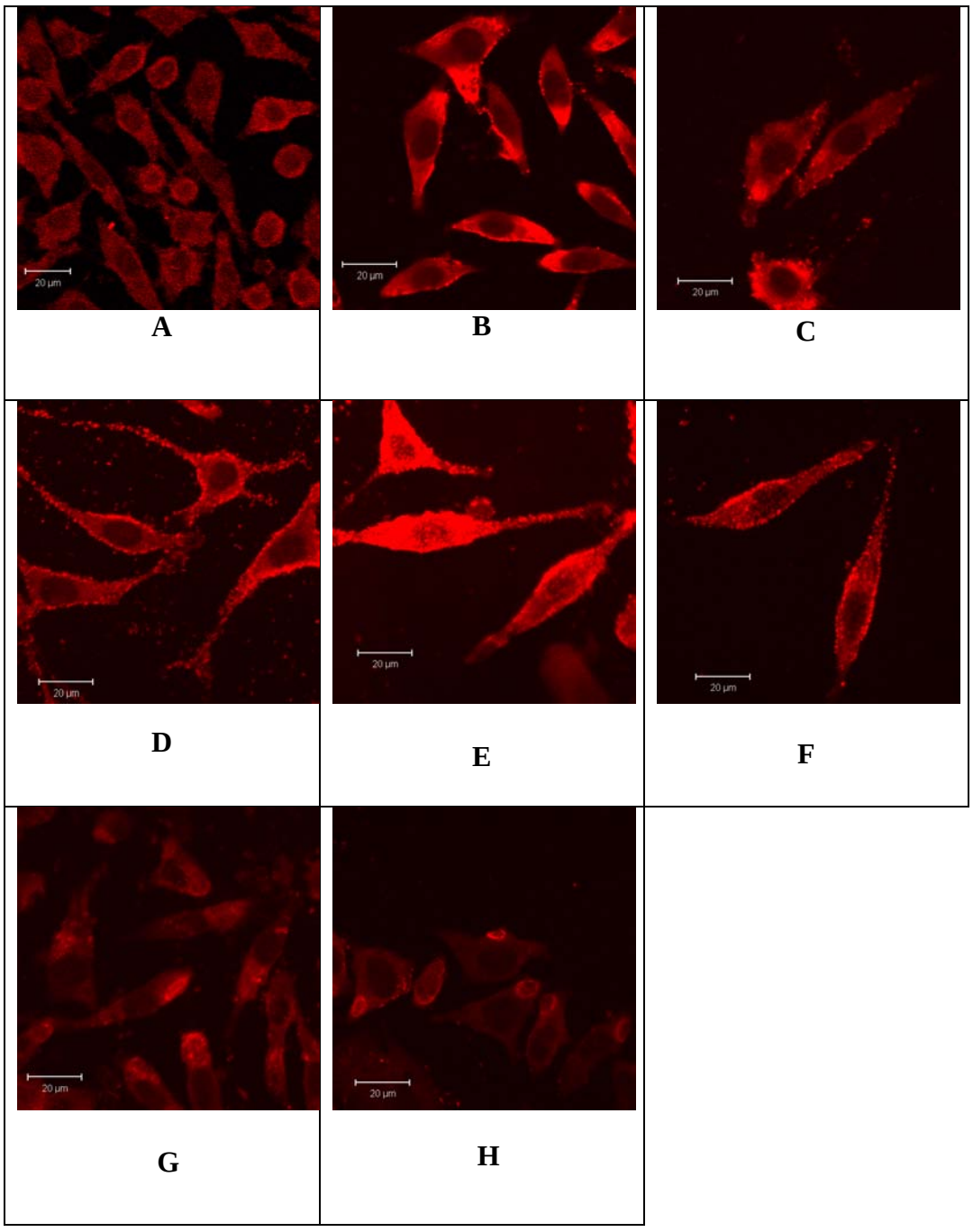

Figure 44. Immunoflorescent detection of αSMA in L929 fibroblasts added with conditioned media from macrophages seeded over SE (B-24h ,E-72h),over UHMWPE(A-24h,D-72h) and TCPS(C-24h,F-72h).The control L929 cells without any conditioned media addition(G and H).

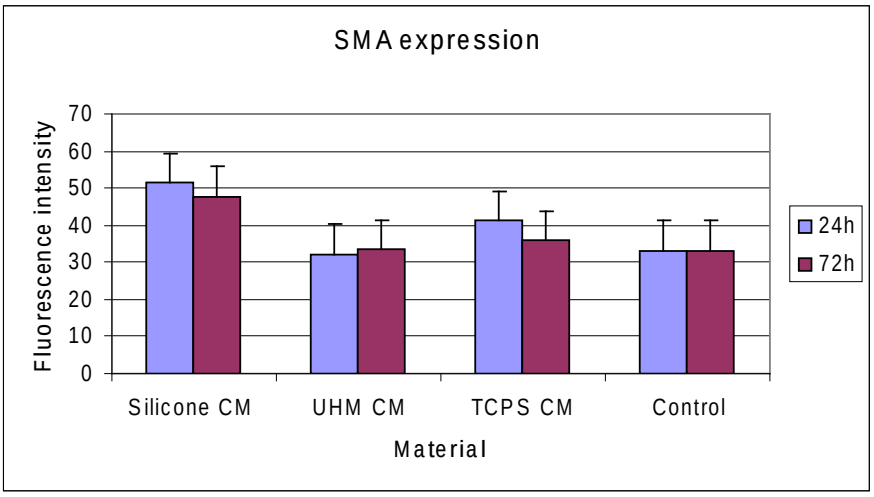

Figure 45. The fluorescence intensity plot of αSMA expression in L929 fibroblasts grown in conditioned media from RAW macrophages grown over different material surfaces. Control cells were L929 cells without any conditioned media treatment.

Figure 46. Western blot images of protein expression of αSMA and Erk in Human lung fibroblasts added with conditioned media from monocytes seeded over SE(C), monocyte derived macrophages seeded over SE(D), monocyte derived macrophages seeded over UHMWPE . A and B represents cell control and media control respectively.

4.4.5.2. Interferon gamma role on fibroblasts (HLF) grown over SE, UHMWPE and Coverslip

Addition of IFNγ did not result in any difference in α SMA expression and Erk was absent in all groups except the positive control (Figure 47). These findings suggest that IFNγ has no direct role in αSMA expression.

Figure 47. Western blot images of protein expression of αSMA and Erk in fibroblast seeded over SE(C), UHMWPE (D), coverslip(E) and grown in presence of IFNγ. A and B represents positive control (Human Airway epithelial cells) and negative control (untreated HLF) respectively.

Phase III

4.4.6. Silicone degradation in Pseudo extra cellular fluid(PECF)

4.4.6.1. *In vitro* leaching of silicone into PECF

After 60 days incubation at 37^0C in pseudo extra cellular fluid, there was considerable level of silicone leaching out ie. 44ppm when compared to the negative control, the extraction vehicle alone (Figure 48). This *in vitro* leaching study supported the data observed *in vivo* by SEM-EDAX and ICP-AES. The high level of silicone leachant observed *in vitro* and absence to low levels detected in peri-implant tissue *in vivo* suggest distant migration of silicone from peri-implant site.

4.4.6.2. Effect of silicone leachants on fibroblast differentiation

It was noted that expression of αSMA was significantly high in L929 fibroblasts activated by silicone extract at a concentration of 200ppm, thus confirming the role of silicone leachants in contraction of the thick fibrous capsule around the implant (Figure 49). This data indicates that an optimum level of silicone release is essential for initiating fibroblast to myofibroblast transition.

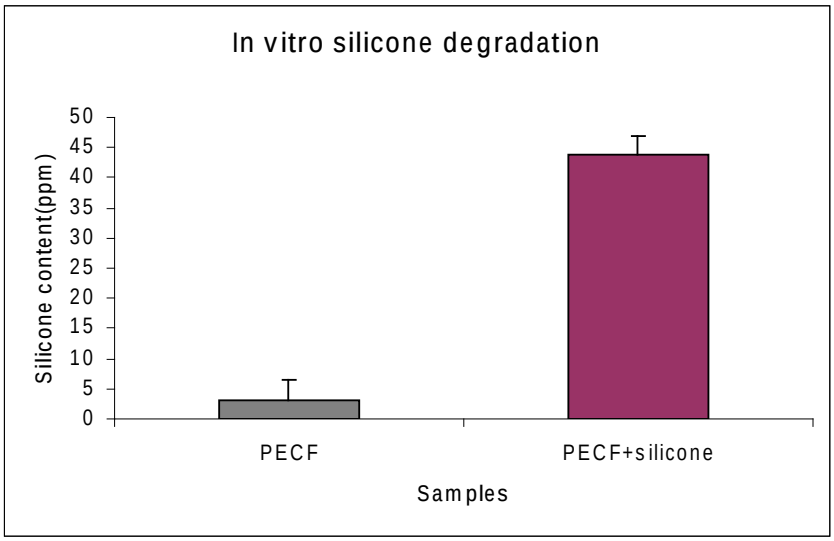

Figure 48. Silicone leaching into Psuedo extracellular fluid.

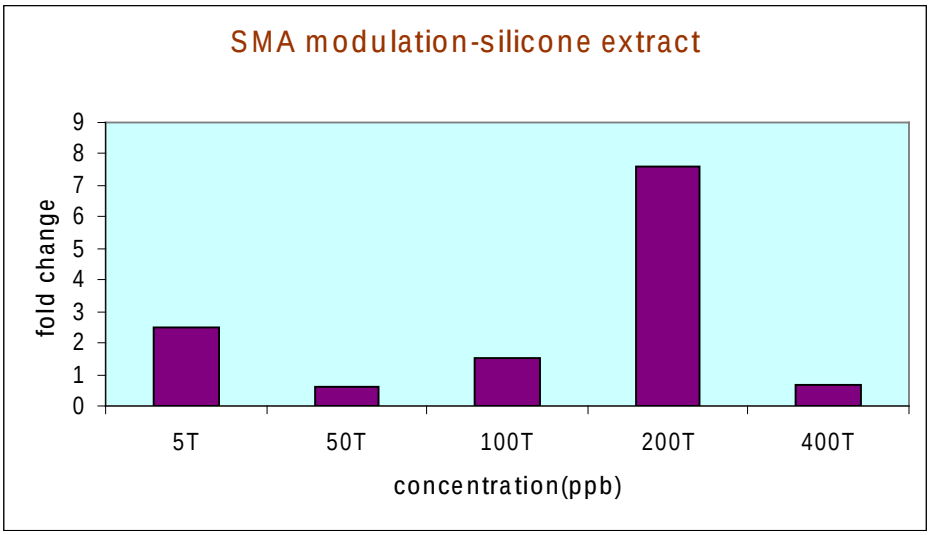

Figure 49. Effect of different concentrations of silicone leachants on myofibroblast differentiation

4.5. Tissue responses to V-P shunt

Ventriculo-peritoneal shunting is the most commonly performed neurological procedure in children with hydrocephalus.

4.5.1. FTIR spectroscopy

The spectral pattern obtained for VP shunt pre-implantation showed peaks matching with spectrum of standard, polydimethylsiloxane (Figure 50). There was similarity between peaks in pre and post implantation periods. No significant changes were noted in surface moieties on VP shunt before and after 180 days post implantation.

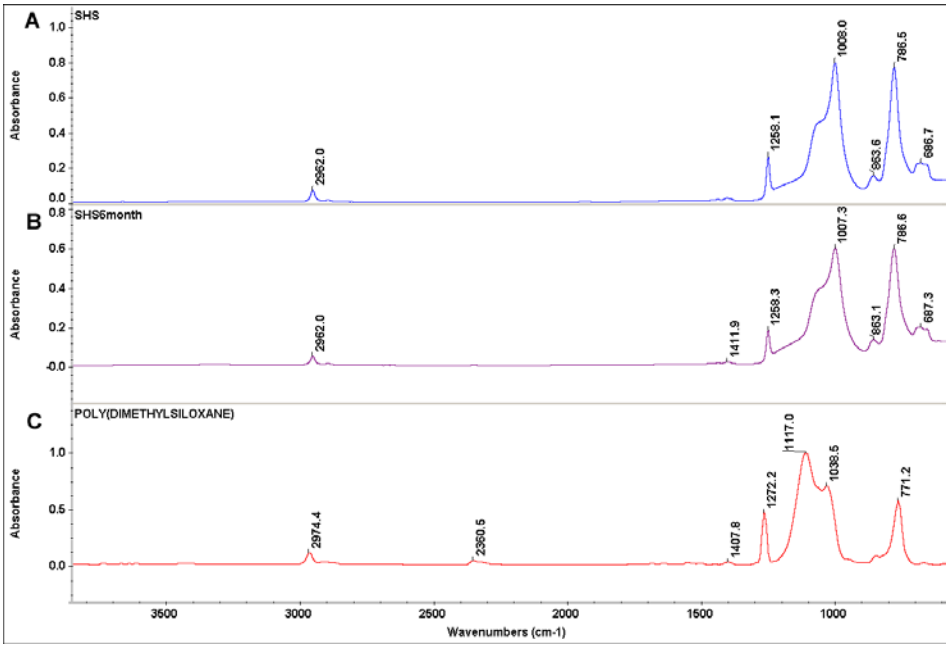

Figure 50. FTIR Spectrum of VP shunt material pre-implantation and 180 days post-implantation

4.5.2. Histology

The initial cell population consisted of macrophages and fibroblast whereas at later stages of 90 days, fibroblasts predominated around VP shunt (Figure 52 A and C). Hematoxylin &Eosin staining revealed formation of a fibrous sheath around the implant. The thickness of this layer seem to be increasing over a time period of 180 days when compared to the UHMWPE. A thick fibrous capsule was observed around VP shunt from 30days (Figure 52A) on wards and it persisted even at 90 days (Figure 52C) whereas around UHMWPE a thinner fibrous capsule was observed (Figure 52B and D).

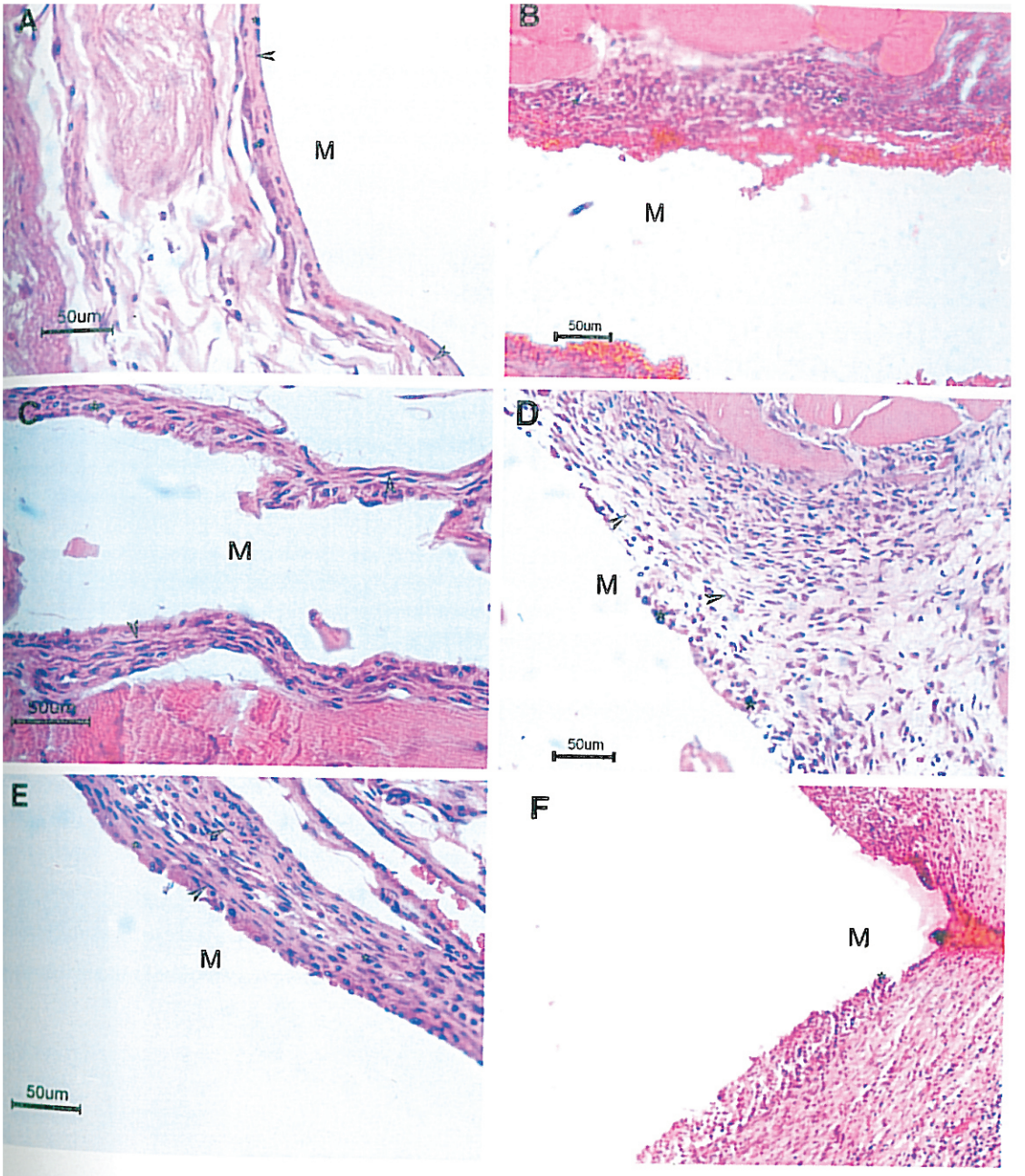

Figure 51: Light micrographs of Haematoxylin & Eosin stained sections of muscle around **Ventriculo-Peritoneal shunt** : 3 days; 7 days; 14 days (A, C, E) and **UHMWPE**: 3 days; 7 days; 14 days (B, D, F)
(M -Implant site, ⮜ - Fibroblast, * - Macrophage)

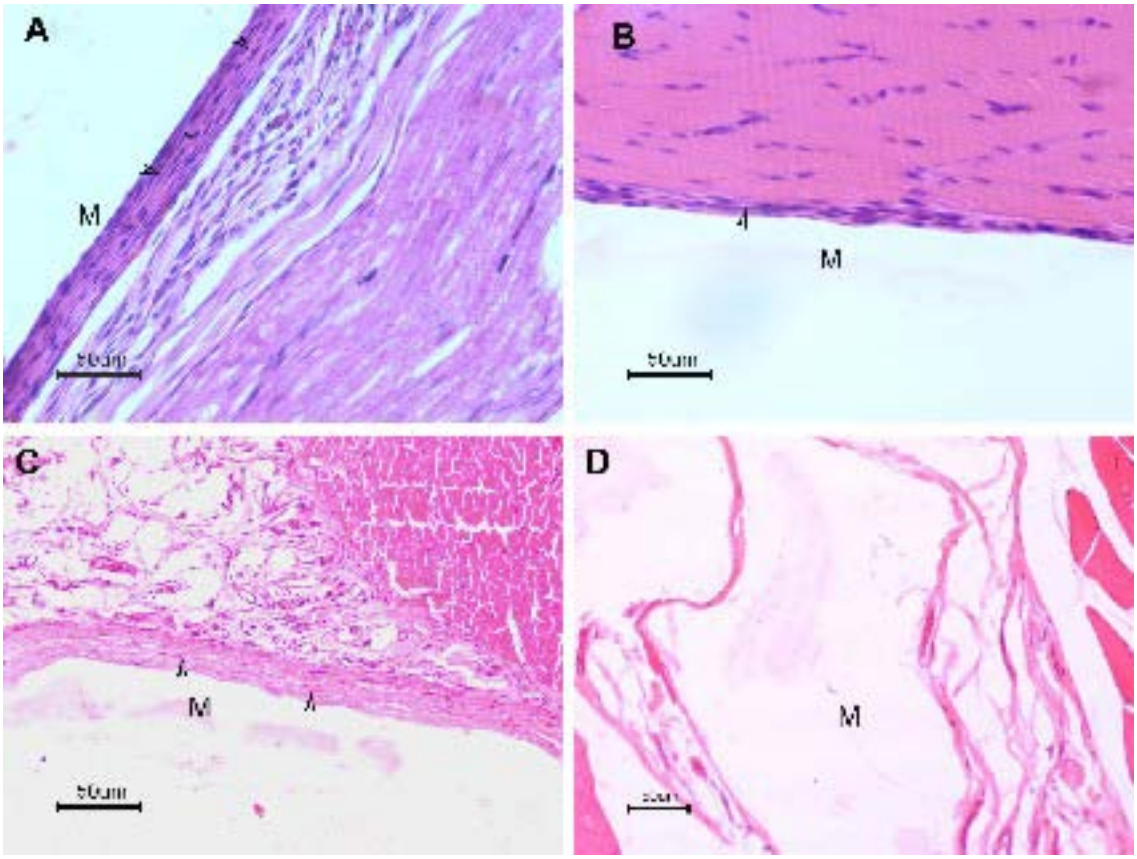

Figure 52: Light micrographs of Haematoxylin & Eosin stained sections of muscle around **Ventriculo-Peritoneal shunt:** 30 days; 90 days (A, C) and **UHMWPE:** 30 days; 90 days (B, D)

(**M** -Implant site, ↑ - Fibroblast, * - Macrophage)

4.5.3. Collagen staining

The data obtained from light microscopy was supported by trichrome staining for collagen. There was a decrease in collagen deposition at 30 days around VP shunt (Figure 53E and Figure 54) which increased at 90 days post implantation (Figure 53G and Figure 54). Whereas around UHMWPE a steady decrease in collagen content was observed (Figure 53F, H and Figure 54).

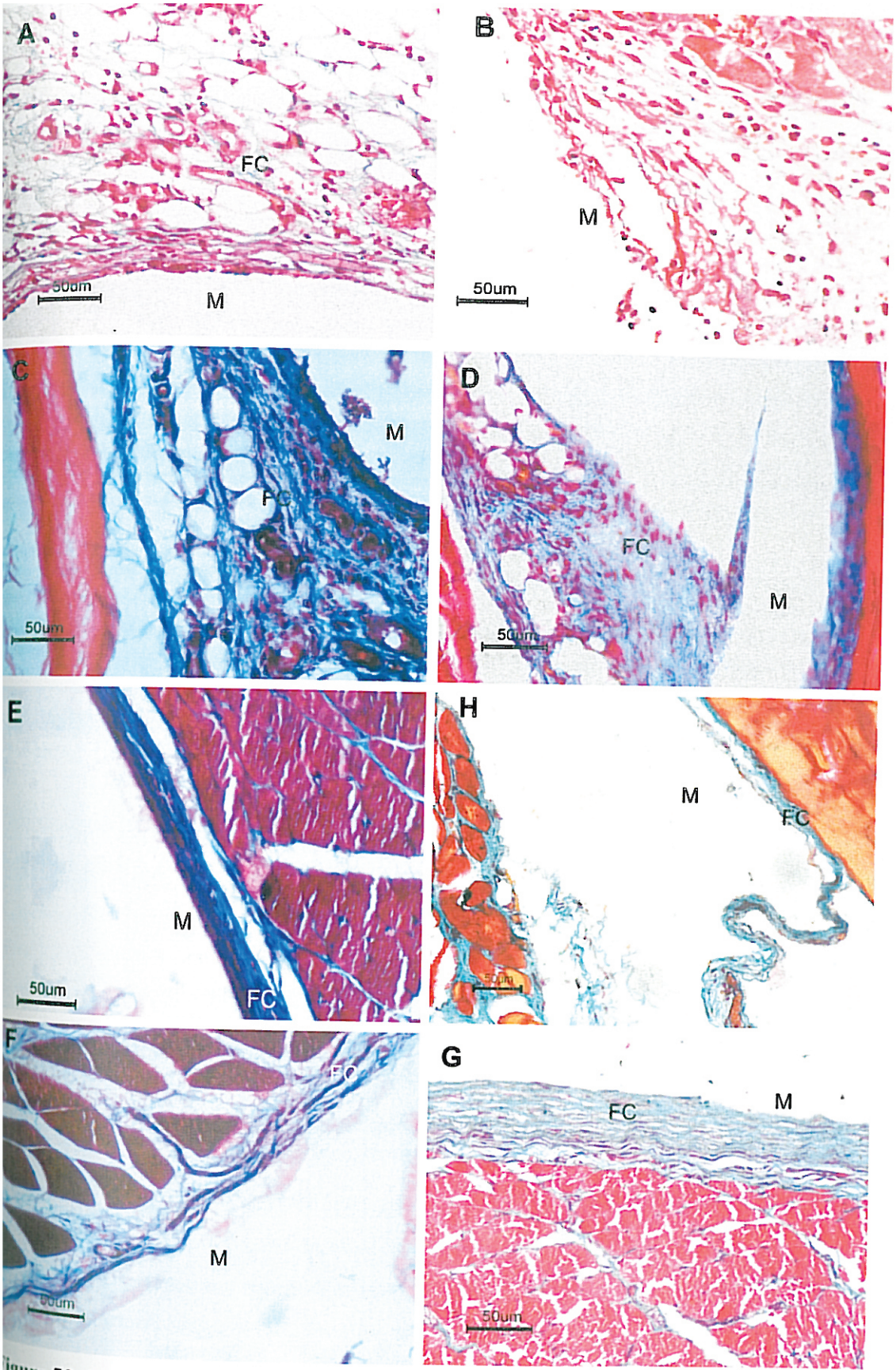

Figure 53: Light micrographs of Masson's trichrome stained sections of muscle around **Ventriculo-peritoneal shunt** : 3 days; 14 days; 30 days, 90 days (A, C, E, G) and **UHMWPE**: 3 days; 14 days; 30 days, 90 days (B ,D ,F ,H)
(M - Implant site, **FC** - Fibrous capsule)

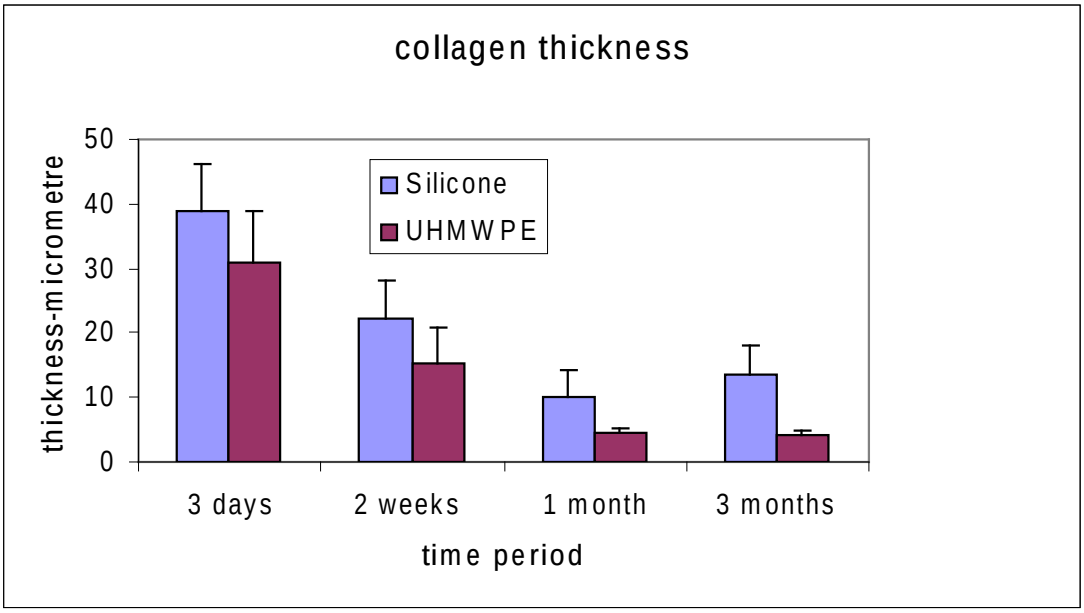

Figure 54: Quantitative evaluation of collagen deposition around VP shunt and UHMWPE

4.5.4. Immunohistochemical analysis

Immunohistochemical staining in 90 day samples revealed persistence of T lymphocytes and macrophages, vimentin and actin positive fibroblasts at tissue material interface of VP shunt (Figure 55-58C). Even though Macrophages and lymphocytes were present around both implants at initial time periods, these cells persisted around silicone VP shunt. But there was notable difference in vimentin and αSMA expression between both the implants (Figure 57, 58 A&C and B&D). Both the markers expressed high and persisted around VP shunt than around UHMWPE.

The cytokines such as TGFβ, TNFα, IL-1α and anti fibrotic cytokines like IFNγ were expressed around VP shunt and UHMWPE. All cytokines were expressed intensely around Silicone VP shunt at 30 days (Figure 59-62A) and persisted at 90 days (Figure 59-62C) whereas around UHMWPE the expression was only at initial time period of 30 days (Figure 59-62B). This indicates normal wound healing around UHMWPE with no chronic inflammation but persistent inflammation around silicone.

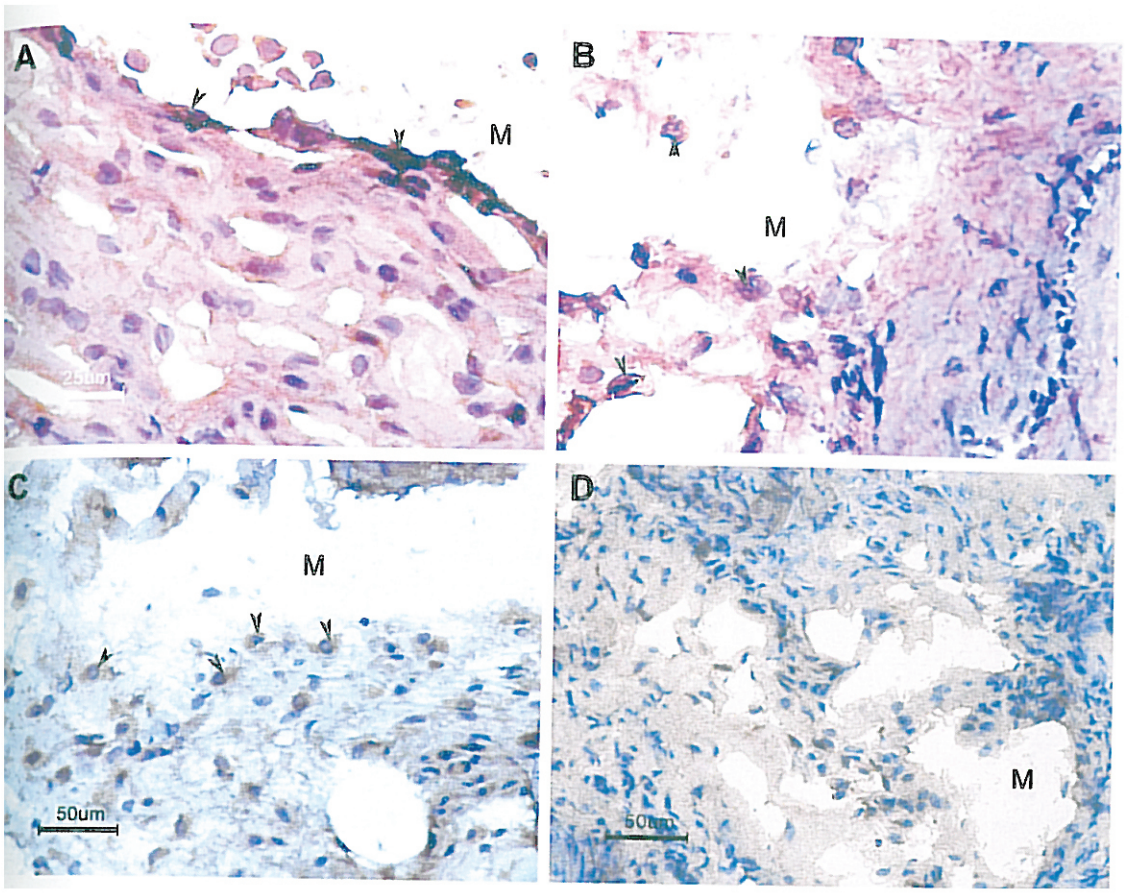

Figure 55: Light micrographs of immunohistochemical staining for ED2 (macrophages) in sections of peri implant tissue around **Ventriculo-Peritoneal shunt**: 30 days; 90 days (A, C) and **UHMWPE**: 30 days; 90 days (B, D)
(**M** - implant site, ▲ - immuno positive cells)

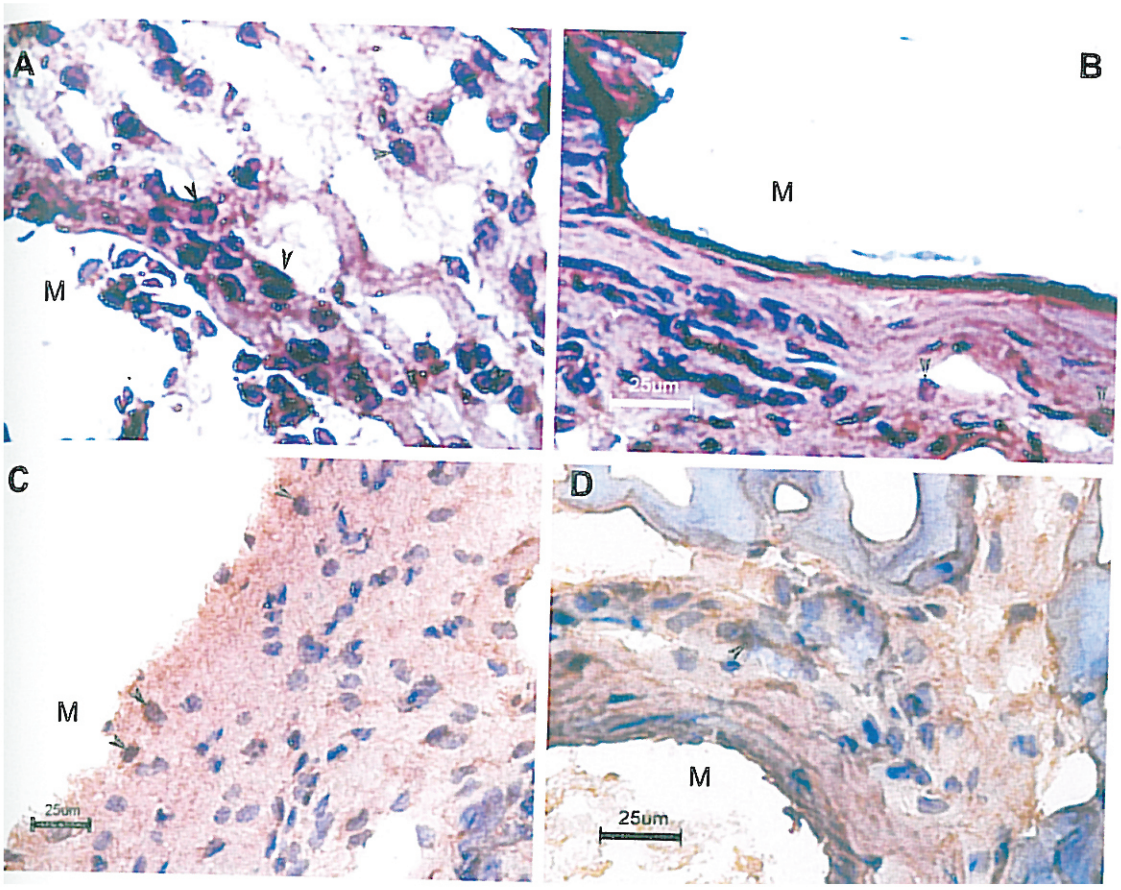

Figure 56: Light micrographs of immunohistochemical staining for CD4 (lymphocytes) in sections of peri implant tissue around **Ventriculo-Peritoneal shunt**: 30 days; 90 days (A, C) and **UHMWPE**: 30 days; 90 days (B, D)
(**M** - implant site, ⋀ - immuno positive cells)

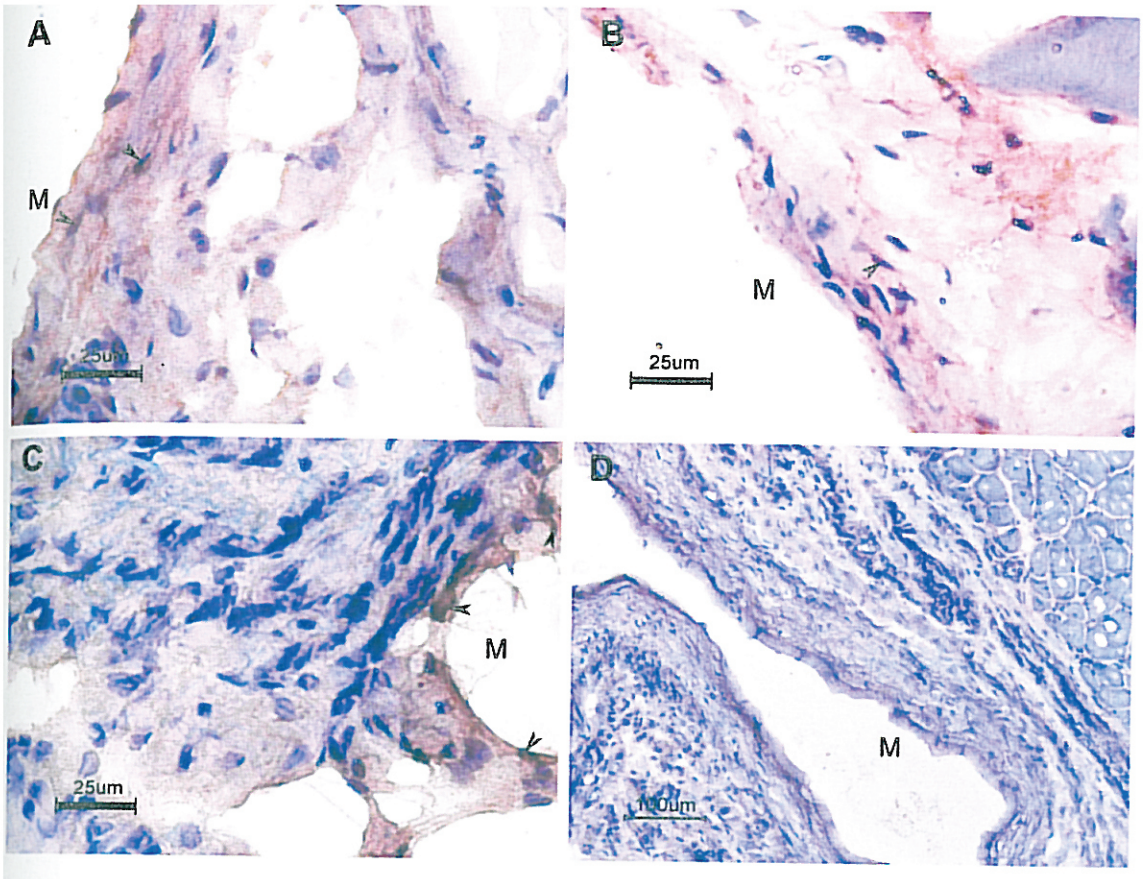

Figure 57: Light micrographs of immunohistochemical staining for vimentin (fibroblasts) in sections of peri implant tissue around **Ventriculo-Peritoneal shunt**: 30 days; 90 days (A, C) and **UHMWPE**: 30 days; 90 days (B, D)
(**M** - implant site, ⮜ - immuno positive cells)

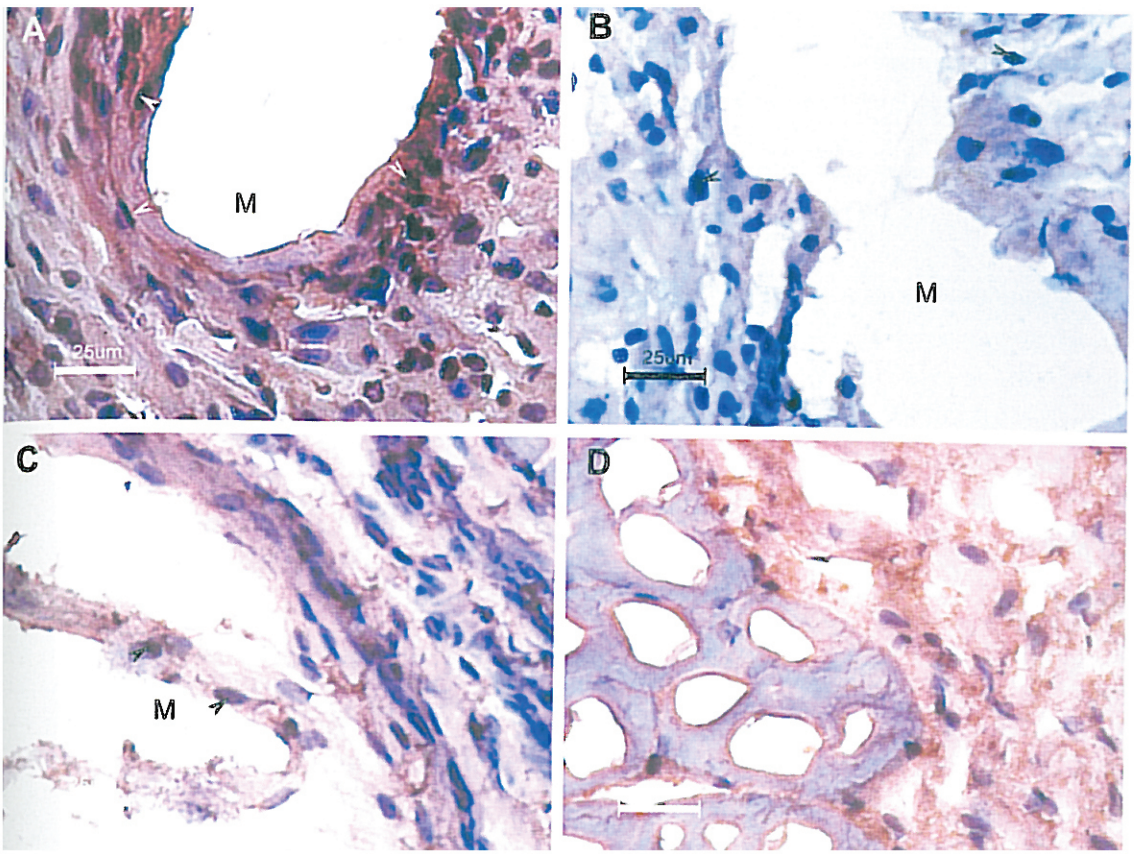

Figure 58: Light micrographs of immunohistochemical staining for αSMA (myofibroblasts) in sections of peri implant tissue around **Ventriculo-Peritoneal shunt**: 30 days; 90 days; 180 days (A, C, E) and **UHMWPE**: 30 days; 90 days; 180 days (B, D, F).
M - implant site, ▲ - immuno positive cells)

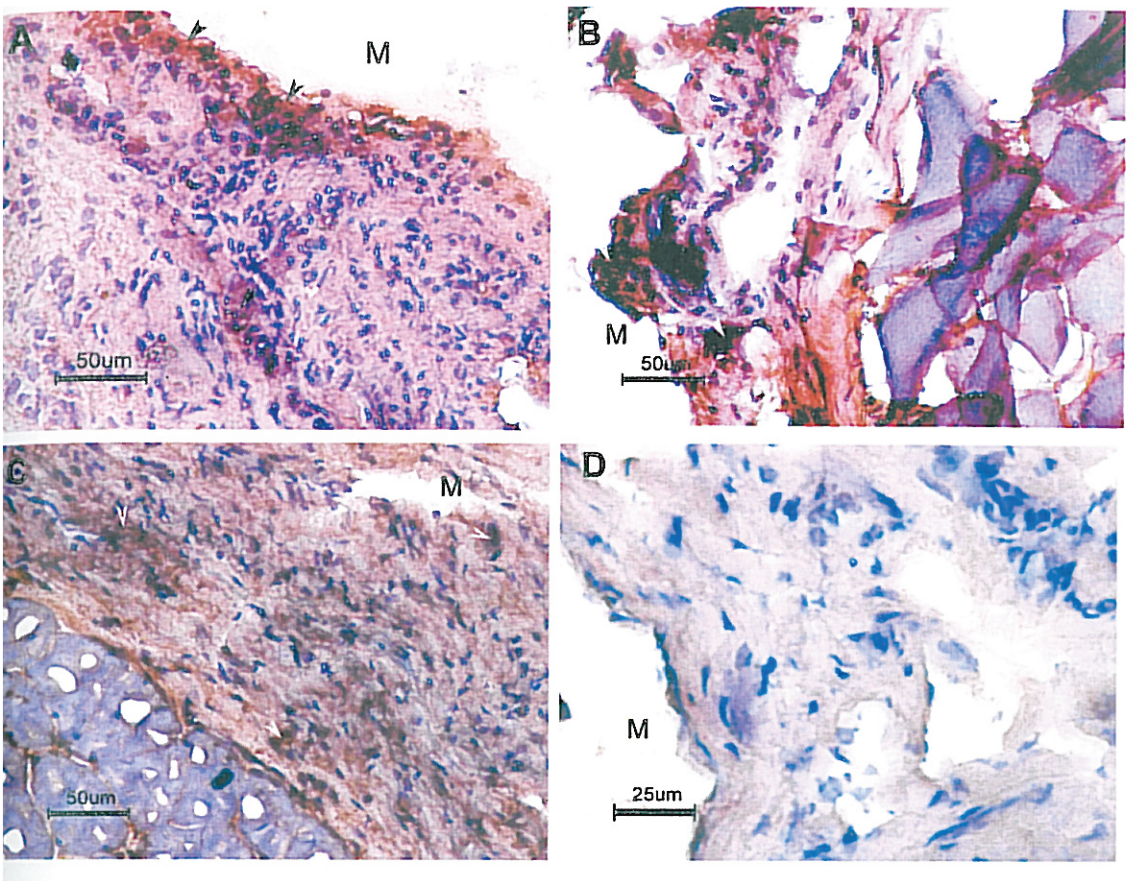

Figure 59: Light micrographs of immunohistochemical staining for TGFβ in sections of peri implant tissue around **Ventriculo-Peritoneal shunt**: 30 days; 90 days (A, C) and **UHMWPE**: 30 days; 90 days (B, D)
(M - implant site, ⮜ - positive staining)

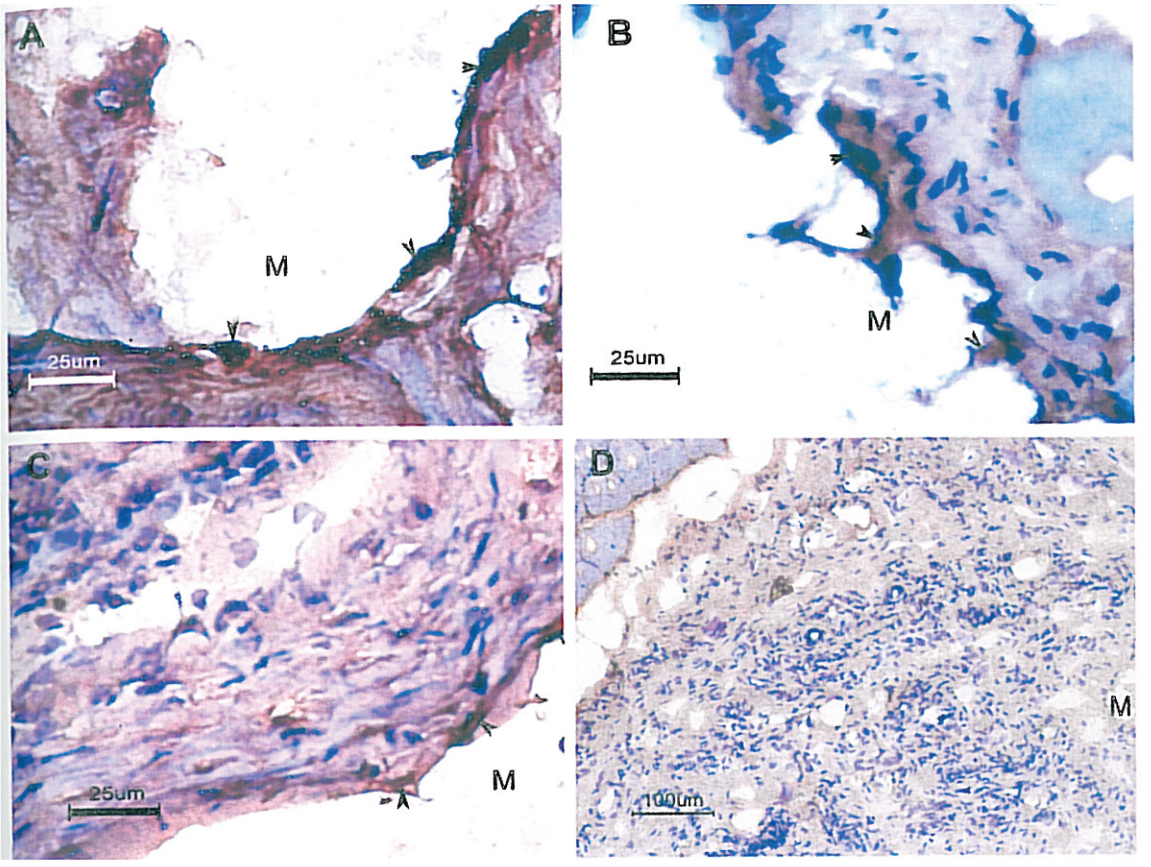

Figure 60: Light micrographs of immunohistochemical staining for TNFα in sections of peri implant tissue around **Ventriculo-Peritoneal shunt**: 30 days; 90 days (A, C) and **UHMWPE**: 30 days; 90 days (B, D)
(**M** - implant site, ⮝ - positive staining)

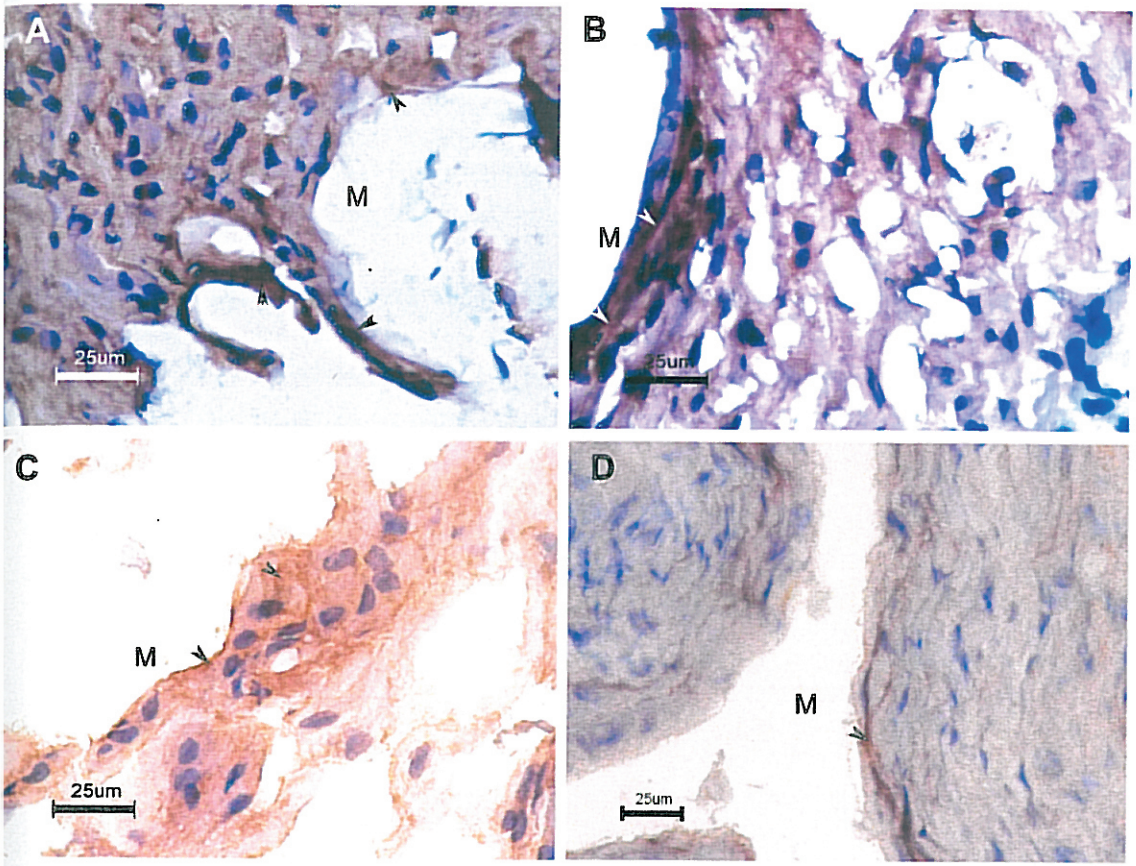

Figure 61: Light micrographs of immunohistochemical staining for IL-1α in sections of peri implant tissue around **Ventriculo-Peritoneal shunt**: 30 days; 90 days (A, C) and **UHMWPE**: 30 days; 90 days (B, D)
(**M** - implant site, ⮝ - positive staining)

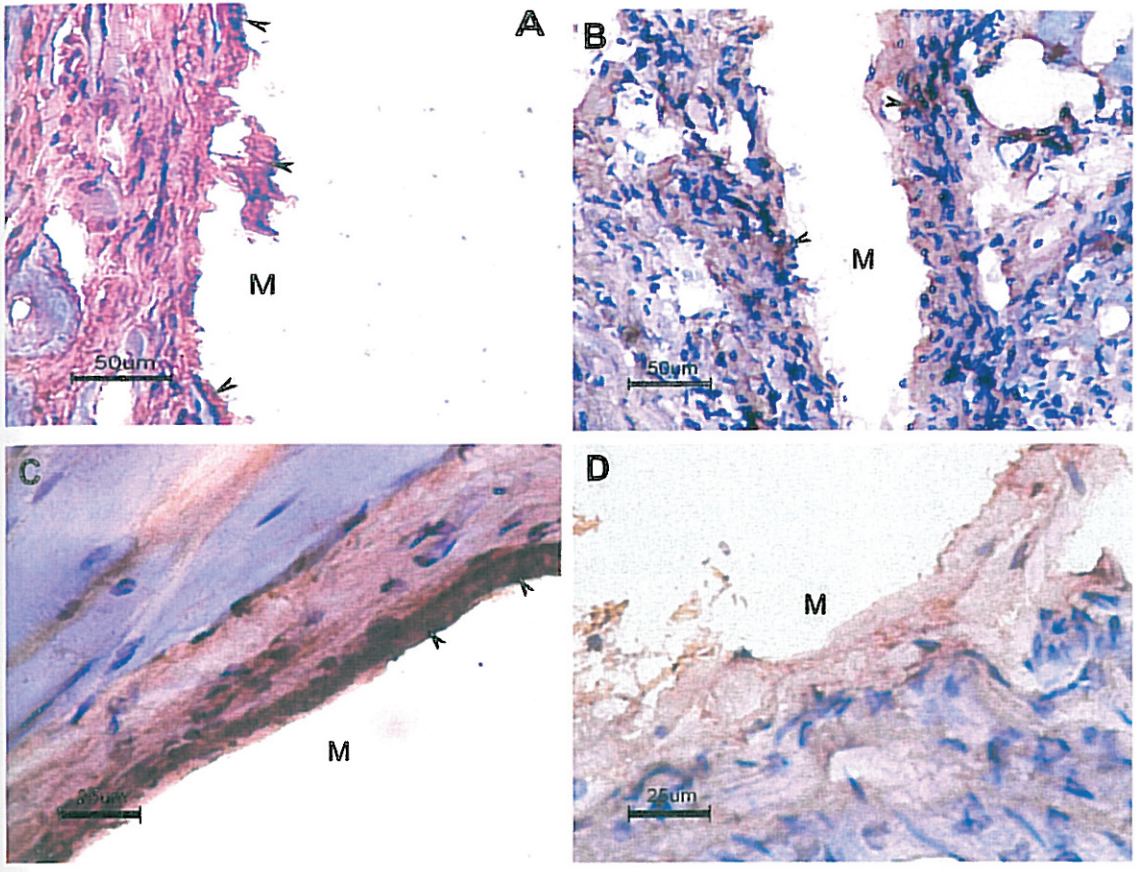

Figure 62: Light micrographs of immunohistochemical staining for IFNγ in sections of peri implant tissue around **Ventriculo-Peritoneal shunt**: 30 days; 90 days (A, C) and **UHMWPE**: 30 days; 90 days (B, D)
(**M** - implant site, ⮝ - positive staining)

Earlier reports demonstrated the presence of antibody responses to shunt bound proteins and polymeric substances suggesting an immunological response behind sterile shunt malfunctions (Vandevord PJ *et al.*, 2004). This and the expression of pro fibrotic and anti fibrotic cytokines suggest a cell-cell interaction between these cells and fibroblasts suggesting an active role of these immune cells in the formation of a thick fibrous sheath around shunt tubing, leading to blockage and shunt failure.

The results of this investigative study shows an apparent difference in fibrous capsule formation and the persistence of myofibroblasts around silicone implants, both around SE and VP shunt as opposed to UHMWPE following long term implantation. The modulatory role of various immune cells and their cytokines in the foreign body response to implants have been monitored in a time dependant manner.

Chapter 5

SUMMARY, CONCLUSIONS & FUTURE DIRECTIVE

5.1. Summary

The formation of extensive fibrosis around silicone implants that lead to capsular contracture and implant failure is a multifaceted problem in which several factors are engaged. Identification of molecule/s involved would aid in devising newer ways to prevent the occurrence of excessive fibrosis around otherwise useful silicone implants.

Data obtained from our study indicates the importance of the silicone material itself in formation of a thick fibrous peri-implant capsule, both in tissue expanders and ventriculo-peritoneal shunts and fibroblast to myofibroblast transformation. Silicone elicits thick fibrous capsule with presence of myofibroblasts both to tissue expander and shunt material in long term. The role of the immune cell, macrophage and its cytokines particularly TGF-β and IL-6 on fibroblast to myofibroblast transformation has also been elucidated. *In vitro* studies also emphasize the salient role of Interleukin-6 as a prominent cytokine that decides the fate of wound healing around a biomaterial. Erk is a key molecule involved in TGF beta as well as Interleukin-6 pathway**.** Macrophages through the secreted cytokines, trigger Erk pathway in fibroblasts which relate to high αSMA expression indicative of fibroblast to myofibroblast transition.

The interaction of macrophages with silicone results in the release of pro fibrotic

cytokines which do have an enhancing effect on fibroblast to myofibroblast transformation. Differential expression of cytokines, with a shift from pro inflammatory to pro fibrotic cytokines around silicone implant during the different phases of wound healing was observed. The effective monitoring of this cytokine levels in an experiment model will be an indicator of normal wound healing versus a chronic inflammatory condition.

Role of T lymphocytes in fibrous tissue remodeling is evident from the mounting presence of IL-10 but IFN γ has no stimulatory effect in fibroblast to myofibroblast transition both *in vivo* and *in vitro*.

The cellular adherence was less on silicone surface at all time periods than over the more hydrophilic UHMWPE, which could be a factor in formation of compact fibrous layer around the implant.

Though the level of silicone in peri-implant tissue *in vivo* was very low, there was a definite leaching of silicone *in vitro* .This may be due to initial migration of the silicone from the surface of the material into peri-implant tissue and then further away to distant organs. Continued release of leachants from silicone implant by spalliation into the surrounding milieu, stimulates macrophages to release fibrogenic cytokines that are involved in a thick fibrous capsule formation around the implant. There exists a dynamic cycle of silicone release, activation of macrophages, release of cytokines and increased collagen deposition along with formation of myofibroblasts. This provides a plausible mechanism behind long term failure of silicone implants due to peri-implant contracture leading to severe pain. The schematic diagram (Figure 63) illustrates the summary of this study:

5.2. Conclusion

This study throws light on role of material surface and degradation products in the activation of monocytes and macrophages, release of cytokines, transformation of fibroblasts to myofibroblasts and collagen deposition in the extensive fibrosis around silicone implants leading to clinical contracture and pain. It also elucidates the importance of the cytokine, IL-6 in addition to TGFβ in the transition of fibroblasts to myofibroblasts.

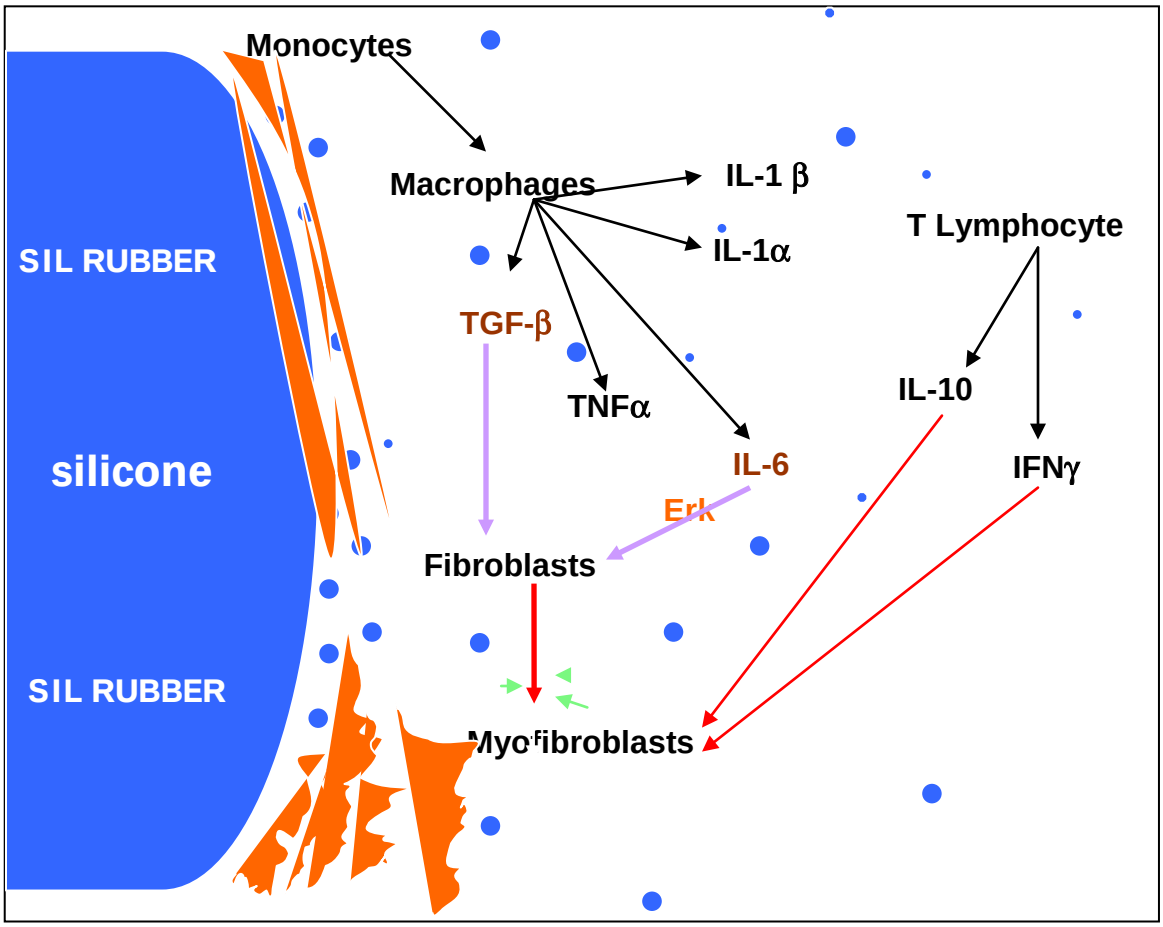

Figure 63: Schematic Diagram of summary of this study

5.3. Future plans

Further investigations on the role of individual silicone leachants in fibroblast, myofibroblast modulation are necessary to get detailed insight on nature of molecular interactions in peri-implant tissue. Such studies would help in deciphering signaling molecules and pathways which could be targeted to prevent long term contracture and failure of silicone prostheses.

BIBLIOGRAPHY

Abbondanzo SL, Young VL, Wei MQ and Miller FW. Silicone gel filled breast and testicular implant capsules: a histologic and immunophenotypic study. *Mod Pathol* 1999; 12(7): 706-713.

Agnew WF, Todd EM, Richmond H, Chronister WS. Biological evaluation of silicone rubber for surgical prosthesis. *J Surg Res* 1962 ; 2: 357–36.

Akdis CA and Blaser. Mechanisms of interleukin-10-mediated immune suppression**.** *Immun* 2001; 103(2): 131-136.

Anderson JM and Jones JA. Phenotypic dichotomies in the foreign body reaction. *Biomat* 2007; 28(34):5114-5120.

Anderson JM. Biological responses to materials. *Ann Rev mat Res.* 2001; **31**: 81-110.

Arai T, Abe K, Matsuoka H, Yoshida M, Mori M, Goya S, Kida H, Nishino K, Osaki T, Tachibana I, Kaneda Y and Hayashi S. Introduction of the interleukin-10 gene into mice inhibited bleomycin-induced lung injury *in vivo*. *Am J Physiol Lung Cell Mol Physiol* 2000; 278(5): L914-L922.

Arepalli SR, Bezabeh S and Brown LS. Allergic reaction to platinum in silicone breast implants. *J Long-term Eff Med* 2002; 12(4): 299-306.

Arion HG ."Retromammary prosthesis". *C R Soc Fr Gynecol* 1965:5.

Backovic A,Wolfram D, Del-Frari B, Piza H, Huber LA,Wick G .Simultaneous analysis of multiple serum proteins adhering to the surface of medical grade polydimethylsiloxane elastomers. *J Immunol Methods* 2007; 328:118-127.

Bal BT, Yılmaz H, Aydın C, Karakoca S and Tokman B. Histopathologic study of rat connective tissue responses to maxillofacial silicone elastomers. *J mat sci: mat med* 2009; 20(9):1901-1907.

Baldwin CM and Kaplan EN. Silicone induced human adjuvant disease? *Ann plast surg* 1983; 10: 270-273.

Barnard JJ, Todd EL, Wilson WG, Mielcarek R, Rohrich RJ. Distribution of organosilicon polymers in augmentation mammoplasties at autopsy. *Plast reconstr Surg* 1997; 100(1): 197-205.

Barnes BJ, Karin M. Mechanisms of disease: Nuclear factor κB-a pivotal transcription factor in chronic inflammatory diseases. *New Engl JMed* 1997; 336:1066-107.

Bayston R, Ashraf W, Bhundia C.. Mode of action of an antimicrobial biomaterial for use in hydrocephalus shunts. *J Antimicrob Chemother* 2004; 53: 778–782.

Behling CA and Spector M. Characterization of the *in vivo* cellular response to selected polymers. In Biological and biomechanical performance of biomaterials. (Eds) Christel P, Eunier A and Lee AJC, Elsevier science Publishers B.V.1986: 327-330.

Benesch J, Askendal A and Tengvall P. Quantification of adsorbed human serum albumin: a comparison between radio immuno assay (RIA) and simple null ellipsometry. *Coll.surf.B.Biointerfaces* 2000; 20(1):51-62.

Beno DW, Espinal R, Edelstein BM and Davis BH. Administration of prostaglandin E1 analog reduces rat hepatic and Ito cell collagen gene expression and collagen accumulation after bile duct ligation injury. *Hepatol* 1993; 17: 707–714.

Bente J, Irene WH, Allan W, Soren F, Henning B, Birthe T, Joseph MK, Samsoe BD, Jorgen H. Anti polymer antibodies in Danish with silicone breast implants. *J Long-term Eff Med* 2004; 14(2): 73-79.

Bhat SV. Overview of Biomaterials in Biomaterials. (Eds) Bhat SV. Narosa publishing house, Delhi, 2002: 4.

Boch AL, Hermelin E, Sainte-Rose C, Sgouros S. Mechanical dysfunction of ventriculoperitoneal shunts caused by calcification of the silicone rubber catheter. *J Neurosurg* 1998; 88: 975–982.

Bondurant S, Ernster V, Herdman R (Eds). Committee on the Safety of Silicone Breast Implants . Safety of Silicone Breast Implants. Institute of Medicine. 1999; 21.

Bonfield TL, Colton E and Anderson J.M. Protein adsorption of biomedical polymers influences activated monocytes to produce fibroblast stimulating factors. *J Biomed Mater Res* 1992; 26: 457- 465.

Border WA and Ruoslahti E. Transforming growth factor-beta in disease: The dark side of tissue repair. *J Clin Invest* 1992; 90: 1–7.

Brodbeck WG, Voskerician G, Ziats NP, Nakayama Y, MatsudaT and Anderson JM. *In vivo* leukocyte cytokine mRNA responses to biomaterials are dependent on surface chemistry. *J Biomed Mater Res* 2003; 64 A: 320-329.

Bronzena SJ, Fenske NJ, Cruse CW, Espinoza CG, Vasey FB, Germain BF and Espinoza LR. Human adjuvant disease following augmentation mammoplasty. *Arch dermatolo* 1988; 124:1383-1386.

Browd SR, Gottfried ON, Ragel BT, Kestle JR. Failure of cerebrospinal fluid shunts: part II: Overdrainage, loculation, and abdominal complications. *Pediatr Neurol* 2006b; 34: 171–176.

Browd SR, Ragel BT, Gottfried ON, Kestle JR**.** Failure of cerebrospinal fluid shunts: part I: obstruction and mechanical failure. *Pediatr Neurol* 2006a ; 34: 83–92.

Brown SL, Duggirala HJ and Pennello G. An association of silicone gel breast implant rupture and fibro myalgia. *Curr Rheumatol Rep* 2002; 4(4):293-298.

Bucky LP, Ehrlich HP, Sohoni S and May JW . The capsule quality of saline –filled smooth silicone, textured silicone, and polyurethane implants in rabbit: a long term study. *Plast Reconstr Surg* 1995; 95 (5):937-938.

Buttner C, Skupin A, Rieber AP. Transcriptional activation of the type I collagen genes COL1A1 and COL1A2 in fibroblasts by interleukin-4: analysis of the functional collagen promoter sequences. *J Cell Physiol.* 2004; 198 (2):248-58.

Celli B, Textor S and Covnat DM. Adult respiratory distress syndrome following mammary augmentation. *Am j of med Sci* 1978; 275: 81-85.

Coleman DJ , Sharpe DT, Naylor IA, Chander CL, Cross SE. The role of the contractile fibroblast in the capsules around tissue expanders and implants. *Br J Plat Surg* 1993; 46(7):547-556.

Coleman DJ, Foo IT, Sharpe DT. Textured or smooth implants for breast augmentation? A prospective controlled trial. *Br J Plast Surg.*1991; 44: 444-448.

Collins P, Hockley AD, Woollam DH. Surface ultrastructure of tissues occluding ventricular catheters. *J Neurosurg* 1978; 48: 609–613.

Cornelissen AMH, Maltha JC, VondenHoff JW and Kuijpers- Jagtman AM. Local injection of IFNgamma reduces the number of myofibroblasts and the collagen content in palatal wounds. *J Dent Res* 2000; 79: 1782-1788.

Darby I, Skalli O and Gabbiani G. Alpha-smooth muscle actin is transiently expressed by myofibroblasts during experimental wound healing. *Lab Invest* 1990; 63: 21-29.

de Aquino HB, Carelli EF, Neto BAG, Pereira CU. Nonfunctional abdominal complications of the distal catheter on the treatment of hydrocephalus: an inflammatory hypothesis? Experience with six cases. *Child's Nerv Syst* 2006 ; 22: 1225–1230.

de Jong WH, Kallewaard M, Goldhoorn CA, Verhoef CM, Johannes WJ, Jan B, Schouten SAG and Loveren HV. Long term exposure to silicone breast implants does not induce antipolymer antibodies. *Biomat* 2004; 25: 1095-1103.

de Waal MR, Abrams J, Bennett B, Fidgor C, de Vries J. Interleukin-10 inhibits cytokine synthesis by human monocytes: An autoregulatory role of Il-10 produced by macrophages. *J Exp Medicine* 1991;174: 1209-1220.

Del Bigio MR. Biological reactions to cerebrospinal fluid shunt devices: a review of the cellular pathology. *J Neurosurg* 1998; 42: 319–325.

Del Bigio MR, Fedoroff S. Short-term response of brain tissue to cerebrospinal fluid shunts *in vivo* and *in vitro*. *J Biomed Mater Res* 1992; 26: 979–987.

Denel TF, Kawahara RS, Mustoe TA, Piercer GF. Growth factors and wound healing :platelet derived growth factor as a model cytokine. *Annu Rev Med* 1991; 42: 567-584.

Desmouliere A, Chaponnier C, Gabbiani G. Tissue repair, contraction and the myofibroblast. *Wound repair regen* 2005; 13(1):7-12.

Desmoulière A, Christelle Guyot and Giulio Gabbiani .The stroma reaction myofibroblast: a key player in the control of tumor cell behavior. *Int J Dev Bio* 2004; 48:509-517.

Desmouliere A, Geinoz A, Gabbiani F and Gabbiani G. Transforming growth factor-beta 1 induces alpha-smooth muscle actin expression in granulation tissue myofibroblasts and in quiescent and growing cultured fibroblasts. *J Cell Biol* 1993; 122(1):103-111

Desmouliere A, Guyot C and Gabbiani G. The stroma reaction myofibroblast: a key player in the control of tumor cell behaviour. *Int J dev Biol* 2004; 48:509-517.

Desmouliere A, Redrad M, Darby I, Gabbiani G. Apoptosis mediates the decrease in cellularity during the transition between granulation tissue and scar. *Am J Pathol* 1995; 146: 56-66.

Desmouliere A, Rubbia-Brandt L, Abdin A, Walz J, Maciera-Coelho A, Gabbiani G. Alpha smooth muscle actin is expressed in a subpopulation of cultured and cloned fibroblasts and is modulated by gamma-interferon.*Exp cell res* 1992 a ; 201: 64-73.

Dolores W, Christian R, Harald N, Hildegunde P, Georg W. Cellular and molecular composition of fibrous capsules formed around silicone breast implants with special focus on local immune reactions. *J Autoimmun* 2004; 23: 81-91.

Ducheyne P and Hastings GW. Metal and ceramic biomaterials: strength and surface, Vol.2, CRC press, Boca Raton FL 1984: 79-105.

Dugina V, Fontao L, Chaponnier C, Vasilev J, Gabbiani G. Focal adhesion features during myofibrobalstic differentiataion are controlled by intracellular and extracellular factors. *J Cell Sci* 2001; 114: 3285-3296.

Dumitru.S. (Ed) Polymeric Biomaterials, 2nd edition, New York: Marcel dekker, 2002.

Duncan MR, Frazier KS, Abramson S, Williams S, Klapper H, Huang X and Grotendorst GR Connective tissue growth factor mediates transforming growth factor β-induced collagen synthesis: Down-regulation by cAMP. *FASEB J* 1999; 13: 1774–1786.

Eltze E, Bettendorf O, Rody A, Jackisch C, Herchenröder F, Böcker W, Pfleiderer B. Influence of local complications on capsule formation around model implants in a rat model. *J Biomed Mater Res* 2003 ; 64A (1): 12-19**.**

Eming AS, Werner S, Bugnon P, Wickenhauser, Siewe L, Utermöhlen O, Jeffrey M, Krieg DT and Roers A. Accelerated Wound Closure in Mice Deficient for Interleukin-10. *Am J Pathol* 2007; 170: 188-202.

Endo LP, Edwards NL, Longley S, Corman C and Panush RS. Silicone and rheumatic diseases. *Arthritis Rhuem* 1987; 17:112-118.

Eyden B. Electron microscopy in the study of myofibroblastic lesions. *Semin Diagn Pathol* 2003 ; 20(1):13-24.

Eyden B. The myofibroblast: an assessment of controversial issues and a definition useful in diagnosis and research. *Ultrastruct pathol* 2001; 25(1): 39-50.

FDA Breast Implant Consumer Handbook, 2004-06-08.

Fernell E, Hadberg B, Hadberg G,Von Wendt L. Epidemiology of infantile hydrocephalus in sweden.Birth prevalence and general data. *Acta Paediatr Scand* 1986; 75:975-981.

Flassbeck D, Pfliederer B,Grumping R,Hirner AV. Determination of low molecular weight silicones in plasma and blood of women after exposure to silicone breast implants by GC/MS. *Anal chem* 2001; 73:606-611.

Friedman DW, Orland PJ and Greco RS. Biomaterials: An Historical perspective. Implantation biology: The host response and Biomedical Devices. CRC Press 1994: 1-12.

Friemann J, Bauer M, Golz B, Rombeck N, Hohr D, Erbs G, Steinau HU, Olbrisch RR. Physiologic and pathologic patterns of reaction to silicone breast implants. *Zentral bl chir* 1997; 122:551-564.

Furukawa F, Matsuzaki K, Tahashi Y, Yoshida K, Sugano Y, Yamagata H, Matsushita M, Seki T, Inagaki Y, Nishizawa M, Fujisawa J and Inoue K. p38 MAPK mediates fibrogenic signal through smad3 phosphorylation in rat myofibroblasts. *J Hepatol* 2003; 38: 879-889.

Gabbiani G. The evolution of the Myofibroblast concept: a key cell for wound healing and fibrotic diseases. *G gerontol* 2004; 52:280-282.

Gabbiani G. Evolution and clinical implications of the myofibroblast concept. *Cardiovasc Res* 1998; 38: 545-548.

Galluci RM., Lee BG and Tomasek JJ. IL-6 modulates alpha smooth muscle actin expression in dermal fibroblasts from Il-6 deficient mice. *J invest Dermatol* 2006; 126: 561-568.

Garcia JEL, Cabo MRM, Mates F, Rodriguez, Losada JP, Lopez AJ and Arellano JLP. Effect of cyclosporine-A on inflammatory cytokine production by U937 monocyte- like cells. *Mediat Inflamm* 2000; 9: 169–174.

Garton HJ, Piatt JH, Jr. Hydrocephalus. *Pediatr Clin North Am* 2004; 51: 305–325.

Gayou R, Rudolph R. Capsular contraction around silicone mammary prosthesis. *Ann Plast Surg* 1979; 2: 62-71.

Ghosh AK, Yuan W, Mori Y, Chen S and Varga J. Antagonistic Regulation of Type I Collagen Gene Expression by Interferon-γ and Transforming Growth Factor-β integration at the level of p300/CBP transcpritional coactivators. *J Biol Chem* 2001**;** 276 (14)**:** 11041-11048.

Giulietti A, Overbergh L, Valckx D, Decallonne B, Bouillon R, Mathieu C. An overview of real time quantitative PCR: applications to quantify cytokine gene expression. *Methods* 2001 ; 25(4):386-401.

Gorczyca DP, De Bruhl ND, Ahn CY , Hoyt A, Sayre JW, Nudell P, McCombs M, Shaw WW and Bassett LW. Silicone breast implant ruptures in an animal model: comparison of mammaography, MR imaging , US and CT. *Radiology* 1994; 190:227- 237.

Goumans MJ and Mummery C. Functional analysis of the TGFb receptor/Smad pathway through gene ablation in mice. *Int J Dev Biol* 2000; 44: 253-265.

Granchi D, Cavedagna D, Ciapetti G, Stea S, Schiavon P, Giuliani R and Pizzoferrato A. Silicone breast implants: The role of immune system on capsular contracture formation. *J Biomed Mater Res* 1995; 29: 197-202.

Grinnell F. Fibroblasts, myofibroblasts, and wound contraction *J Cell Biol* 1994; 124: 401-404.

Guerret S, Desmoulière A, Chossegros P, Costa AMA, Badid C, Trépo C, Grimaud JA and Chevallier M. Long-term administration of interferon-α in non-responder patients

with chronic hepatitis C: Follow-up over 5 years of liver fibrosis. *J Viral Hepat* 1999; 6: 125–133.

Hanlon TPO', Okada S, Love LA, Dick G, Young VL and Miller FW. Immunohistopathology and T cell receptor gene expression in capsules surrounding silicone breast implants. *Curr Top Microbiol Immunol* 1996; 210: 237-242.

Hansmann H. A new method of fixation of fragments in complicated fractures. *Verein Duetsches Geselschaftfur chirurgie* 1886; 15: 134.

Henderson B. Therapeutic modulation of cytokines. *Ann Rhuem Dis* 1995; 54: 519-523.

Hinz B and Gabbiani G. Cell-matrix and cell-cell contacts of myofibroblasts: role in connective tissue remodeling. *Thromb Haemost* 2003; 90: 993-1002.

Hinz B, Dugina V, Ballestrem C, Wehrle-Haller B and Chaponnier C. α-Smooth Muscle Actin is Crucial for focal adhesion maturation in myofibroblasts. *Mol Biol Cell* 2003; 14(6): 2508–2519.

Holmich LR, Friis S, Fryzek JP, Vejborg IM, Conrad C, Sletting S, Kjoller K, McLaughlin JK and Oisen JH. Incidence of silicone breast implant rupture. *Arch Surg* 2003; 138(7):801-806.

Holmich LR, Kjoller K, Fryzek JP, Hoier-madsen M, Vejborg I, Conrad C, Sletting S, McLaughlin JK, Breiting V and Friis S. Self-reported diseases and symptoms by rupture among unselected Danish women with cosmetic silicone breast implants. *Plast Reconstr Surg* 2003 ; 111(2):723-734.

Homsy CA, Hodge R, Gordon EE, Braggs BS, Esterella M. Biochemical Engineering materials screening and monitoring. *J Biomed Mater Res* 1969; 3: 235-245.

Hunt J, Farthing M J, Baker, L R, Crocker PR. Silicone in the liver: Possible late effects. *Gut* 1989; 30:239-242.

Inagaki Y, Nemoto T, Kushida M, Sheng Y,Higashi K, Ikeda K, Kawada N, Shirasaki F, Takehara K, Sugiyama K, Fujii M,Yamauchi H, Nakao A, Crombrugghe BD, Watanabe T and Okazaki I. Interferon alfa down-regulates collagen gene transcription and suppresses experimental hepatic fibrosis in mice. *J Hepatol* 2003; 38(4): 890-899.

Ishidoya S, Morrisey J, McCracken R, Reyes A, and Klahr S. Angiotensin II receptor antagonist ameliorates renal tubulointerstitial fibrosis caused by unilateral ureteral obstruction. *Kidney Int* 1995; 47: 1285–1294.

ISO 10993-12. Biological evaluation of Medical devices-Part 12: Sample preparation and reference materials. 2nd edition, 2002-12-15.

ISO 10993-13. Identification and quantification of degradation products from polymeric medical devices, first edition, 1998

ISO 10993-6: Biological evaluation of Medical devices-tests for local effects after implantation.2nd Edition: 2007

James SJ, Pogribna M, Miller BJ, Bolon B and Muskhelishvili L. Characterization of cellular response to silicone implants in rats: implications for foreign-body carcinogenesis. *Biomat.* 1997; 18 :667-675.

Jones JA, Chang DT, Meyerson H, Colton E, Kwon K, Matsuda T, Anderson JM. Proteomic analysis and quantification of cytokines and chemokines from biomaterial surface-adherent macrophages and foreign body giant cells. *J Biomed Mater Res* 2007 ; 83A:585-596.

Kalousdian S, Karlan M.S, Williams M.A. Silicone elastomer cerebrospinal fluid shunt systems. Council on Scientific Affairs, American Medical Association. *J Neurosurg* 1998; 42: 887–892.

Kamel M, Protzner K, Fornasier V, Peters W, Smith D and Ibanez D. The peri-implant breast capsule: An immunophenotypic study of capsules taken at explantation surgery. *J Biomed Mater Res Part B: Appl Bio mat* 2001; 58**:** 88-96.

Kämpfer H, Paulukat J, Mühl H, Wetzler C, Pfeilschifter J, Frank S. Lack of interferon-gamma production despite the presence of interleukin-18 during cutaneous wound healing. *Mol Med* 2000; 6(12):1016-1027.

Katzin WE, Feng L, Abbuhi M and Klein MA. Phenotype of lymphocytes associated with the inflammatory reaction to silicone gel breast implants. *Clin diagn lab immunol* 1996; 3(2):156-161.

Kessler DA. The basis of the FDA's decision on breast implants. *New Engl J Med* 1992; 326: 1713-1715.

Kossovsky N, Freiman CJ. Silicone breast implant pathology. Clinical data and immunologic consequences. *Arch Pathol Lab Med* 1994; 118: 686–693.

Kossovsky N, Frieman CJ. Physicochemical and immunological basis of silicone pathophysiology. *J Biomater Sci Polym Ed* 1995; 7(2):101-113.

Kumagai YA, Chiyuki and Shiokawa Y .Scleroderma after cosmetic surgery: four cases of human adjuvant disease. *Arthritis Rheum* 1979; 22:532-537.

Laitung JK, McClure J and Shuttleworth CA. The fibrous capsules around static and dynamic implants: their biochemical, histological and ultrastructural characteristics. *Ann Plast Surg* 1987; 19:208-216.

Leask A and Abraham DJ. TGF beta signaling and the fibrotic response. *FASEB J* 2004; 18:816-827.

Legrand AP, Georgi M ,Pavlov S, France GM, Famery R, Bresson B, Zhang Ze, Guidoin R. Degenerative mineralization in the fibrous capsule of silicone breast implants.*J Mater Sci Mater Med.* 2005; 16(5):477-85.

Lin PH, Hirko MK, Fraunhofer VJA and Greisler HP. Wound healing and inflammatory response to biomaterials. In Wound closure biomaterials and devices.1st Ed. Chu CC, Greisler HP, Fraunhofer VJA .CRC Press, 1997: 7-24.

Lin Z, Kondo T, Ishida Y, Takayasu T and Mukaida N. Essential involvement of IL-6 in the skin wound healing process as evidenced by delayed wound healing in IL-6 deficient mice. *J Leukocyte Biol* 2003; 73:713-721.

Loh IH, Lin HL and Chu CC. Plasma modification of synthetic absorbable sutures. *J Appl Biomater* 1992; 3: 131-146.

Lopez GP, Ratner BD, Tidwell CD, Haycox CL and Rapoza RJ. Glow discharge plasma deposition of tetraethyleneglycoether for fouling-resistant biomaterial surfaces. *J Biomed Mater Res* 1992; 26(4): 415-439.

Lord GH. Regulation and reason for biocompatibility testing, Techniques of biocompatibility testing, Vol. 1, CRC press Inc, Boca Raton, 1986: 1-33.

Luttikhuizen DT, Harmsen MC and VanLuyn MJA. Cellular and molecular dynamics in the foreign body reaction. *Tissue Eng* 2006; 12: 1955-1970.

Majno G and Joris I. Chronic Inflammation .In Cells, Tissues and Diseases: Principles of General Pathology. (Eds) Majno G and Joris I. Blackwell Sciences, 1996: 442-470.

Mallat A, Preaux AM, Blazejewski S, Rosenbaum J, Dhumeaux D and Mavier P. Interferon alfa and gamma inhibit proliferation and collagen synthesis of human Ito cells in culture. *J Hepatol* 1995; 21: 1003–1010.

Manabe N, Chevallier M, Chossegros P, Causse X, Guerret S, Trépo C and Grimaud JA. Interferon-α2b therapy reduces liver fibrosis in chronic non-A, non-B hepatitis: A quantitative histological evaluation. *J Hepatol* 1993; 18: 1344–1349.

Mancino D, Vuotto ML and Minucci M. Effects of a crystalline silica on antibody production to T-dependant and T-independent antigens in Balb/c mice. *Int Arch Allergy Appl Immunol* 1984; 73: 10-13.

Mauviel A, Temime.N, Charron D, Loyau.G and Pujol JP. Induction of the interleukin-1β production in human dermal fibroblasts by interleukin-1α and tumor necrosis factor-α. Involvement of protein kinase- dependent and adenylate cyclase-dependent and adenylate cyclase-dependent regulatory pathways**.** *J Cell Biochem* 1991; 47(2): 2174 – 183.

Messer RLW, Lewis JB, Wataha JC, Adama Y and Tseng WY. Cytokine secretion from monocytes persist differentially after activator removal-one mechanism of long term biological response to implants. *J Biomed Mater Res: part B Appl biomat* 2007; 83B: 58-63.

Millonig G, Niederegger H, Rabl W, Hochleitner BW, Hoefer D, Romani N, Wick G. Network of vascular- associated dendritic cells in intima of healthy young individuals. *Arterioscler Thromb Vasc Biol* 2001; 21:503-508.

Moulin V, Castilloux G, Auger FA, Garrel D, O'Connor-McCourt MD, Germain L . Modulated Response to Cytokines of Human Wound Healing Myofibroblasts Compared to Dermal Fibroblasts. *Exp Cell Res* 1998; 238(1): 283-293.

Naim JO, Satoh IM, Buehner NA, Ippolito KML, Yoshida H, Nusz D, Kurtelawicz L, Cramer SF and Reeves WH. Induction of Hypergammaglobulinemia and Macrophage Activation by Silicone Gels and Oils in Female ASW Mice. *Clin Diagn Lab Immunol* 2000; 7(3): 366-370.

Norde W and Lyklema J. Why Proteins Prefer Interfaces? In The Vroman effect. (Eds) Bamford CH, Cooper SL, Tsuruta T , VSP, 1992:1.

Pages G, Guerin S, Grall D, Bonino F, Smith A, Anjuere F. Defective thymocyte maturation in p44 MAP kinase (Erk 1) knockout mice. *Science* 1999; 286: 1374-1378.

Peters W, Smith D, Lugowski S. Silicon assays in women with and without silicone gel breast implants- a review. *Ann Plast Surg* 1999 ; 43(3): 324-30.

Petillo O, Barbarisi A, Margarucci S, deRosa A and Peluso G. Fibroblast cell activation- a highly orchestrated reaction to Biomaterial implantation. Integrated biomaterial science (Eds). Barbucci R, KluwerAcademic/ plenum publishers, 2002: 660-663.

Pfleiderer B, Garrido L. Migration and accumulation of silicone in the liver of women with silicone gel-filled breast implants. *Magn Reson Med* 1995; 33(1): 8-17.

Phan SH. The Myofibroblast in Pulmonary Fibrosis. *Chest* 2002; 122 (6): 2865-2895.

Picha GJ and Goldstein JA. Analysis of the soft–tissue response to components used in the of breast implants: a rat animal model. *Plast Reconstr Surg* 1990; 87: 490-500.

Pollock H. Breast capsular contracture: a retrospective study of textured versus smooth silicone implants. *Plast Reconstr Surg*1993; 91: 404-407.

Postlethwaite AE, Raghow R, Stricklin GP, Poppleton H, Seyer JM and Kang AH. Modulation of fibroblast functions by interleukin 1: increased steady-state accumulation of type I procollagen messenger RNAs and stimulation of other functions but not chemotaxis by human recombinant interleukin 1 alpha and beta. *J Cell Biol* 1988; 106(2):311-318.

Prakash S, Paul WE and Robbins PW. Fibrosin, a novel fibrogenic cytokine modulates expression of myofibroblasts. *Exp mol path* 2007; 82: 42-48.

Rees DA, Badley RA, Bayley SA, Couchman JR, Smith CG and Woods A. Surface components in fibroblast adhesion and movement. In Cellular Interactions. (Eds). Jingle JT and Gordon JL, Elsevier, 1981.

Robinson MJ and Cobb MH. Mitogen –activated protein kinase pathways. *Curr opin cell biol* 1997; 9:180-186.

Ross R, Everett NB and Tyler R. Wound healing and collagen formation.The origin of the wound fibroblast studied in parabiosis. *J Cell Biol* 1970; 271:4916-4922.

Rudolph R, Abraham J, Vecchione T, Guber S and Woodward M. Myofibroblasts and free silicon around breast implants. *Plast Reconstr Surg* 1978; 62: 185-196.

Ruiz-de-Erenchun RMD, Herrerias JD and Hontanlla BMD. Use of transforming Growth factor-(beta)1 inhibitor peptide in periprosthetic capsular fibrosis: Experimental model with tetraglycerol Dipalmitate. *Plast Reconstr Surg* 2005; 116(5):1370-1378.

Ruiz-Ortega M and Egido J. Angiotensin II modulates cell growth-related events and synthesis of matrix proteins in renal interstitial fibroblasts. *Kidney Int* 1997; 52: 1497–1510.

Sappino AP, Schürch W, Gabbiani G. Differentiation repertoire of fibroblastic cells: Expression of cytoskeletal proteins as marker of phenotypic modulations. *Lab Invest* 1990; 63: 862-866.

Schmidt S, Horch K, Normann R. Biocompatibility of silicone-based electrode arrays implanted in feline cortical tissue. *J Biomed Mater Res* 1993; 27: 1393–1400.

Sefton MV, Cholakis CH and Lianos G. Preparation of non thrombogenic materials by chemical modification, Blood Compatibility,Vol1,Williams,D.F.(Ed.)CRC press, Boca Raton, FL, 1987: 51-198.

Sekhar LN, Moossy J and Guthkelch AN. Malfunctioning ventriculoperitoneal shunts, Clinical and pathological features**.** *J Neurosurg* 1982; 56(3): 411-416.

Serini D, BochatanRiallat ML, Geinoz RP, Borsil A, Zardi L and Gabbiani G. Thefibronectin domain ED-a is crucial for myofibroblatsic phenotype induction by transforming growth factor beta 1.*J Cell Biol* 1998; 142: 873-888.

Sgouros S and Dipple SJ. An investigation of structural degradation of cerebrospinal fluid shunt valves performed using scanning electron microscopy and energy-dispersive X-ray microanalysis. *J Neurosurg* 2004; 100: 534–540.

Shanklin DR and Smalley DL. Dynamics of Wound Healing after Silicone Device Implantation. *Exp Mol Pathol* 1999; 67(1):26-39.

Shanklin DR and Smalley DL. Silicone immunopathology. *Sci and Med*1996; 3(5): 22.

Shao R, Shi Z, Gotwals PJ, Koteliansky VE, George J and Rockey DC. Cell and molecular regulation of endothelin-1 production during hepatic wound healing. *Mol Biol Cell* 2003; 14: 2327–2341.

Silver RM, Swahn EE, Allen JA, Sahn S, Green W, Maize JC and Garen PD. Demonstration in silicon in sites of connective tissue disease in patients with silicone gel breast implants. *Arch dermatol* 1993; 129: 63-68.

Smalley DL, Shanklin DR, Hall MF, Michael V, Stevens and Hanissian A. Immunologic stimulation of T lymphocytes by silica after use of silicone mammary implants. *FASEB J* 1995; 9: 424-427.

Spilizewski KL, Marchant RE, Anderson JM and Hiltner A. *In vivo* leukocyte interactions with NHLB-DTB primary reference materials: polyethylene and silica-free polydimethylsiloxane.*Biomat* 1987; 8: 12-17.

Su B and Karin M. Mitogen-activated protein kinase cascades and regulation of gene expression. *Curr Opin Immunol* 1996; 8(3): 402-411.

Tanaka K, Sano K, Yuba K, Katsumura K, Nakano T, Tanaka K, Kobayashi M, Ikeda T and Abe M. *Inter immunopharm* 2003;3: 1273-1277.

Tavazzani F, Xing S, Waddell JE, Smith D and Boynton EL. *In vitro* interaction between silicone gel and human monocyte- macrophages. *J Biomed Mater Res* 2005; 72(2):161-167.

Tomasek JJ, Gabbiani G, Hinz B, Chaponnier C and Brown RA. Myofibroblasts and mechanoregulation of connective tissue remodeling. *Nat rev Mol Cell Biol* 2002; 3(5): 349-363, 2002.

Tredget EE, Wang R, Shen Q, Scott PG, Ghahary A. Transforming growth factor-beta mRNA and protein in hypertrophic scar tissues and fibroblasts: antagonism by IFN-alpha and IFN-gamma *in vitro* and *in vivo*. *J interferon cytokine res* 2000; 20(2):143-151.

Vandevord PJ, Gupta N, Wilson RB, Vinuya RZ, Schaefer CJ, Canady AI, Wooley PH. Immune reactions associated with silicone-based ventriculo-peritoneal shunt malfunctions in children. *Biomat* 2004; 25(17):3853-3860.

Vojdani A, Campbell A and Brautbar N. Immune functional impairment in patients with clinical abnormalities and silicone breast implants. *Toxicol Ind Health* 1992; 8(6): 415-429.

Webb K, Hlady V, Tresco PA. The relative importance of surface wettability and charged functional groups on NIH 3T3 fibroblast attachment, spreading and cytoskeletal organization. *J Biomed Mater Res* 1998; 41(3): 422 - 430 .

Weinzweig J, Schnur PL, MCconnell JP, Harris JB, Petty PM., Moyer TP and Nixon D. Silicon analysis of breast and capsular tissue from patients with saline or silicone gel breast implants.Correlation with connective-tissue disease. *Plast Reconstr Surg* 1998; 101(7): 1836-1841.

Wells AF, Daniels S, Gunasekaran S and Wells KE. Local increase in hyaluronic acid and interleukin 2 in the capsule surrounding silicone breast implants. *Ann Plast Surg* 1994; 33:1-5.

Weng H, Mertens PR, Gresner AM and Dooley S. IFN-γ abrogates profibrogenic TGF-β signaling in liver by targeting expression of inhibitory and receptor Smads. *J Hepatol* 2007; 46: 295-303.

Wesolowski SA and Dennis C. Fundamentals of vascular grafting. (Ed)Sigmund A.McGraw-Hill, New York, 1963.

Williams DF. Introduction to the use of Implants . In Reconstructing the body: Implants in surgery. Vol 1 (Eds)Williams DF and Roaf R.Liverpool University Press, 2000: 2.

Williams DF. The Williams Dictionary of Biomaterials. (Ed.) Williams DF. Liverpool university press, 1999:42.

Winding, Christensen L, Thomsen JL, Nielsen M, Breiting V, Brandt B. Silicon in human breast tissue surrounding silicone gel prosthesis. A scanning electron microscopy and energy dispersive X-ray investigation of normal, fibrocytic and peri- prosthestic breast tissue. *Scand J Plast Reconstr Surg Hand Surg* . 1988; 22(2):127-130.

Ziats NP, Miller KM and Anderson JM. *In vitro* and *in vivo* interactions of cells with biomaterials. *Biomat* 1988; 9: 5-13.

Appendix I

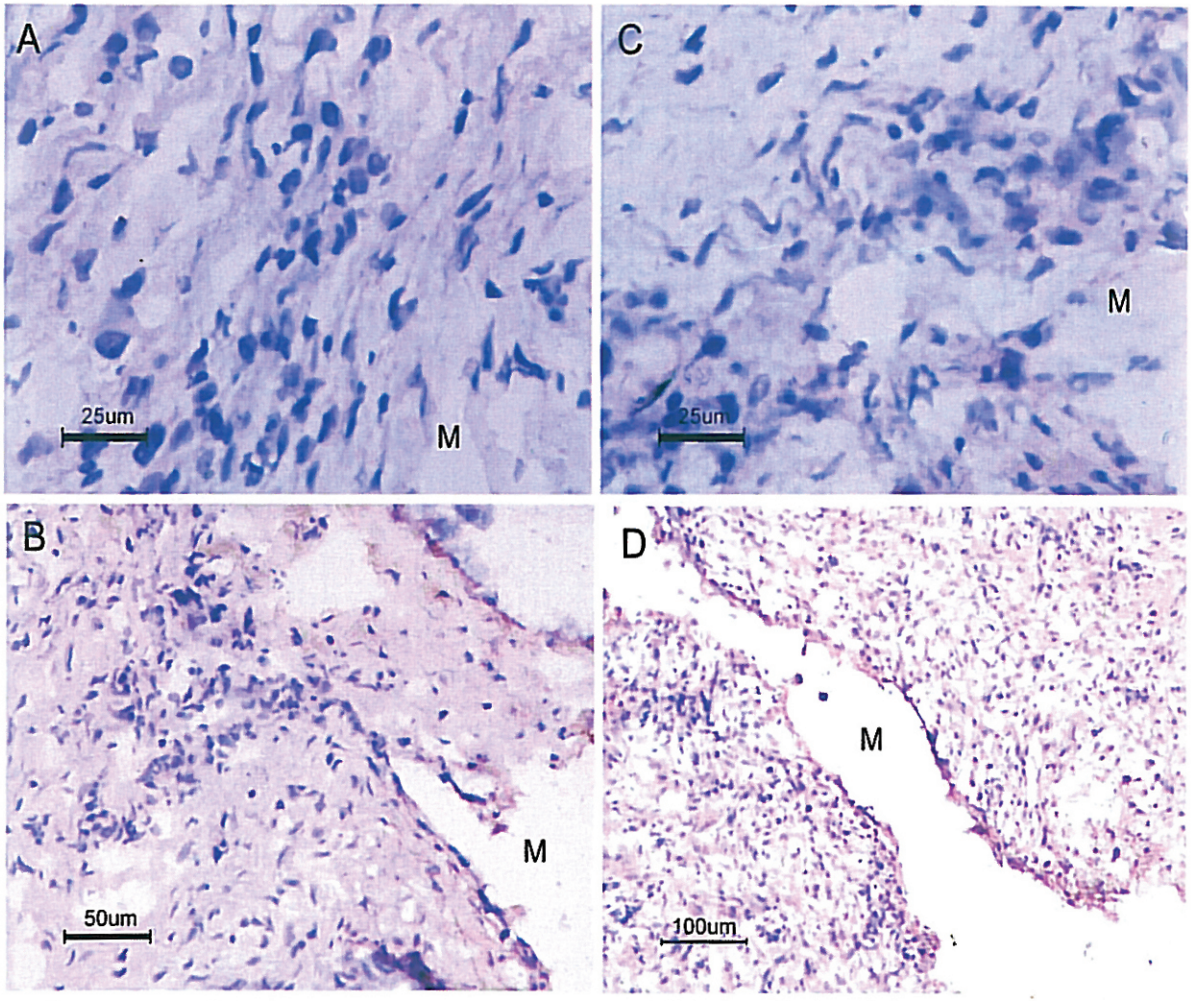

Light micrographs of negative control for immunohistochemical staining: ED2 (A), CD4(C), α SMA (B), Vimentin (D).

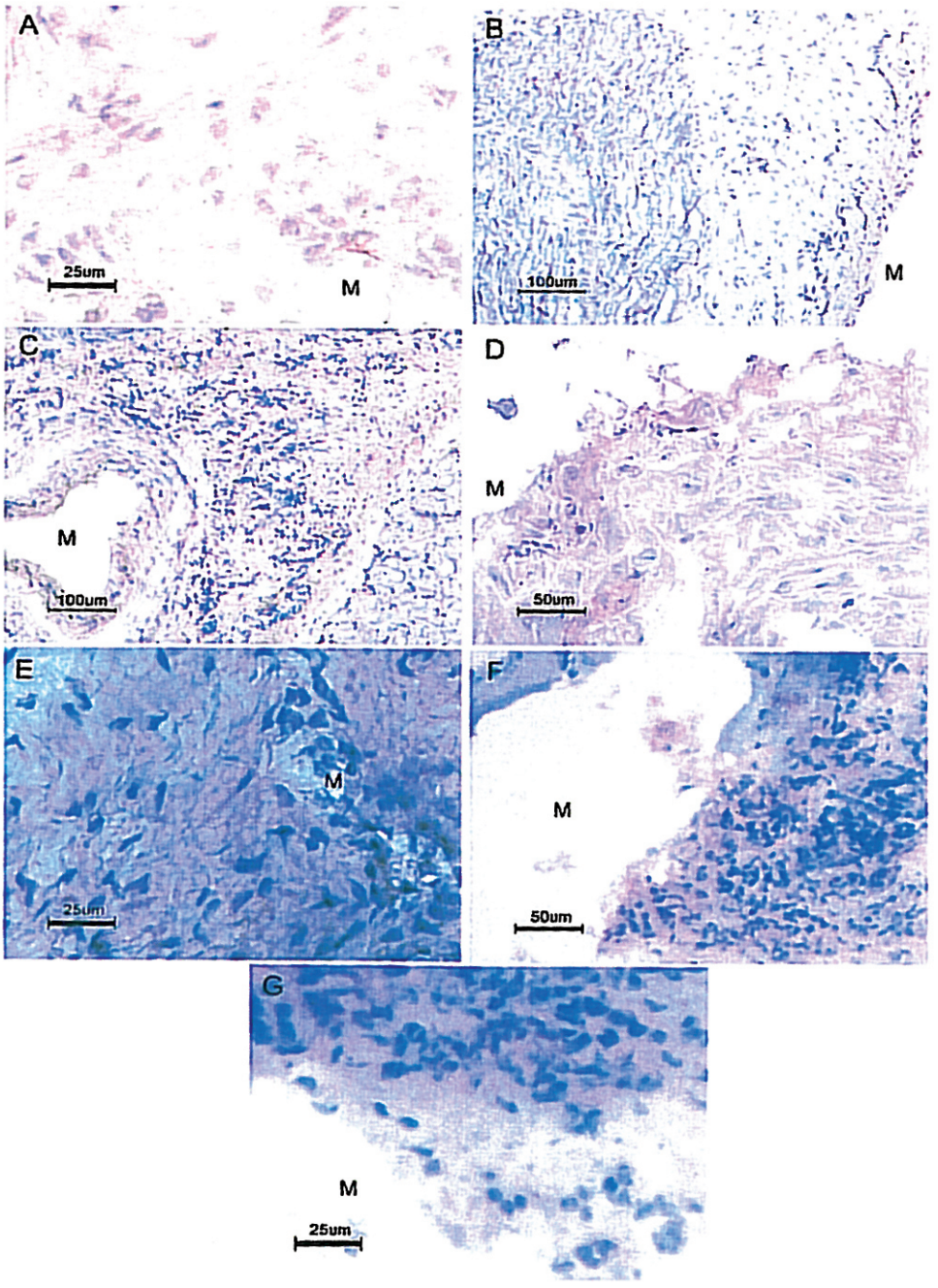

Light micrographs of negative control for immunohistochemical staining: TGFβ (A) TNFα (B), IL-1α(C), IL-1β (D), IFNγ (E), IL-6 (F), IL-10 (G).

Appendix II

Primary antibodies used for the immunohistochemical analysis

Antibody	**Cat. No.**	**Dilution**
ED2 (macrophage lysosomal antigen)	MCA 342R	1:100
CD4 (T lymphocytes)	MCA 55G	1:100
Vimentin (fibroblasts)	sc-7557	1:200
Alpha Smooth muscle actin, αSMA (myofibroblasts)	sc-1615	1:100
Transforming Growth factorβ	sc-146	1:250
Tumor Necrosis factorα	sc-1350	1:500
Interleukin 1α	sc-1254	1:500
Interleukin 1 β	MCA1397	1:250
Interferonγ	MCA1301	1:25
Interleukin-6	sc-1265	1:500
Interleukin-10	sc-1783	1:250